Harpur Hill, Buxton
Derbyshire, SK17 9JN
T: +44 (0)1298 218000
F: +44 (0)1298 218986
W: www.hsl.gov.uk

HEALTH & SAFETY LABORATORY

Technical Assessment of Petroleum Road Fuel Tankers
Work Package 1 Extension - Full scale testing of Lakeland tanker
AT11-1475

ES/2015/32

Report Approved for Issue By:	**Nigel Corlett BEng (Hons), MSc, PhD, ACSM**
Date of Issue:	**18 September 2015**
Lead Author:	**Chris Atkin BEng (Hons) CEng, MIMechE**
Contributing Author(s):	**James Hobbs MEng, PhD CEng, MIMechE, Liz Geary PhD, Duncan Webb BSc (Hons)**
Technical Reviewer(s):	**Michael Stewart MSc, PhD, FIMechE**
Editorial Reviewer:	**Rob Richardson BEng (Hons) CEng, MIMechE**
HSL Project Number:	**PE05832**

External Report

Production of this report and the work it describes were undertaken under a contract with the Department of Transport. Its contents, including any opinions and/or conclusion expressed or recommendations made, do not necessarily reflect policy or views of the Health and Safety Executive.

DISTRIBUTION

Steve Gillingham	Principal Engineer, Department for Transport
DfT Research Consortium	As requested by DfT
Nigel Corlett	HSL, Head of Engineering and Personal Safety Unit
Authors	
Duncan Webb	HSL Project Manager
HSL Reports and Papers Library	PDF Only

Report Approved for Issue by:	**Nigel Corlett BEng(Hons), MSc, PhD, ACSM**
Date of issue:	**18 September 2015**
Lead Author:	**Chris Atkin BEng (Hons) CEng, MIMechE**
Contributing Author(s):	**James Hobbs MEng, PhD CEng, MIMechE, Liz Geary PhD, Duncan Webb BSc (Hons)**
HSL Project Manager:	**Duncan Webb BSc (Hons)**
Technical Reviewer(s):	**Michael Stewart MSc, PhD, FIMechE**
Editorial Reviewer:	**Rob Richardson BEng (Hons) CEng, MIMechE**
HSL Project Number:	**PE05832**

CONTENTS

Last page = [121]

1 LIST OF FIGURES

2 LIST OF TABLES

3 EXECUTIVE SUMMARY

Background

This work has been undertaken as part of the Department for Transport (DfT) technical assessment of petroleum road fuel tankers. On 18 December 2014 DfT published findings including research on fuel tankers which were non-compliant with ADR, which were taken into account in a decision on their continued use (a Written Ministerial Statement to Parliament on "Petroleum road fuel tankers compliance" refers). This research was summarised in Project Report PPR724 "Technical Assessment of Petroleum Road Fuel Tankers - Summary Report (all Work Packages)" (TRL, 2014) which covered the three work packages (WPs) as follows:

- WP1 – Full scale testing and associated modelling; Health and Safety Laboratory (HSL).
- WP2 – Detailed Fracture and Fatigue Engineering Critical Assessment (ECA); TWI Ltd.
- WP3 – Accident data and regulatory implications, and production of an overall summary report of the research; TRL Ltd.

The work described in this report is an extension of WP1 and WP2, conducted by HSL and TWI, respectively.

Objectives

1. Preparation and topple test of an ADR-compliant tanker using the same or equivalent approaches as those used for previous tests; including full data-gathering instrumentation, but without subsequent modelling of the tanker impact.

2. Metallographic examinations of sections removed from the tanker after the topple test and detailed numerical analyses (static finite element modelling) of the front and rear bulkheads and their joints with the tanker shell.

Main Findings

The 2011/12 ADR-compliant road fuel tanker AT11-1475, supplied from service by Lakeland tankers maintained its internal and external integrity when subject to the HSL tanker topple test. Radiographic and metallographic examinations revealed some issues relating to the quality of the circumferential welds at the extrusion bands.

Test Methods, including tanker preparation

A single ADR-compliant Lakeland tanker was topple tested using the HSL topple test. This was a 10-banded, 6-compartment road fuel tanker numbered AT11-1475, with the tank manufactured in 2011, and the tanker assembled in 2012.

Tanker AT11-1475 was supplied by Lakeland Tankers after having been taken out of service at the end of a rental contract. Before delivery to HSL, the tanker was radiographed and assessed to obtain information on the condition of the circumferential welds. The same suitably qualified radiographic contractor was used as for the previous work in this research programme. The radiographs indicated defects, to a greater or lesser extent, in all the circumferential welds. The overall percentage of the length of welds radiographed that indicated lack of fusion defects was 23.4%. However, since the design of the circumferential joint has features which are known to complicate radiographic interpretation, these results may require further examination to be certain of the findings, and as such may be viewed as a worst-case. TWI findings from examinations of samples taken from the front and rear circumferential welds, which included radiographic and metallographic assessments, are more definitive and reported at the end of this summary. Prior to delivery to HSL, the tanker was fully ADR inspected by the same qualified

inspection body as used for the previous work in this research programme. The minor remedial work arising from the inspection was conducted by Lakeland Tankers before the tanker was prepared for the topple test.

Using the method developed and demonstrated to be reliable in previous work for DfT (TRL report PPR724, 2014), the Lakeland tanker was tilted under controlled conditions until it became unstable and fell onto its offside due to the effect of gravity. The tanker was filled with water because fuels were not practical for environmental and safety reasons. Impact on the offside of the tanker avoided damaging filling ports on the tankers nearside. Information on the tanker was used to calculate the approximate angle at which it would become unstable. The ramps were secured to a concrete test pad, with a plate steel landing pad providing a robust and repeatable impact area. After preparation the empty tanker was lifted onto the ramps with its offside at, and parallel to, the bottom of the ramps.

Once ready for test, the tanker was filled with the required volume of water (equivalent to the maximum mass of fuel that could be carried in service) distributed across all compartments. It was then toppled sideways, pivoting around the outer edge of its offside wheels to fall onto the landing pad. The tanker was tilted into the topple position using two parallel winching systems, with wide slings to spread the load and prevent high stress levels on the tanker barrel and comb when winch forces were applied to the slings. Each winching system included a chain hoist and load cell and was anchored to the concrete pad. Tilting the tanker into the topple position was controlled by ensuring the load on each winch line was similar. When the point of instability was reached, the winching lines slackened and the tanker toppled onto its side due to the effect of gravity.

Rectangular steel supports ('steel wheels') replaced the tanker's offside wheels to remove the risk of the tyres coming off the wheel rims during the test, and to avoid variability from uncontrolled shear movement in these tyres during the topple. The tanker was not tested with a tractor unit to avoid uncontrolled variations between tests caused by tractor unit rotation and to avoid possible failure of the kingpin due to unconventional loading. Instead, a steel frame (the '5^{th} wheel' assembly) was fitted at the tanker's kingpin plate to give the support normally provided by the tractor and to keep the tanker at the desired coupling height for the test. The tanker's suspension was blocked rigid to remove sources of uncontrolled variation, such as changes in the ride height, and to keep the tank position fixed relative to the suspension during the topple. Any tanker items not integral to the tank and suspension, or which might adversely affect the impact, or which might contain fuel, hydraulic oil or other environmentally harmful materials, were sealed or removed.

The full data gathering instrumentation for the tanker comprised strain gauges, pressure transducers and accelerometers to provide data for comparison and characterisation of general impact behaviour. In total, 40 such instruments were used. Accelerometer blocks were located at the centre point on the outside of both the front and rear bulkheads. Arrays of strain gauges and pressure transducers were affixed to compartments 1b (rear half of front compartment), 4b (third compartment from the rear) and to the front and rear bulkheads as follows:

- seven pressure transducers in each of the two compartments, located at the midpoint of the compartment close to the inner tanker wall, radiating circumferentially top to bottom on the offside (impact side), the centre being at the estimated point of impact;
- twelve strain gauges for compartment 1b, mounted as gauge pairs in matching positions on the inside and outside of the offside tanker shell. Two gauge pairs measuring longitudinal strain near the rear bulkhead weld, two gauge pairs measuring longitudinal strain near the front bulkhead and two gauge pairs measuring longitudinal and hoop strain at the midpoint.

- six strain gauges for compartment 4b, mounted as gauge pairs in matching positions on the inside and outside of the offside tanker shell. Two gauge pairs measuring longitudinal strain near the rear bulkhead weld, and one gauge pair measuring hoop strain at the midpoint.
- three strain gauges on each end bulkhead, mounted on the outside, towards the offside tanker shell, measuring radial strain.

Two independent data loggers were used: one for compartment 1b and the other for 4b and the end bulkheads. During the test these loggers were synchronised with the high speed video and acquired data at 50,000 samples per second, or one sample every 0.02 millisecond. The test was recorded using fifteen video cameras ranging from standard speed (25 frames per second) to high speed (1,000 frames per second). Frames from the high speed video were analysed to obtain accurate measurements of acceleration and impact velocity at the front and rear of the tanker.

After preparation, and before the topple test, the tanker was pressure tested to confirm that the integrity of the tanker had not been adversely affected by the preparations for the topple test. Also, before the topple test, the internal welds at the extrusion bands were visually inspected and the locations and characteristics of fillet welds between the extrusion band and the shell were mapped. The external circumferential weld caps were surveyed and were found to be broadly comparable with expectations based on the experience from previous tests. The tanker was laser scanned on arrival at HSL, after being lifted onto the ramps, immediately after testing (lying on its side), and after being lifted back onto its wheels. This was to confirm that tanker preparation and recovery had caused no damage to the tanker, and to record any changes to the tanker shape after impact.

Once surveyed and prepared, including fitting all instrumentation, the manway lids were refitted and pneumatic pressure tests conducted to confirm that the tanker was fully sealed and loadworthy. Immediately before the test, the tanker was filled with water (using a calibrated water meter) to give a mass that was equivalent to the maximum rated laden mass of the tanker. The tanker was, thus, filled with 31,244 litres of water, with each compartment filled to about 70% of its maximum capacity. These volumes were below the maximum rated laden volumes for fuel because of the higher density of water.

Immediately after impact, impact features found by visual examination were recorded. The tanker was then emptied and lifted back upright onto its wheels. After recovery, further visual examinations and pressure tests were conducted to establish the internal and external integrity of the tank and its compartments.

Topple test results

The overall event duration was a few seconds with most deformation occurring in the first 100 ms. The impact was close to uniform along the length of the tanker, with the rear hitting the ground approximately 8 ms before the front of the tanker. The impact velocities of 4.8 m/s (1.94 rad/s) at the front and 4.1 m/s (1.97 rad/s) at the rear of the tanker lay within the range of 1.75 to 2.62 rad/s which has been reported for rollovers in real accidents.

The pressure and strain data in both compartments were broadly consistent with expectations based on the impact events, tanker structural design and experience from previous tests. Peak pressures occurred at the 90 degrees from bottom dead centre position which is where the initial impact occurred. In general, strains near the welds were higher than those at the compartment centre, with some yielding and plastic deformation observed in the strain behaviour near the

welds. During impact, high speed video captured free travelling flexural waves propagating away from the impact line around the circumference of the tanker. Such waves should result in more pronounced ripples in the circumferential strain than the longitudinal strain at the centre of the compartment, and there was some evidence of this in the data.

After the test, the tanker exhibited a deformation shape with the impact area flattened along the length of the tanker. The impact caused a permanent reduction in tanker diameter of approximately 90 mm at the rear and 61 mm at the front of the tanker.

Immediately after the test, no external leaks could be seen, although there were slow drips from some pressure relief valves on the tanker's manlids. During emptying there was no evidence of internal leaks at any of the bulkheads. **Importantly, after the tanker was righted, ADR pressure tests confirmed that external and internal integrity had been maintained for all compartments and pressure relief valves, and detailed visual examination of the impact damage did not reveal any cracks that would compromise the integrity of the tanker.**

HSL supplied TWI with samples from the front and rear of the tanker, including both the damaged offside and the undamaged nearside, for radiographic and metallographic examinations and in support of detailed numerical analyses.

Metallographic examinations and detailed numerical analyses

Metallographic examinations and detailed numerical analyses have been undertaken to provide supplementary information about the performance of the petroleum road fuel tanker AT11-1475 after topple testing. These investigations found that:

- No through wall ruptures were observed in any of the samples taken from the front or rear welds of AT11-1475.
- The samples from the front circumferential joint did not exhibit any significant lack of fusion defects.
- The samples of the rear circumferential joint exhibited variable root penetration in the main circumferential welds. This resulted in some internal surface-breaking, lack of root fusion defects being observed with typical defect depths ranging from 1.0 mm to 2.0 mm.
- For the rear weld samples, the joints were found to exhibit good alignment, typically within 0.5 mm, and the height of the weld caps of the main circumferential welds was found to be typically in excess of 3.0 mm. The combination of low misalignment and large weld caps likely contributed to the good performance of the joints under the topple test. However, the excessive weld cap size was seen to correlate with lack of root penetration (and lack of root fusion defects) in many samples.
- Finite element modelling of a static, idealised representation of the end dish under topple test conditions, in conjunction with a forming limit diagram methodology, correctly predicted that the front swept dish and rear end dish of AT11-1475 would not rupture during the topple test. The model also accurately predicted the tanker front swept dish and rear end dish deformations and, therefore, represents a valuable approach for future assessments of tanker performance under these conditions.

In light of the metallographic examinations, RTN Lakeland have considered the findings from the examinations of the circumferential welds and are working with TWI to review welding practices, welding procedure qualification records and associated welding procedure specifications. HSL have been informed that the plan is to develop a new suite of welding procedure specifications which accommodate all aspects of the tanker welding process and take into account the latest best practice and practicalities of manufacture.

4 INTRODUCTION

This work has been undertaken as part of the Department for Transport (DfT) technical assessment of petroleum road fuel tankers.

On 18 December 2014 DfT published findings including research on fuel tankers which were non-compliant with ADR[1], which were taken into account in a decision on their continued use (a Written Ministerial Statement to Parliament on "Petroleum road fuel tankers compliance" refers). This research was summarised in Project Report PPR724 "Technical Assessment of Petroleum Road Fuel Tankers - Summary Report (all Work Packages)" (TRL, 2014 [1]) which covered three work packages (WPs) as follows:

- WP1 – Full scale testing and associated modelling; Health and Safety Laboratory (HSL).
- WP2 – Detailed Fracture and Fatigue Engineering Critical Assessment (ECA); TWI Ltd.
- WP3 – Accident data and regulatory implications, and production of an overall summary report of the research; TRL Ltd.

4.1 SCOPE OF WORK

The work described in this report is an extension of WP1 and WP2, conducted by HSL and TWI, respectively, with the objectives:

1. Preparation and topple test of an ADR-compliant tanker using the same or equivalent approaches as those used for previous tests; including full data-gathering instrumentation, but without subsequent modelling of the tanker impact.

2. Metallographic examinations of sections removed from the tanker after the topple test and detailed numerical analyses (static finite element modelling) of the front and rear bulkheads and their joints with the tanker shell.

Item 1 was conducted by HSL, with TWI conducting item 2. The tanker tested was a 10-banded, 6-compartment configuration (Section 6.1), manufactured by Lakeland (number AT11-1475).

Where this report refers to previous topple tests, unless another report reference is provided, the details are given in HSL report 14/39/04, published by DfT at the same location as PPR724.

[1] *Publically available material; current location of overall summary and more detailed reports:* *https://www.gov.uk/government/publications/petroleum-road-fuel-tankers-technical-assessment*

5 TANKER TEST METHOD

5.1 SUMMARY OF DIFFERENT TEST METHODS CONSIDERED

In early discussions with DfT on impact testing of tankers, the research consortium considered three different methodologies to carry out the tests as shown in Table 1.

Table 1 Summary of the test methods considered

Method	Advantages	Limitations
1. Tanker rollover whilst in motion	Closer to a real-life scenario.	This method is not the most suitable for validating a numerical model as there will be a larger variation in the dynamic response of each tanker being tested compared with 3. (below). For example, the impact velocities will vary more between each test than in 3. Also there will probably be a greater variation in which part of the tank strikes the ground first.
2. Drop tests of a tank	A well-controlled test. The tank orientation could be controlled so impact occurs on specific areas of interest. Would follow a similar test method for packages used to transport radioactive materials (covered by IAEA regulations). May be useful when considering accident scenarios involving direct impacts on the tank (e.g. rear impact or side impact crashes)	Test method more suitable for assessments of the tank alone. Test is different to rollover conditions. Dynamic response of the internal fluid may not be typical of an accident scenario.
3. Sideways topple test of a tanker when stationary	A well-controlled test without the practical difficulties in 1. and 2. Will provide data that should be suitable for validation of a model. Closer to a real-life scenario than 2. Closer to the ADR regulatory test for IBCs (clause 6.5.6.11 described Section 5.2 below).	Not as close to a road-going accident scenario as 1.

The methodology followed, in agreement with DfT, was the topple test (number 3 in Table 1), with the tanker filled with water to represent the fuel: petroleum, diesel or fuel oil were not practical for environmental and safety reasons. The tanker would be toppled in a sideways direction onto flat ground, so the topple height was almost zero as the pivot line was close to the ground. This was considered the most practical and appropriate method within the timescales required to deliver the test work.

The tanker would be positioned close to the point of instability and then 'nudged' to roll it onto its side using a controlled and repeatable method. The impact is on the tanker's offside, because the ports on the nearside need to be accessible for filling. This is shown in Figure 1.

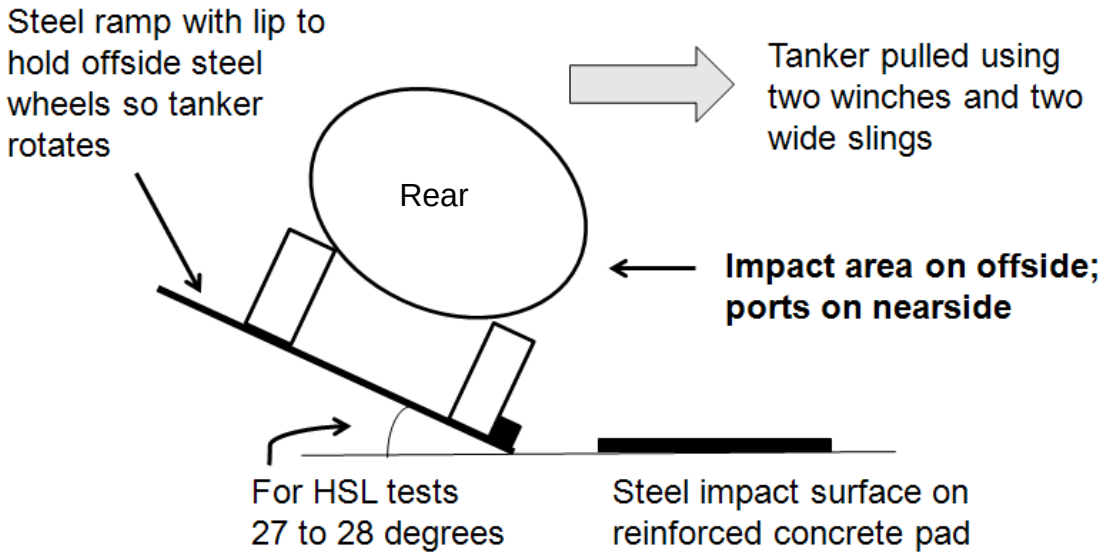

Figure 1 The key features of the HSL tanker topple test

HSL calculated that a tanker of the type to be tested, filled to its maximum gross weight with water rather than road fuel, is stable at around 27 to 33 degrees of tilt. Therefore an initial angle of around 27 to 28 degrees would reduce the horizontal pull force required to topple the tanker.

5.2 ADR TEST METHOD FOR TANKS

The ADR regulations [2] were referenced to assess what impact test methods are required for tanks. In ADR there are currently no mandatory impact test requirements for petroleum road fuel tankers. However, there are topple test requirements for intermediate bulk containers (IBCs)[2], which are shown below for information.

[2] *An Intermediate bulk container (IBC) is a reusable industrial container designed for the transport and storage of bulk liquid and granulate substances. They can normally be stacked, and common sizes are 1 040 litres and 1 250 litres. Cube shaped IBCs give particularly good storage capacity compared to palletized drums.*

6.5.6.11 Topple Test

6.5.6.11.1 Applicability

For all types of flexible IBC, as a design type test.

6.5.6.11.2 Preparation of the IBC for test.

The IBC shall be filled to not less than 95% of its capacity and to its maximum permissible gross mass, the contents being evenly distributed.

6.5.6.11.3 Method of testing.

The IBC shall be caused to topple on to any part of its top on to a rigid, non-resilient, smooth, flat and horizontal surface.

6.5.6.11.4 Topple Height

Packing Group I	*Packing Group II*	*Packing Group III*
1.8m	*1.2m* **(same group as an LGBF code petroleum tanker)**	*0.8m*

6.5.6.11.5 Criteria for passing the test.

No loss of contents. A slight discharge, e.g. from closures or stitch holes, upon impact shall not be considered to be a failure of the IBC provided that no further leakage occurs.

HSL installed a 20 mm thick steel landing pad, bolted to a 150 mm deep reinforced concrete slab to satisfy 6.5.6.11.3. Regarding 6.5.6.11.2, HSL did not fill the tankers to maximum volumetric capacity for reasons discussed in Section 7.

5.3 RAMP DESIGN

HSL placed the tanker at a pre-set angle on a ramp as described in Section 5.1. As well as reducing the winching force required to topple the tanker, it also reduced the risk of the tanker sliding towards the winches as the force was applied.

HSL designed two steel ramps constructed at an angle of 25^{o} (one to go under the trailer, and the other to go under a bespoke 5^{th} wheel assembly (described in Section 5.4)).

The ramps consisted of a 20 mm thick top plate welded to a triangular steel frame underneath; the frame was constructed of rectangular hollow sections (RHS) to provide the angle and support the load of a fully-loaded tanker.

Stability calculations showed that, for a fully-loaded tanker, this would require a winching force in the range of four to seven tonnes. To reduce this force, HSL manufactured 1^{o} wedges to go underneath the upper wheels to raise the angle to $26^{o} – 27^{o}$ as shown in Figure 2. This reduced the calculated winching force to between two and five tonnes.

FES150501_01

Figure 2 Tanker on the ramps showing the wedges under the nearside wheels in preparation for a topple test

Figure 2 also shows the two restraint slings that HSL used to secure the tanker on the ramp. HSL had carried out calculations to demonstrate the tanker would be stable on the ramp at this angle (whilst empty, during filling and when filled). However, as a safety precaution these two restraint slings were attached to the tanker and each anchored to a separate steel bracket bolted into the concrete pad (similar to those for the winching lines shown in Figure 7). Therefore, if the tanker did become unstable and started to topple (e.g. in high winds) the restraints would hold the load[3].

The tanker is shown on the ramps in Figure 3.

[3] *In still conditions, the tests showed the tanker does remain stable on the ramp without the need for the restraints.*

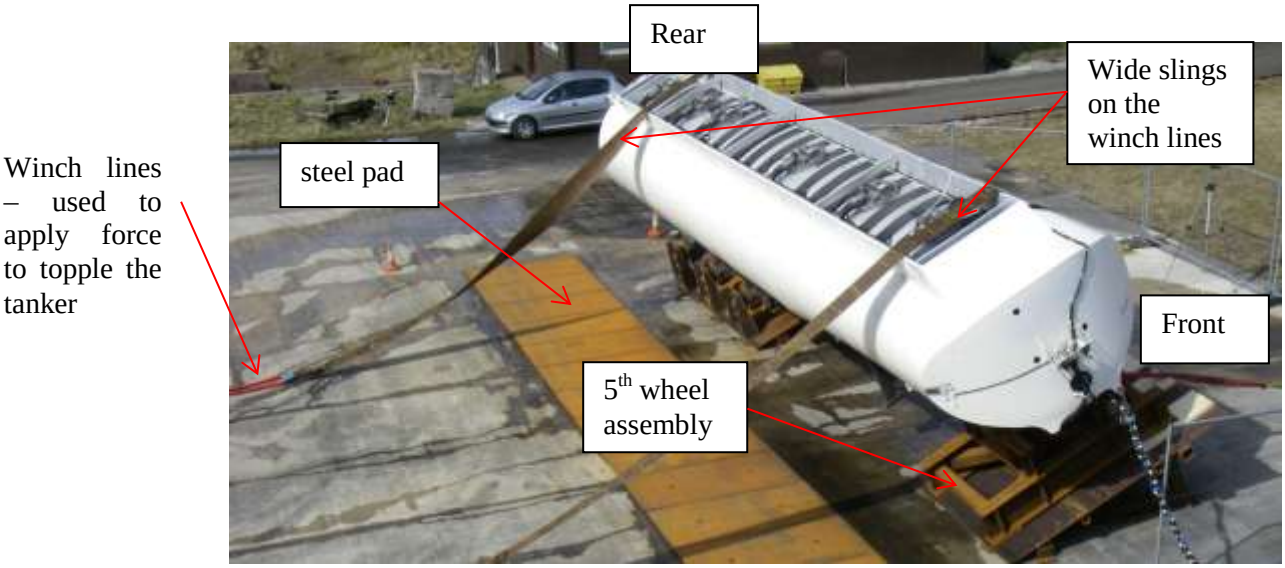

FES140501_02

Figure 3 AT11-1475 on the ramps before test

To prevent the tanker sliding off the ramp, and to provide a pivot point, a 20 mm x 20 mm steel strip was welded along the lower side of the ramps (this can be seen in Figure 5).

5.4 TANKER PREPARATION

All tanker components that could affect the impact, such as brackets, mudguards, flexible hoses, the box containing firefighting equipment etc. were removed. This ensured that the tank would impact directly on the ground during the test, and the method would be repeatable for tests on other tankers.

The tanker was not tested with a tractor unit as tractor unit rotation, and possible failure of the kingpin due to unconventional loading, would have caused variations in the test that would not be repeatable from one test to the next. A steel frame, the 5th wheel assembly, was bolted to the kingpin plate on the underside of the tanker near the front to provide support (see Figure 4). The assembly was designed and manufactured by HSL using I-beams and cross-bracing. It supported the tanker at the same nominal height and replicated the wheel track as if coupled to a tractor unit.

FES150501_03

Figure 4 Front of the tanker and 5th wheel assembly

To eliminate the risk of the tyres coming off the rims, and shear movement in the tyres as the tanker is winched to the topple position, the nearside wheels were replaced with rectangular steel supports: referred to as *steel wheels* (see Figure 5).

FES150501_04

Figure 5 Tanker on ramps with steel wheels fitted to its offside and the steel strip on the ramp

Both the 5th wheel assembly and the steel wheels were designed to keep the vehicle track (the width from the outside of the tyres on one side to the outside of the tyres on the other side) as close to the true dimension as practical (2,550 mm). In addition, the tanker suspension was blocked on all tankers by installing brackets between the axles and chassis rail (Figure 6).

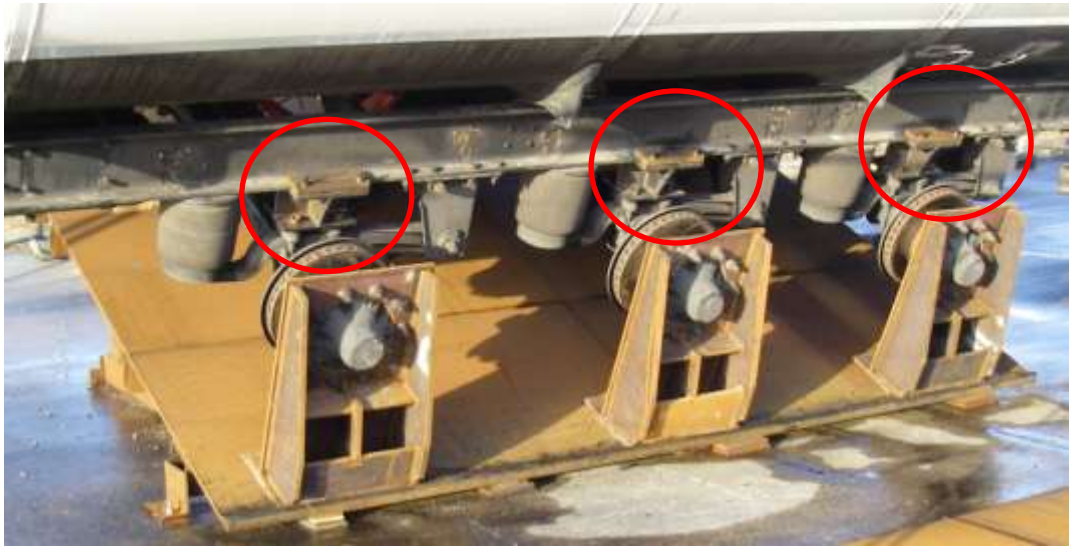

FES150501_05

Figure 6 Chassis rail showing the brackets blocking the suspension

These brackets were fitted to ensure that:

- winching the tanker to the topple position was controlled — any movement between tanker and chassis could cause the tanker to topple prematurely in an unpredictable manner;
- the tanker toppled in a repeatable way — movement of the suspension could vary between tankers. This would cause variations and present difficulties when comparing the results with the predictions; and
- there was no risk the suspension would fail due to the shear forces acting on it when the tanker was in a raised position.

After all the preparation work, including fitting the instrumentation, had been completed in the laboratory, the empty tanker was transferred to the test pad.

5.5 WINCHING METHODS

The method chosen was to winch the tanker using two chain hoists attached to anchor brackets bolted into the concrete pad. Chain hoists have a high gear ratio so the load can be applied in a more controlled manner. However, as chain hoists are not specifically designed to be used as winches, HSL investigated this matter and confirmed that there was no risk of the chain hoists being unable to support the load, or reductions in the safe working load. Recommendations were made to check the hoist remained lubricated, as some hoists have an oil breather which may leak oil when used in the horizontal position: this was not an issue for the chain blocks that HSL chose.

One of the chain hoists and winching lines are shown in Figure 7.

The winches were shackled, via textile slings, to steel brackets that had been bolted into the concrete; these brackets had been proof loaded to 5 tonnes. At the other end, the slings were placed over the top of the tanker, then 'choked' onto the 5th wheel assembly at the front, and around the middle or rear axle at the back. Flat, textile webslings (300 mm wide) were used around the tanker body to spread the winching load and prevent high stresses on the tanker barrel and comb: these are shown in Figure 7.

Each winch had a load cell in the line so the *Winch Master* (standing between the two load lines) could observe the force in each line and instruct either of the winch operators to haul the 'pull chain' quicker or slower, in order to keep the forces balanced on each line.

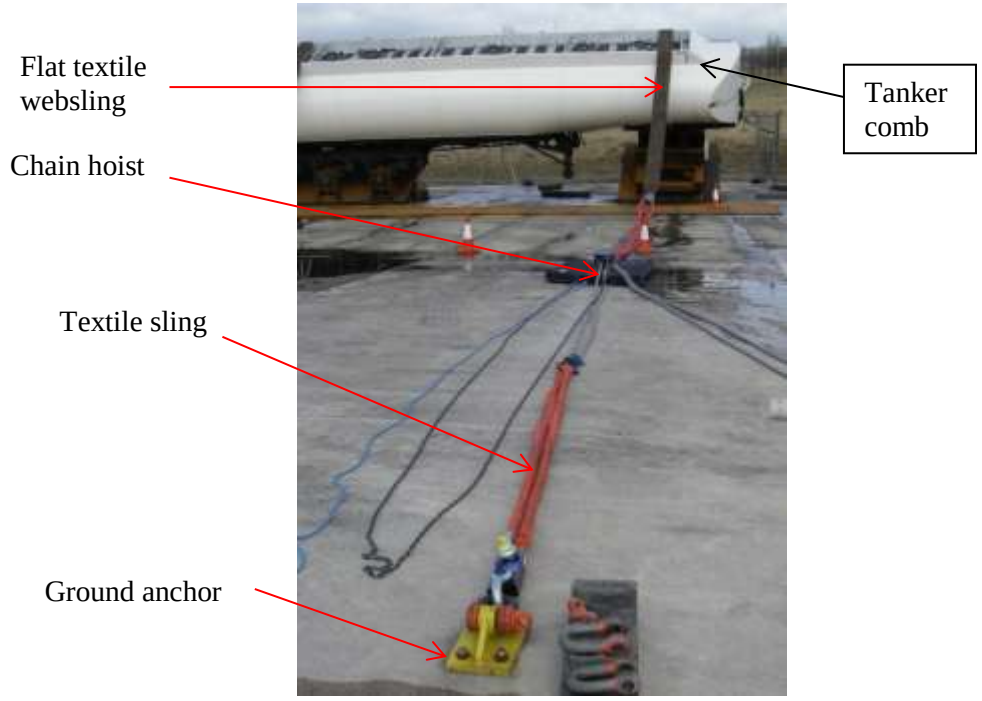

Figure 7 Method of winching the tanker

5.6 TEST ASSURANCE

The *Test Officer* maintained a short track sheet to ensure the tests were carried out in a controlled manner, and instrumentation and video operators were prepared. The sheet was signed after each step had been carried out. Maximum load in the winch lines (1,100 kgf on each line) was reached once the upper (nearside) wheels had lifted a short distance from the ramp. As the winches continued to rotate the tanker, the load required on the winch lines began to decrease. This is due to the horizontal distance between the tanker's centre of gravity and the pivot line reducing as the tanker begins to rotate. So the turning force (moment) required to continue to rotate the tanker reduces. At the point of instability, the winch lines went slack as the tanker toppled.

The test was conducted at 13:30 on 27th March 2015, ambient temperature was approximately 8°C.

6 PRE-TEST SURVEYS AND TANKER CONSTRUCTION

6.1 TANKER CONSTRUCTION

The tanker used for the test, AT11-1475, was ADR-compliant and manufactured by Lakeland Tankers with a 10-banded, 6-compartment configuration. The tank was manufactured in 2011, with the tanker assembled in 2012. Tanker AT11-1475 was supplied for topple test by Lakeland after having been taken out of service at the end of a rental contract.

The bands are where tanker shell sections and a baffle or bulkhead are welded together. For all except the front band (Band A/10), this joint uses an extrusion band as the joining section. The front band's "swept" shape uses a double-sided corner joint. Bands were numbered A/y to J/y with Band A at the front, Band J at the rear and y the number of bands on the tanker, in this case 10. This is consistent with the numbering used in the previous research. As only a 10-banded tanker is considered in this report, the "/10" is not always used and the bands may be described with the letter only.

Figure 8 shows the band and compartment numbering convention.

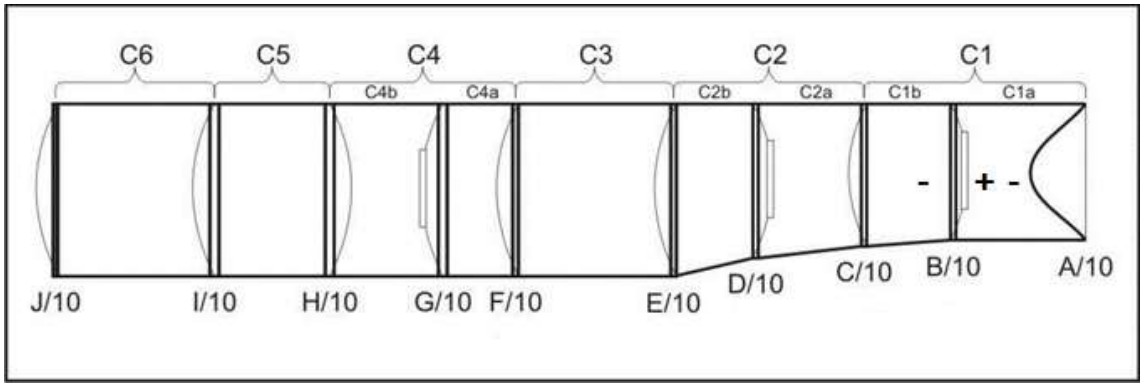

Figure 8 Band and compartment numbers

Bulkheads are solid, while baffles have a central hole and sub-divide compartments. The front and rear ends of the tanker are classed as bulkheads, but may also be called "end-dishes". Baffles are located at bands B, D and G, with bulkheads located at the other bands.

The foremost weld on a band has been designated "+", and the rearmost "-". For example, in Compartment 1a, A- and B+ can be viewed from within the compartment.

6.2 TANKER RADIOGRAPHY

6.2.1 Method

Before delivery to HSL the tanker was radiographed and assessed to provide information on the condition of the circumferential welds. The same suitably qualified radiographic contractor that had been used for previous work in this research programme conducted Computed Radiography and assessed the results to EN ISO 10042: 2005 [3] Quality Level 'C'. For all bands except A, the Single Wall, Single Image (SWSI) approach was used with the SWSI source outside the tanker and the image plate (film) inside the tanker. Curvature of the bulkheads/baffles meant that the circumferential welds were only accessible (for placing the image plate) on the concave side of the baffle plates. Band A used the Double Wall, Single Image (DWSI) approach

Radiographs were taken on both offside and nearside of the tanker, from the lowest accessible position on the band to the comb. Radiographs in the comb area were also taken. The curvature of the "swept-back" band A restricted radiography of this band.

Bands were divided into shorter sections for the individual radiograph exposures, which combined to form the overall radiography of the band. In general these sections were 35 cm long, with other lengths where necessary.

6.2.2 Results reported

The radiography report noted where the following features were found on the individual radiograph sections, and over what lengths:

- lack of fusion (LOF);
- intermittent lack of fusion;
- linear porosity;
- porosity;
- isolated pores;
- lack of penetration (LOP); and
- inclusions.

An overall acceptance or rejection for each individual radiograph section was given in the radiography report, together with summaries of the number of defects and percentage length of defects in terms of total radiographed length in each band. Contractor 1 also provided photos of the tanker and the radiograph starting positions in the radiography reports.

6.2.3 Summary of radiograph results

Figure 9a illustrates the areas radiographed for the different bands, and Figure 9b gives a summary of the radiographic results for the tanker by band. Lack of fusion was, to a greater or lesser extent, found in all bands, and averaged 23.4% of the overall length radiographed, with variation from 1.4% to 96.1% across the bands. The full report is given in Appendix 1.

Since the design of the circumferential joint has features which are known to complicate radiographic interpretation, these results may require further examination to be certain of the findings, and as such may be viewed as a worst-case interpretation. TWI findings from examinations of samples taken from the front and rear circumferential welds, which included radiographic and metallographic assessments, are more definitive and are reported in Section 10.

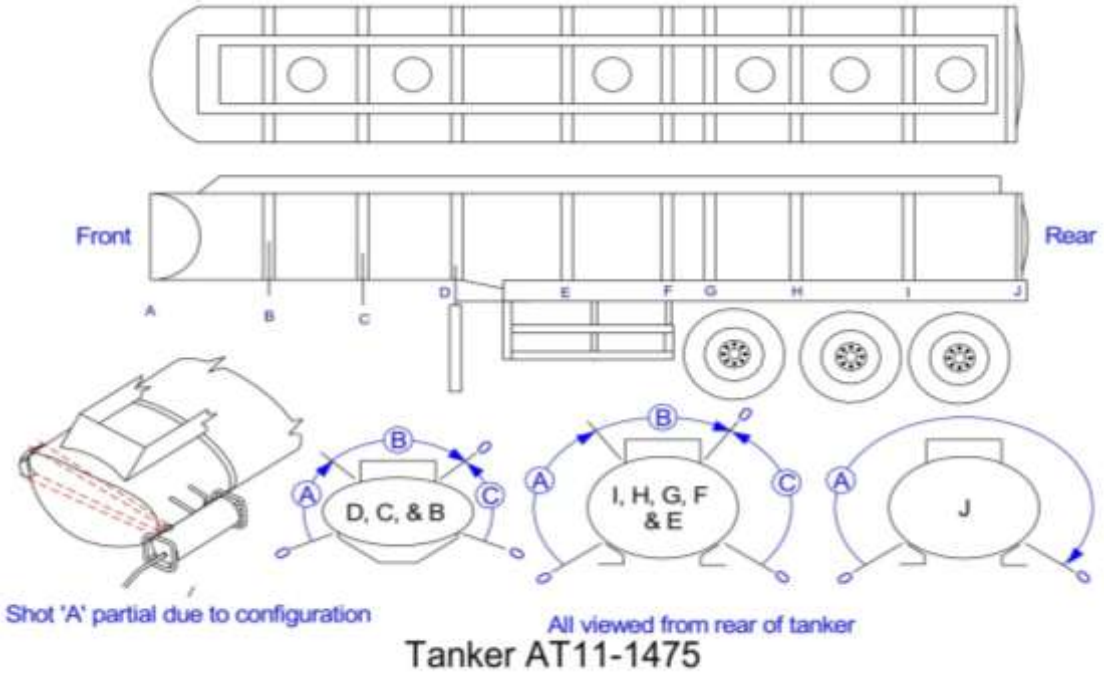

Figure 9a Areas of bands radiographed

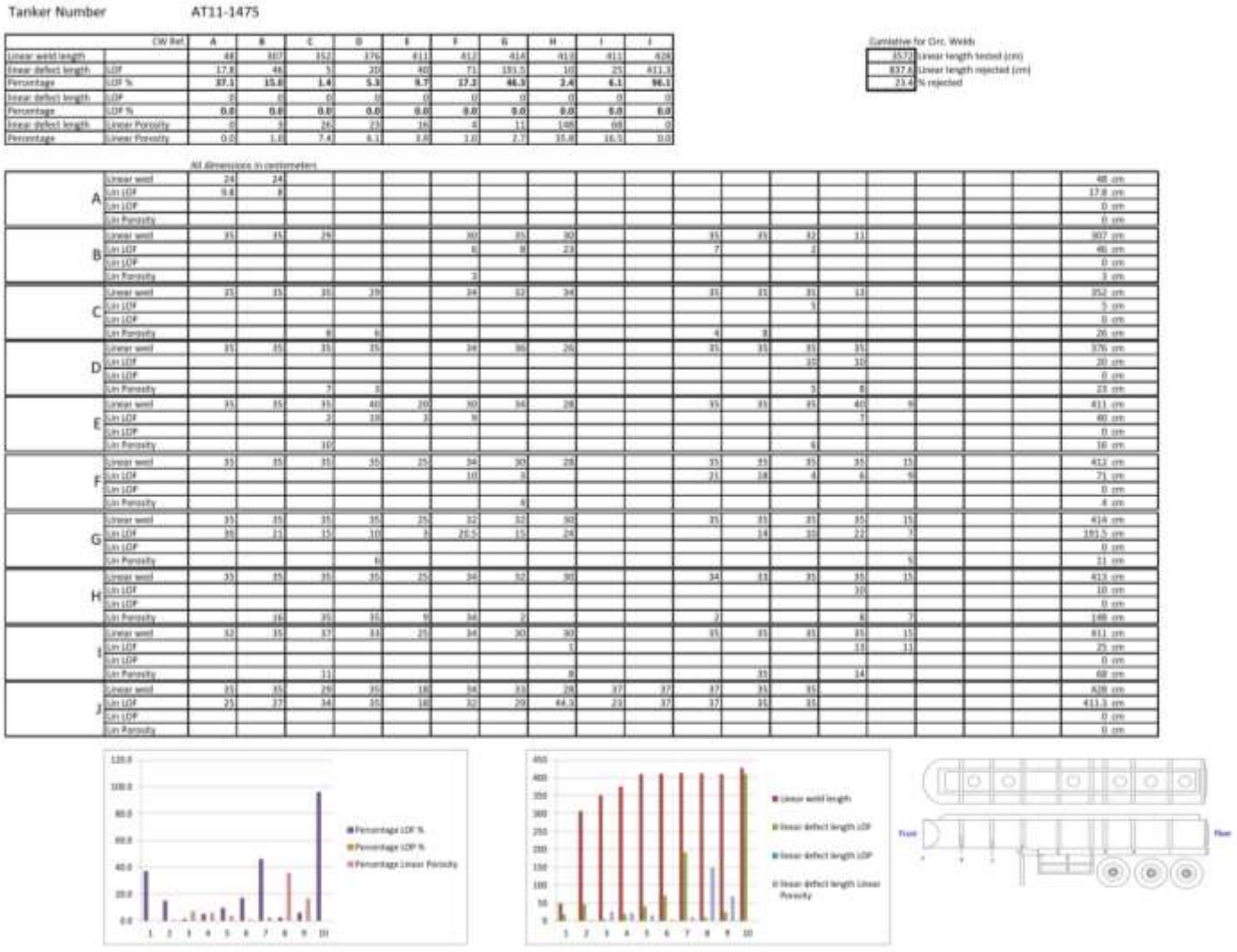

Figure 9b Radiography Summary

6.3 INTERNAL SURVEY

A detailed internal survey of the fillet welds in the compartments of the tanker was carried out prior to testing. All compartments were photographed. Where accessible and the fillet weld was not continuous, the circumference of the tanker was marked out in 0.2 m intervals before photographs were taken: an example photograph is shown in Figure 10.

A map of the location of the fillet welds was then produced from the photographs. An example of a fillet weld map is shown in Figure 11. The numbers shown denote the distance in metres around the circumference from the bottom dead centre. Fillet welds were observed at locations marked in magenta. The full set of fillet weld maps is included in Appendix 2.

In the previous work, the alignment of the main welds was also checked. Where no fillet weld was present, a 1 mm feeler gauge was offered to the gap between the nose of the extrusion band and the tanker shell. However, the design of the welded joint in AT11-1475 included a gap between the shell and the extrusion band. So where there was no fillet weld, it was possible to insert a 1 mm feeler gauge into the gap between the nose of the extrusion band and the tanker shell. While these gaps were recorded, for clarity they have not been marked on the fillet weld maps.

The fillet weld is not a structural weld, but is added for manufacturing purposes. As such the details may vary, and are divided into three categories in this report:

Continuous – no gaps around full circumference.

Stitched – short, reasonably repeatable lengths of fillet weld separated by reasonably repeatable gaps.

Intermittent – variable lengths of fillet weld separated by gaps – gap length around circumference much less than fillet weld length.

FES150501_10

Figure 10 Photograph inside compartment 5 showing location and fillet weld

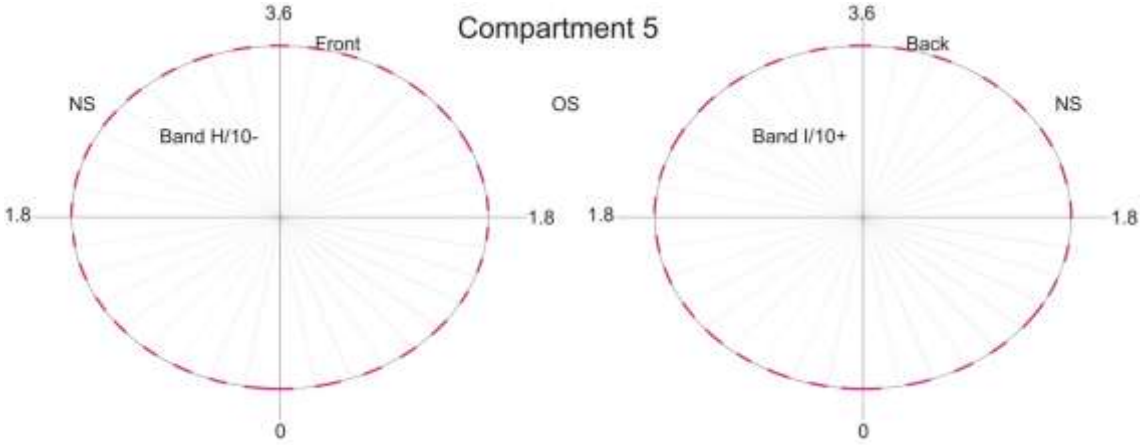

Figure 11 Example of a fillet weld map

6.3.1 Compartment 1

This compartment contained a baffle at Band B. Therefore A-, B+, B- and C+ could be seen from this compartment.

A-: Weld design does not include fillet as there is no extrusion band.

B+, B-, C+: Continuous fillet weld.

6.3.2 Compartment 2

This compartment also contained a baffle, at Band D. Therefore C-, D+, D- and E+ could be seen from this compartment.

C-, D+, D-, E+: Continuous fillet weld.

6.3.3 Compartment 3

E- : Continuous fillet weld.

F+: Intermittent fillet weld.

6.3.4 Compartment 4

This compartment contained a baffle, at Band G. Therefore F-, G+, G- and E+ could be seen from this compartment.

F-, G+: Intermittent fillet weld. As these bands were in the front part, through the baffle, (compartment 4a) it was not possible to gain full access to measure the gap lengths.

G-, H+: Stitched fillet weld.

6.3.5 Compartment 5

H-, I+: Stitched fillet weld.

6.3.6 Compartment 6

I-, J+: Stitched fillet weld.

6.4 ADR AND TANK INTEGRITY INSPECTIONS

AT11-1475 was given a combined 2 year VT and 6 year ADR inspection by a tanker inspection contractor on 17th February 2015 before delivery to HSL (at the radiography contractor's site). The tanker passed the hydraulic test (392 mbar), leakproofness test (200 mbar), EPRV lift/reseal test (Emergency Pressure Relief Valve; 250 mbar) and Vapour tightness/PV Vent Valve test. The inspection found some minor remedial works were needed – these were addressed by Lakeland after the tanker was delivered to HSL and before HSL prepared the tanker for the topple test.

A further inspection by the tanker inspection contractor was performed on 20th March 2015, after the tanker had been prepared for testing at HSL. This was undertaken to confirm that the integrity of the tanker had not been adversely affected by the preparations for the topple test. Again, the tanker passed the hydraulic test (392 mbar), leakproofness test (200 mbar), EPRV lift/reseal test (250 mbar) and Vapour tightness/PV Vent Valve test. For leakproofness, one compartment at a time was pressurised to 200 mbar, then sealed; the duration of the test was five minutes. All compartments were within 5 mbar pressure drop pass/fail criterion; Table 2 gives the pressure drops in the compartments after five minutes. All the EPRVs opened at pressures between 265 and 293 mbar, and re-sealed at pressures between 244 and 269 mbar, within the acceptable limits for a petroleum tanker.

Table 2 Pneumatic pressure test

Compartment No.	1	2	3	4	5	6
Pressure drop after 5 minutes (mbar)	1	1	1	2	1	3

Tank integrity tests were repeated after the topple tests; the results are given in Section 9.4.

6.5 LASER SCANNING OF THE TANKER AND WELDS

The laser scan approaches were the same as those in previous tests.

6.5.1 Laser scanning the tanker

For accurate information on the deformation of the tanker due to the testing, all tankers were laser scanned at the following times:

- On arrival at HSL.
- After being lifted onto the ramps
- After the topple test (lying on its side)
- After being lifted back onto its wheels

The laser scanner was a Leica Scanstation C10, serial number 1260769. It was last serviced on 8/12/2014, which included a calibration. Its user manual states:

Accuracy of single measurement
Position:* 6 mm
Distance:* 4 mm
Angle (horizontal/vertical): 60 μrad / 60 μrad (12" / 12")

Modelled surface
precision/noise:** 2 mm
Target acquisition 2 mm std. deviation
Dual-axis compensator Selectable on/off, resolution 1", dynamic range +/- 5', accuracy 1.5"

* At 1 m – 50 m range, one sigma
** Subject to modelling methodology for modelled surface

The laser scanner works on the 'time of flight' of a pulsed laser. The laser turns on and off 50,000 times a second, the time for each pulse to be reflected back to the scanner is used to calculate the distance to the surface which the pulse has reflected off.

6.5.2 Laser scans of the damage profile

Parameters describing the deformation profile along the length of the tanker were calculated using the laser scans of the tanker both on its side and after righting. Some measurements are included in the damage assessment in Section 9.4.

6.5.3 Laser scanning the weld caps

HSL surveyed the external circumferential weld cap dimensions for the tanker.

The scanner was a Romer Absolute Arm 7525SI, Arm Serial Number: 7525-2505-FA, Scanner Serial Number: 14-25-016. It was calibrated on 15/09/2014 and the user manual states that the scanning system accuracy is ±0.032 mm.

The weld cap data consisted of cap height, cap width, cap spacing and misalignment measurements taken in circumferential strips from both sides of each band on the tanker (like a set of ribs) as illustrated in Figure 12.

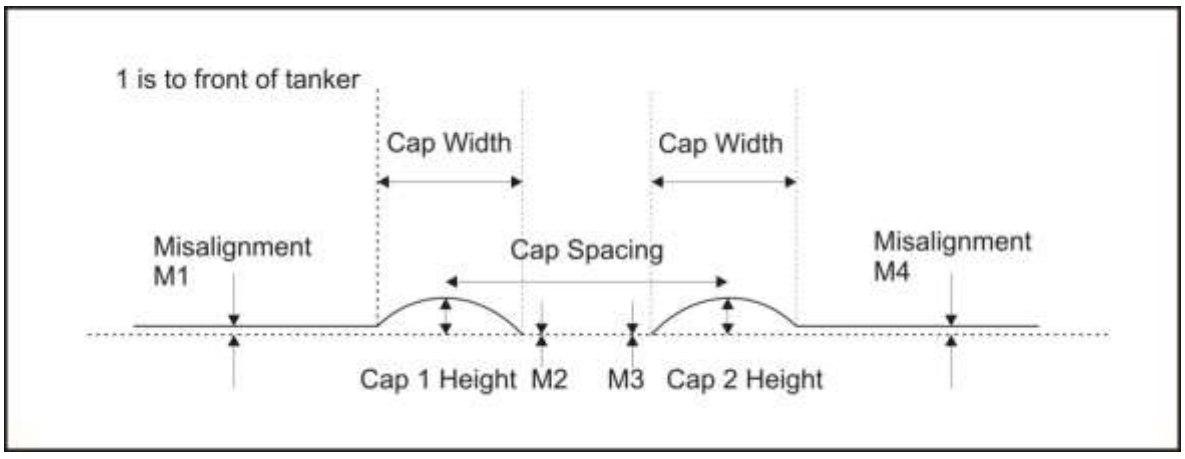

Figure 12 Profile of the circumferential weld caps

The external circumferential weld caps were found to be broadly comparable with expectations based on the experience from previous tests. The measurements are given in Appendix 3 for information.

7 TANKER FILLING – WEIGHT CONTROL

DfT and its research consortium agreed to follow the same approach used in previous topple tests and fill the tanker to maximum mass (*not* volume), equivalent to the maximum laden mass of fuel that could be carried in service. The identification plate on the chassis stated that the maximum gross weight was 38,000 kg, and the unladen mass value provided by Lakeland was 5,520 kg. The quantity of water to fill each compartment was found by converting the nominal capacity of petrol to the equivalent mass of water (that is, multiplying by the density of petrol, 0.73 kg/litre)

The tanker was filled from a fire hydrant, and the water flow into each compartment was measured using a calibrated water meter. The volume of water in each compartment is shown in Table 3.

Overall, the tanker was filled with 31,244 litres or kg of water, with each compartment filled to about 70% of its maximum capacity. Combined with the unladen mass of 5,520 kg, this gives 36,764 kg compared to the maximum gross weight of 38,000 kg.

Table 3 Filling volumes (litres unless otherwise stated)

	C1 (front)	**C2**	**C3**	**C4**	**C5**	**C6 (rear)**	**TOTAL**
Nominal Capacity (from tanker plate)	7,600	7,600	7,000	7,600	6,000	7,000	42,800
Ullage (from tanker plate)	332	400	351	373	262	348	2,066
Maximum capacity	7,932	8,000	7,351	7,973	6,262	7,348	44,866
Petrol mass (kg, nominal capacity)	5,548	5,548	5,110	5,548	4,380	5,110	31,244
Water volume required	5,548	5,548	5,110	5,548	4,380	5,110	31,244
Fill volume measured	5,548	5,548	5,110	5,548	4,380	5,110	31,244
Fill order	2	4	6	5	3	1	

Maximum capacity taken from the tanker chassis plate, 0% ullage

8 INSTRUMENTATION AND VIDEO

8.1 DATA LOGGING EQUIPMENT

The test used the same data acquisition system and a similar instrumentation approach to that used in previous topple tests. Data from two accelerometers, 14 pressure transducers and 24 strain gauges were recorded. Strain and pressure measurements were made in two compartments (C1b and C4b). Strain and acceleration measurements were made on both end bulkheads. Two, independent Graphtec GL-7000 loggers, powered through a UPS (Uninterruptable Power Supply), were used. The loggers were set to acquire data at a rate of 50 (50 000 samples per second). Each logger was specific to one compartment in the tanker, with the rear bulkhead accelerometer and both end bulkhead strain gauges on the same logger as C4b and the front bulkhead accelerometer on the same logger as C1b.

The compartments were fitted with pressure transducers and strain gauges on the interior side, with additional strain gauges attached to the exterior side at the equivalent position to the strain gauges on the interior (strain gauge pairs). This allowed both bending and membrane stresses to be obtained[4]. All strain gauges and pressure transducers were located on the impact side (offside) of the tanker.

Cables from the gauges and transducers on the interior side of a compartment were passed through a set of cable glands mounted on a specially designed baffle that was attached to the manway cover on the top of the tanker, where the tanker level probe is normally fitted.

The data was stored on the loggers as binary .GBD files. These were converted and exported to comma separated values (.csv) files. Further analysis was done by importing these files into data analysis software packages.

The loggers were triggered manually before the tanker started to topple, and a synchronisation pulse was provided to both loggers by the high speed video operator.

8.1.1 Strain Gauges

The gauges used were Vishay CEA-13-250UW-350. As variations in the surface temperature of the tanker were insignificant during the tests, no temperature compensation was used. The gauges were installed as follows:

Compartment 1b (Figures 13a and 13b)

- two pairs near the rear bulkhead weld (band C/10) — measuring longitudinal strain;
- two pairs near the midpoint of the compartment — one measuring longitudinal strain, one measuring hoop strain;
- two pairs near the front bulkhead weld (band B/10) — measuring longitudinal strain.

[4] *When the radius of curvature of a shell is large (greater than a factor of ten) in relation to the thickness of the shell, as it is with the tankers, the shell is often referred to as a membrane. If it is exposed to internal pressure alone, as in a pressure vessel, then the stress in the membrane can be considered to be uniform across the thickness. All the stress is parallel to the membrane wall, and bending stress is insignificant. Although the tanker shell is a membrane in the sense that the radius of curvature of the tanker shell is much greater than ten times the wall thickness, because it is being exposed to an impact event rather than a uniform (or uniformly varying) pressure that it would experience during service, the stresses across the wall thickness are not uniform. However the* ***average*** *membrane strain, and the* ***average*** *bending strain, can be obtained from the strain gauge pairs.*

Compartment 4b (Figures 13a and 13c)

- two pairs near the rear bulkhead weld (band H/10) — measuring longitudinal strain;
- one pair near the midpoint of the compartment — measuring hoop strain;

End Bulkheads (Figures 14a, 14b and 14c)

- outer gauges near the bulkhead weld at midpoint – measuring radial strain

All gauges were connected as quarter-bridge, to bridge completion modules on the logger with a three-wire compensation configuration. Gauges were calibrated with shunt resistors at a local junction box before the test. In total there were twenty four (24) strain gauges on each tanker. Table 4 shows the strain gauge numbering system.

Table 4 Strain gauge numbering system

Compartment 1b	**Compartment 4b**	**Rear Bulkhead**	**Front Bulkhead**
1a to 6a – outer skin	7a to 9a – outer skin	13a to 15a – outer skin	10a to 12a – outer skin
1b to 6b – inner skin	7b to 9b – inner skin		
hoop (circumferential) strain gauges – 3a and 3b	hoop (circumferential) strain gauges – 7a and 7b	Radial strain	Strain
longitudinal strain gauges – 1a and 1b, 2a and 2b, 4a and 4b, 5a and 5b, 6a and 6b	longitudinal strain gauges – 8a and 8b, 9a and 9b		

All gauges were installed on the impact side. The longitudinal line passing through the centre of the side gauges was level with the top of the tank supports (i.e. the saddle): this is the 8 o'clock position shown in Figures 17 and 18 (approximately 29^{o} below the horizontal centreline of the tanker).

Figures 13a and 14a give schematics of the strain gauge locations (Figure 19 gives the overall instrumentation position schematic). Figures 13b, 13c, 14b and 14c are photos of the strain gauge locations.

Strain gauge locations in compartments 1b and 4b followed the same approach as previous topple tests.

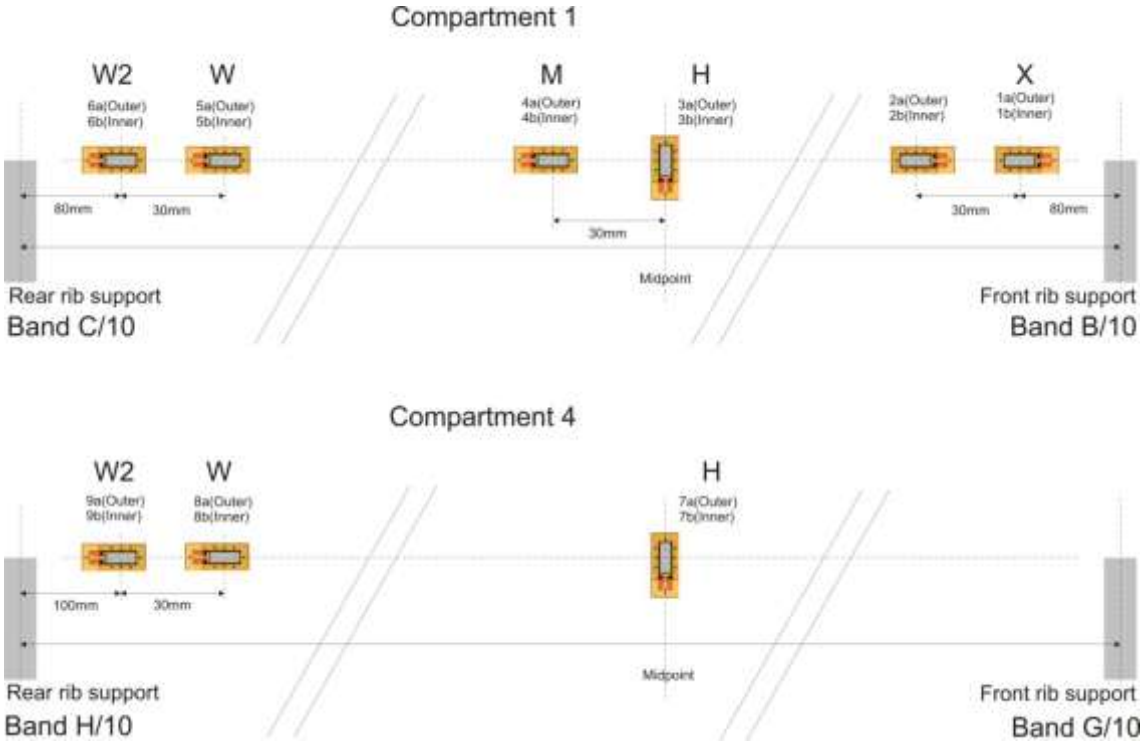

Figure 13a Strain gauge locations - side (not to scale)

Figure 13b Strain gauge locations – compartment 1b

Left to right W2 W M H X

Figure 13c Strain gauge locations – compartment 4b

Left to right W2 W H

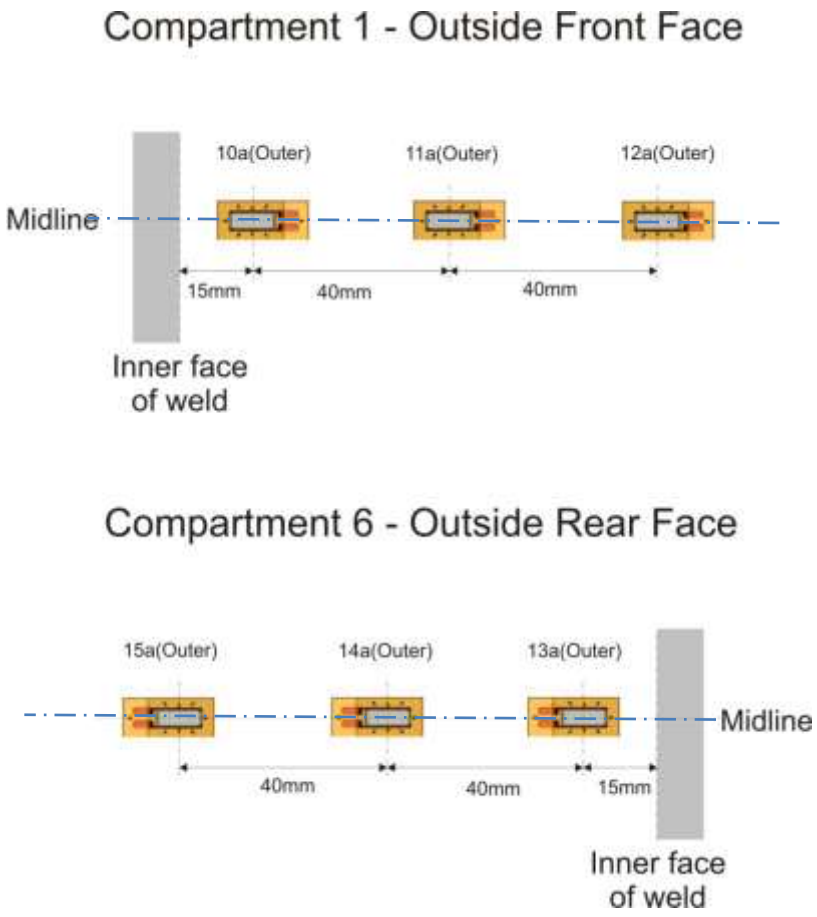

Figure 14a Strain gauge locations – ends (not to scale)

Figure 14b Strain gauge locations – front (compartment 1a)
Left to right 10a 11a 12a

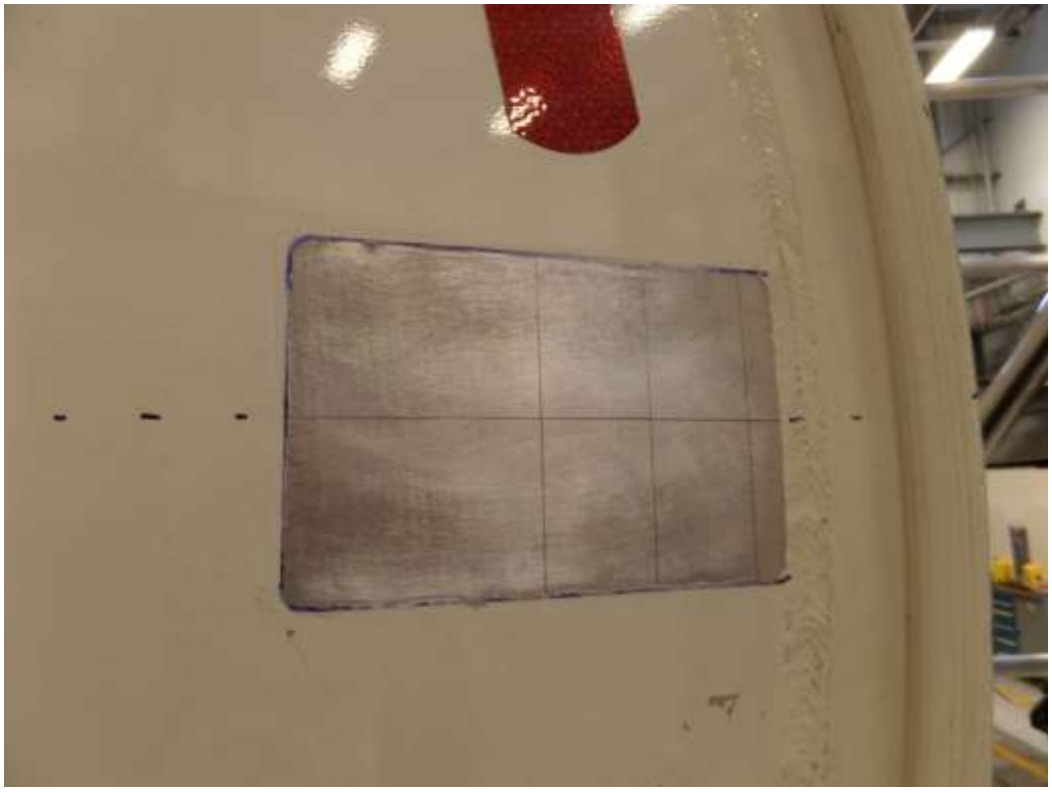

Figure 14c Strain gauge locations – rear (compartment 6)
Left to right 15a 14a 13a

Figure 15 shows a typical variation in strain that may occur across the thickness of the tanker shell during the test.

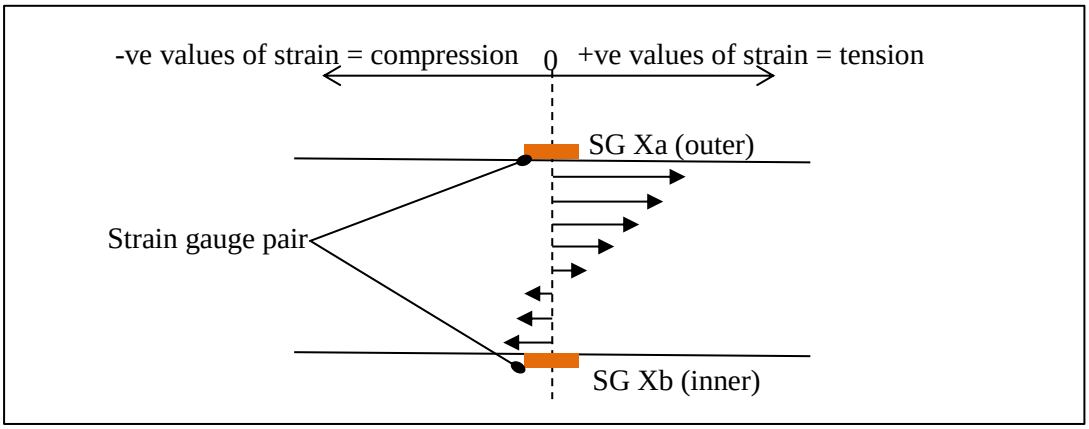

SG = strain gauge

Figure 15 Strain across the thickness of the tanker shell

For *membrane strain* the time-varying strains measured in each pair are added, then divided by two to obtain the *average membrane strain*

$$\frac{Xa_{(t)}+Xb_{(t)}}{2} \qquad (1)$$

Where

$Xa_{(t)}$ is the time varying strain measured by the *outer* strain gauge X

$Xb_{(t)}$ is the time varying strain measured by the *inner* strain gauge X

This is the average strain parallel to the tanker shell.

For *bending strain*, the time-varying strain values of each pair are subtracted, then divided by two, which gives the *average bending strain*

$$\frac{Xa_{(t)}-Xb_{(t)}}{2} \qquad (2)$$

If the membrane strain is positive, then the average state at the measuring point is in tension; if the membrane strain is negative, then the average state at the measuring point is in compression.

If the bending strain is positive, then the tanker shell is flexing outwards (hogging); if the bending strain is negative, then the tanker shell is flexing inwards (sagging).

The example in Figure 15 shows the tanker shell mainly in bending, but with an average tensile loading. Therefore, the *average bending strain* will be greater than the *average membrane strain* as the inner surface of the shell has gone into compression. As the analysis accounts for the direction as well as magnitude of the strain, the difference between the two measured values will be greater than the sum of the two values, so equation (2) will give a greater value than equation (1).

8.1.2 Pressure transducers

Fourteen pressure transducers, seven in each compartment, were placed at approximately 6, 7, 8, 9, 10, 11, 12 o'clock positions on the impact side; the transducers were positioned at the mid-point between the front and rear bulkheads in each compartment. The type of transducer used was a 34.5 bar (with 138 bar over-range) Omega PX709GW-500SGV. The pressure transducers are of the sealed-gauge type, which means the readings are relative to a 1 bar internal reference. Each was supported by two cable conduit connectors that were glued to the inside surface of the tanker using waterproof epoxy glue. All pressure transducers were installed with their longitudinal axes horizontal. The outputs were connected to transducer input modules on the Graphtec data loggers. Figure 16 shows a pressure transducer in position.

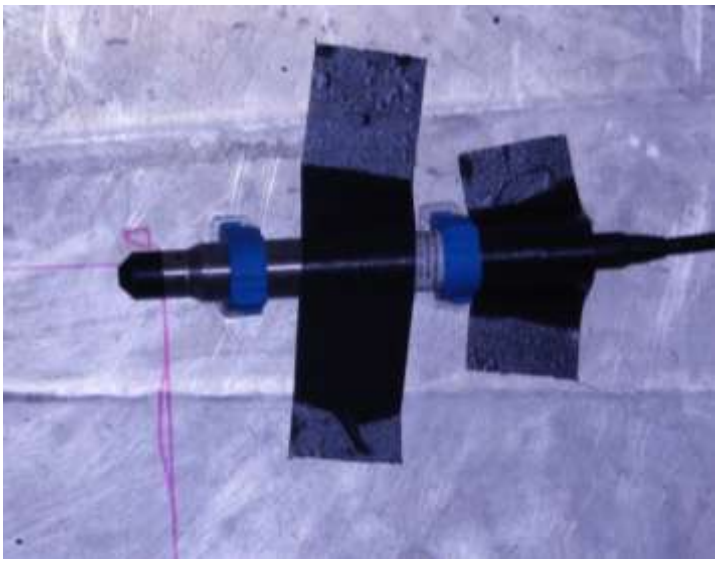

FES 140601_02

Figure 16 Pressure transducer fitted to the inside of a tanker

Figures 17 and 18 give the positions of the pressure transducers in compartments 1b and 4b, respectively.

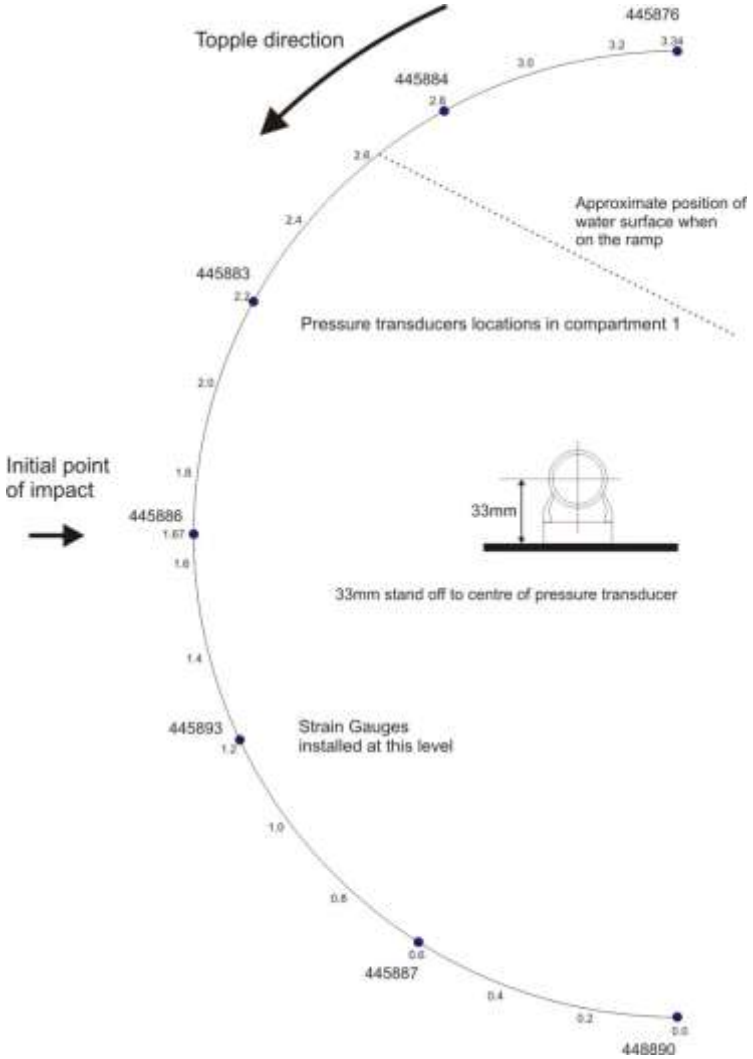

Numbers on the circumference are distances in metres around the tanker surface from 'bottom dead centre' (BDC). The numbers beginning 44xxxx are the serial numbers of the pressure transducers

Figure 17 Pressure transducer locations (tanker in the upright position) – compartment 1b, offside, viewed from the front

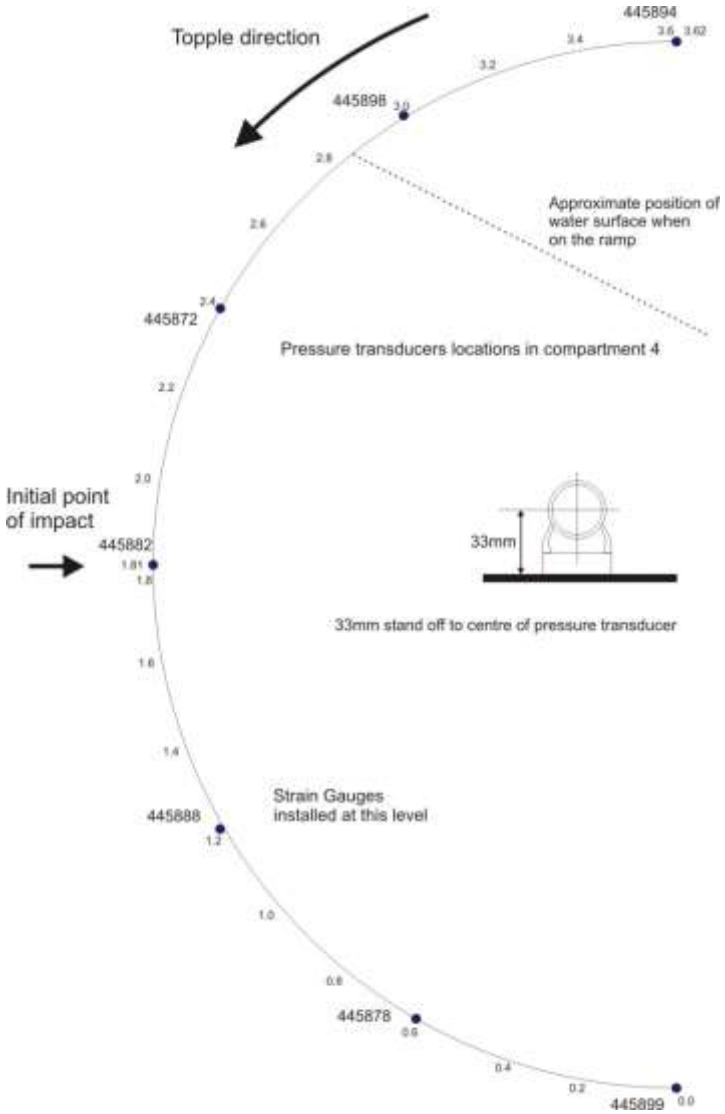

Numbers on the circumference are distances in metres (from BDC). The numbers beginning 44xxxx are the serial numbers of the pressure transducers.

Figure 18 Pressure transducer locations (tanker in the upright position) – compartment 4b, offside, viewed from the front

In Figures 17 and 18, a dotted line has been added to show the approximate position of the water surface when the tanker is resting on the 27° ramps (i.e. tilted over to the left in this figure so the line is horizontal). When placed on the ramp, the depth between the water surface and the lower-most transducers (445888, 445878 and 445899 in Figure 18) is about 1.2 m; so the static pressure acting on these gauges above atmospheric pressure, and prior to winching, will be

$$\text{Static pressure} = \rho g h \text{ N/m}^2$$

Where ρ = density of water = 1,000 kg/m^3
g = acceleration due to gravity = 9.81 m/s^2
h = head of water = 1.2 m (approx.)

So static pressure = 1,000 x 9.81 x 1.2 = 11,772 N/m^2 which is approximately 12,000 N/m^2
or in bar
Static pressure = 12,000 x 10^{-5} bar = 0.12 bar (1.74 psi)

As the tanker is toppling, the head of water will increase on the transducers fitted at higher positions on the tanker body as they become submerged. Also the head of water above the transducers at the greatest depth prior to toppling will also change slightly. This will cause small increases and decreases in static pressure (depending in the gauge location) as the tanker starts to rotate. *However*, in addition to these effects, as the tanker rotates, the water and the pressure transducers are moving together. As the tanker starts to topple, the water will exert less and less pressure on the transducers until, at the point of free fall, the water exerts no additional pressure on the transducers. So at the moment before the tanker impacts, the transducers can be assumed to be measuring atmospheric pressure alone (i.e. zero-gauge pressure).

Strain gauge positions in compartments 1b and 4b followed the same approach as previous topple tests.

8.1.3 Accelerometers

Two single axis accelerometer blocks were located at the centre of the front *and* rear bulkheads of the tanker. The accelerometers at the front and rear were arranged as follows:

- One +/- 50g in the y-axis (vertical axis at impact).

The accelerometer types were *Measurement Specialities* 4000A-050-060, connected to transducer input modules on the Graphtec loggers.

8.1.4 Summary of the Locations of all the Instrumentation

Figure 19 shows the approximate positions of all the pressure transducers, accelerometers, strain gauges and measurement grids.

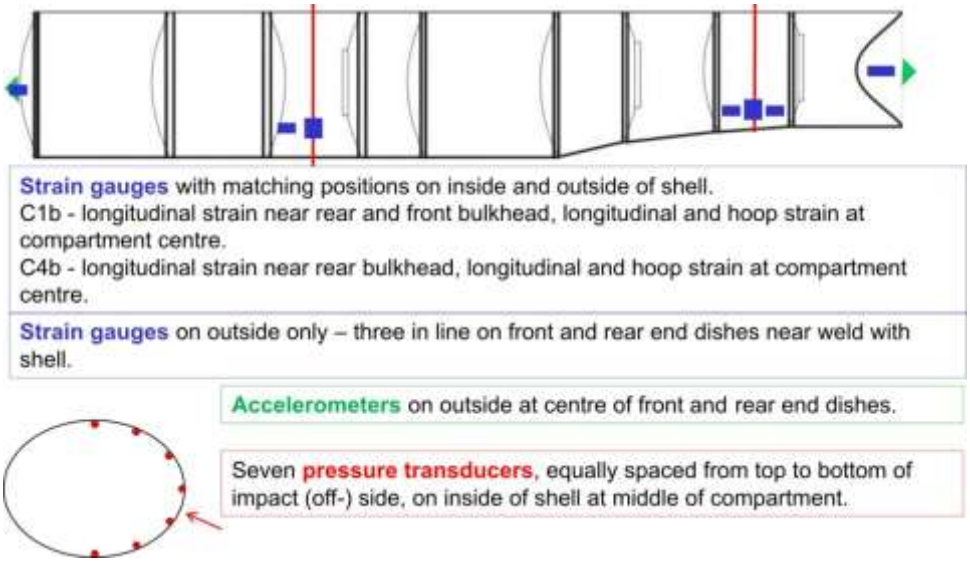

Figure 19 Location of instrumentation

8.2 VIDEO METHODS

Fifteen video cameras ranging from standard speed (25 frames per second) to high speed (1,000 frames per second) were used to record the tests, together with time lapse and stills cameras.

The high speed video images were analysed to obtain the impact velocity and deceleration during impact at the front and rear of the tanker. Targets were placed at each end of the tanker that could be seen on the high speed video. The distance between each target was known; this provided a calibration scale for the high speed video images. The movement of these targets was followed through each consecutive frame of the high speed video. The distance travelled by the targets was divided by the time taken: this gave the linear velocity.

The rotational velocity was then calculated from this using the equation

$$\omega = \frac{v}{r} \text{ rads/sec} \qquad (3)$$

where

v is the impact velocity obtained from the high speed video (m/s)
r is the distance from the pivot point to the target (m)

A frame from the high speed video, showing the targets at the front end of the tanker, is shown in Figure 20.

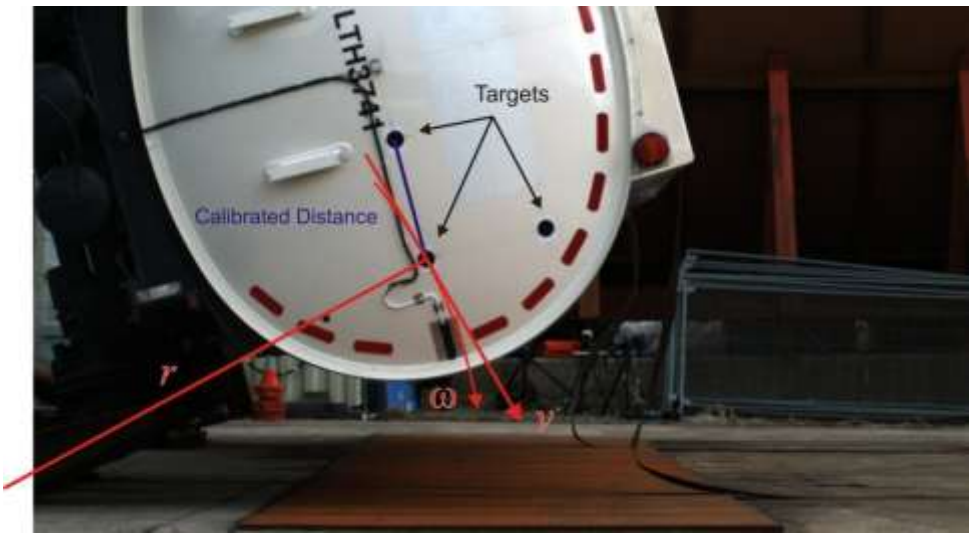

Figure 20 Frame from the high speed video during the topple, showing the targets used to obtain the impact velocity

9 RESULTS AND DISCUSSION

All raw data was analysed to calibrate the transducer outputs, for example voltages, into the relevant scientific units (pressure, acceleration, strain). The measurement and analysis approaches were the same or similar to those used in previous tests.

9.1 IMPACT BEHAVIOUR

The overall impact duration was a few seconds for the test, with most deformation occurring in the first 100 ms. Analysis of high speed video (Section 9.3) gave impact speeds of 4.8 m/s (1.94 rad/s) at the front and 4.1 m/s (1.97 rad/s) at the rear of the tanker, and the rear hitting the ground first, approximately 8 ms before front of the tanker. After first impact, the tanker slid forward, significantly more so at the rear, and simultaneously rolled forward until the comb hit the ground, then rolled back and slid back to near the initial impact position before coming to rest on its side, at approximately 90 degrees to when it is on its wheels.

9.2 ACCELERATION MEASUREMENTS

The accelerometer (RY50 in Figures 21 and 22) signals showed significant ringing, causing the accelerometers to overload and the positive and negative peaks of the signal were 'cropped'. Therefore, the resilient strip between the mounting block and the tanker, to act as a mechanical filter, was allowing some high frequency vibration (ringing) to affect the measurement. Filtering the signal through a low pass filter may not have provided reliable data as some digital filters cannot cope with cropped peaks and troughs effectively. So the data was simply smoothed to reduce the effect of the rapid changes in signal amplitude due to the vibration: for these measurements a 799-point moving average was selected. Although carrying out a moving point average on 'clipped' data can introduce some errors to the average value, as the signal had not been clipped too much, the measurements can still be used for comparative purposes as explained by the second footnote in the next paragraph. These results were then compared with the acceleration calculated from analysing the high speed video (HSV).

The results are shown in Figure 21 for the y-axis accelerometer[5] and high speed video at the front of the tanker, and Figure 22 for the y-axis accelerometer and high speed video at the rear of the tanker. The smoothed data from the accelerometers and high speed video showed good agreement with each other up to the maximum deceleration, given the cropped accelerometer data[6]. After this, the tanker movement, in response to the impact, would have included some rotation about a longitudinal axis within the tanker body. This probably explains why there are differences between the two measurements as the accelerometer and the targets are not at exactly the same position on the tanker body.

[5] *i.e. the accelerometer that is in the vertical position at impact*

[6] *Figures 21 and 22 show the 'raw' acceleration signal has been clipped more on the negative peaks than the positive peaks; so the moving point averaging process is ignoring more data points on the negative side than the positive side. This means the average values are slightly weighted towards the positive (i.e. the calculated average is higher than the true average). However, as these data have not been 'clipped' too much, and as a large number of points have been used in the moving point average, the missing data points do not have a significant effect on increasing the average value.*

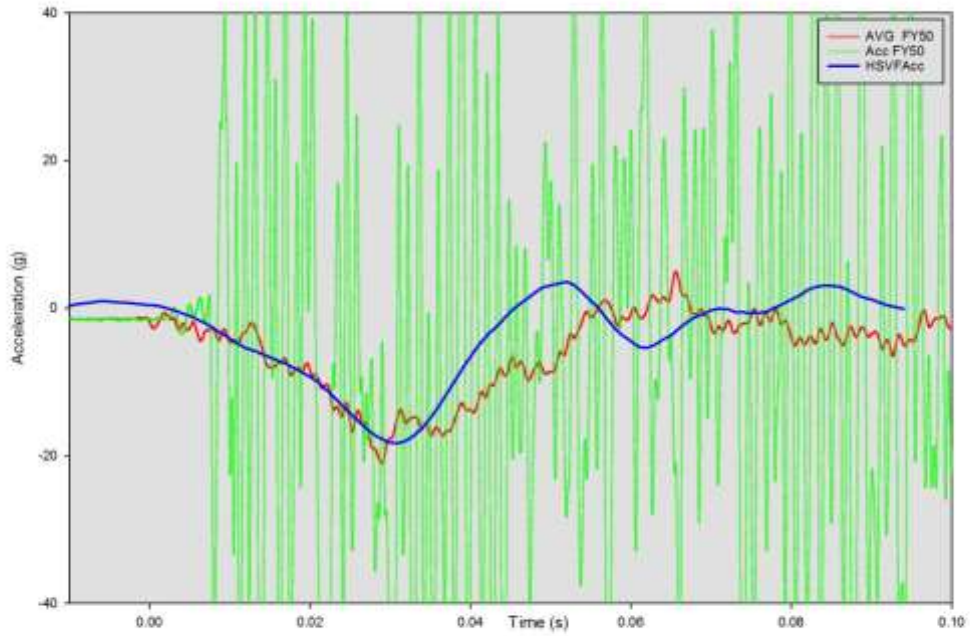

Figure 21 Acceleration measurements; accelerometer (RY50) and HSV analysis; Front

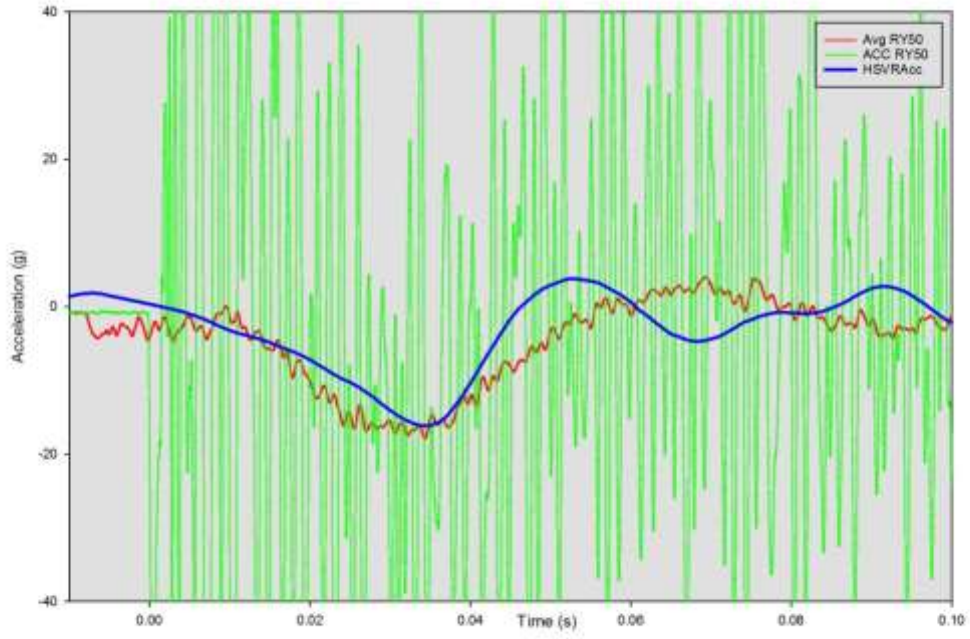

Figure 22 Acceleration measurements; accelerometer (RY50) and HSV analysis; Rear

9.3 IMPACT VELOCITY MEASUREMENTS

The impact velocities obtained from analysing the high speed video were as follows:

- 4.8 m/s at the front of the tanker; and
- 4.1 m/s at the back of the tanker

The radius (*r*) (see Figure 20) at the front of the tanker is 2.48 m, and 2.08 m at the rear. Using equation (3) in Section 8.2

$\omega = \frac{v}{r}$ rads/sec

The rotational velocity at the front was $\omega = \frac{4.8}{2.48} = 1.94$ rads/sec

The rotational velocity at the rear was $\omega = \frac{4.1}{2.08} = 1.97$ rads/sec.

9.4 SUMMARY DAMAGE ASSESSMENT

9.4.1 Deformation of the tanker

Figure 23 shows six images from the high speed video for each end of the tanker in 20 ms steps from the moment of impact to 100 ms later.

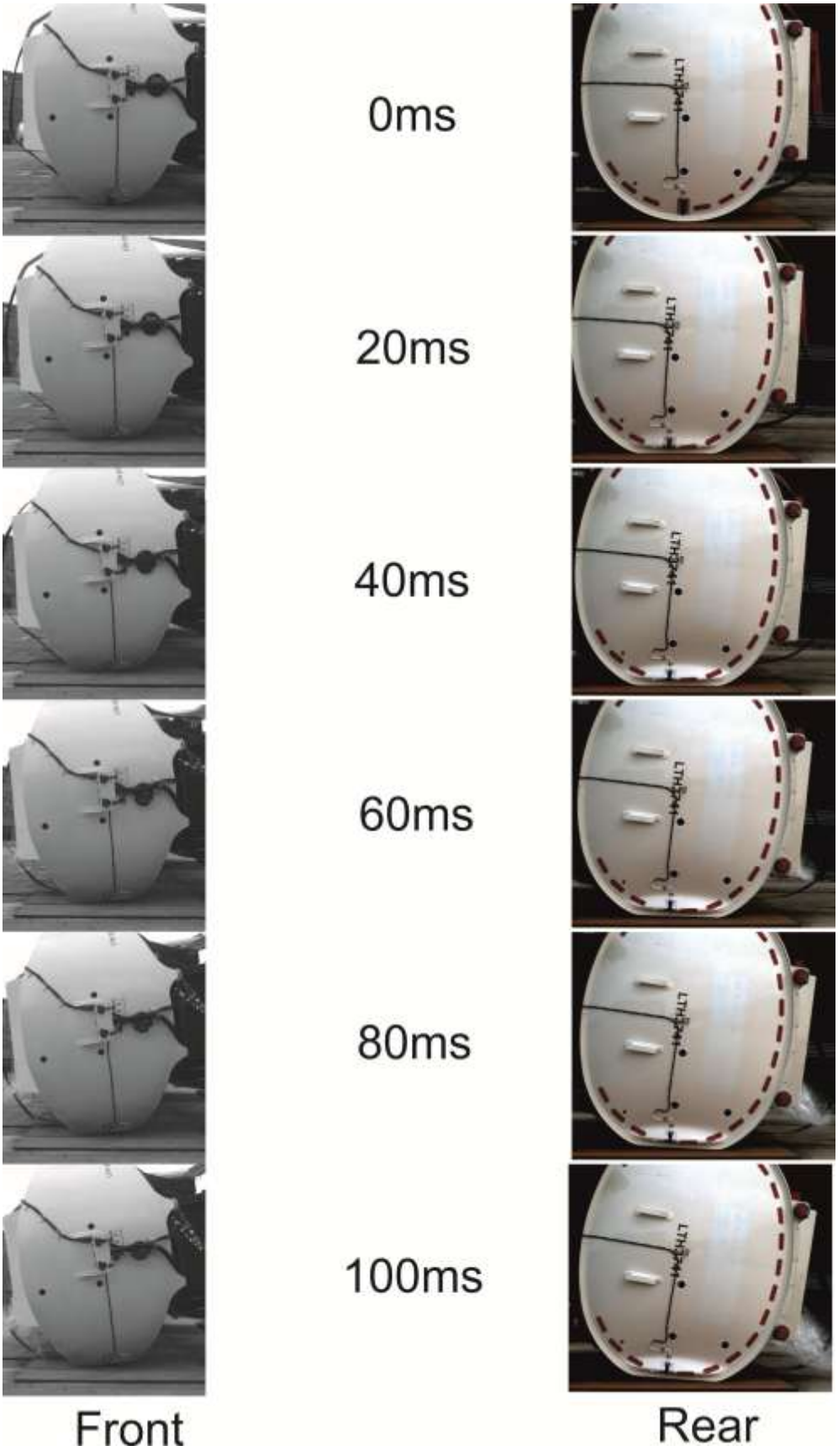

Figure 23 High speed video images during impact

9.4.2 External leaks and internal integrity of compartments

During the initial impact some water was lost through the emergency pressure relief valves (EPRVs). Examination of the videos and stills photography found that the amount of water lost in this way was minimal. Some of the spray from the top of the tanker was from "standing" water on the top of the tanker rather than from the EPRVs.

Immediately after the test, no external leaks could be seen, although there were slow drips from some pressure relief valves on the tanker's manlids. As the EPRVs passed their subsequent lift/reseal test this may not have been a leak through the valves, but rather standing water or water that was lost from the valves during the initial impact.

When the water was pumped out of each compartment, the following observations were made (see Figure 8 in Section 6.1 for compartment numbering, compartment 1 at front to compartment 6 at rear):

- No external leaks were observed.
- When compartment 1 was emptied, the level did not reduce in compartment 2. Conclusion: there was no significant leak at the bulkhead between compartments 1 and 2.
- When compartment 2 was emptied, the level did not reduce in compartment 3. Conclusion: there was no significant leak at the bulkhead between compartments 2 and 3.
- When compartment 3 was emptied, the level did not reduce in compartment 4. Conclusion: there was no significant leak at the bulkhead between compartments 3 and 4.
- When compartment 4 was emptied, the level did not reduce in compartment 5. Conclusion: there was no significant leak at the bulkhead between compartments 4 and 5.
- When compartment 5 was emptied, the level did not reduce in compartment 6. Conclusion: there was no significant leak at the bulkhead between compartments 5 and 6.

After the tanker had been lifted back onto its wheels, the tanker inspection contractor tested the tanker on 09th April 2015. The tanker passed the hydraulic test (392 mbar), leakproofness test (200 mbar), EPRV lift/reseal test (250 mbar) and Vapour tightness/PV Vent Valve test. This meant that, in terms of measured integrity, the tanker was unaffected by the topple test.

Figures 24 and 25 show the general deformation of the tanker after righting. The impact area flattened along the length of the tanker; the flat length is the distance between the lower and upper sides of the deformation, as shown in Figure 24.

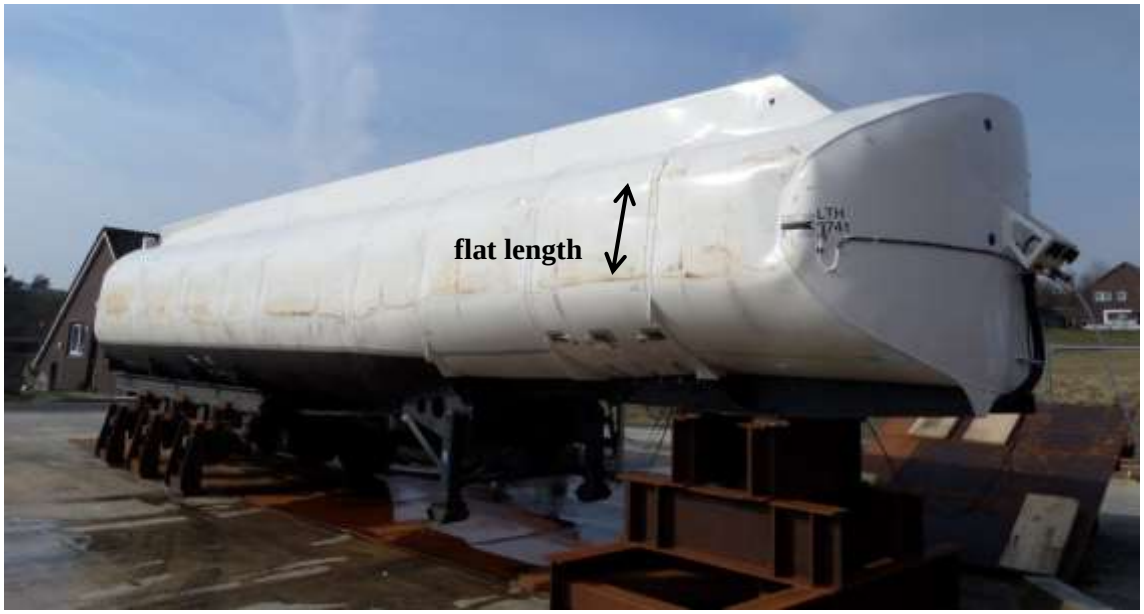

FES150501_24

Figure 24 Side view of damage to tanker after righting

FES150501_25a/b

Figure 25 End views of damage to tanker after righting

The front and rear profiles of the tanker, obtained from laser scans after the test while the tanker was still on its side, are given in Figure 26. Before the test, the approximate width of the tanker at the front was 2,537 mm and the width at the rear was 2,545 mm. After the test the width at the front was 2,476 mm and the width at the rear was 2,455 mm. Therefore, the impact caused permanent deformation of approximately 61 mm at the front and 90 mm at the rear.

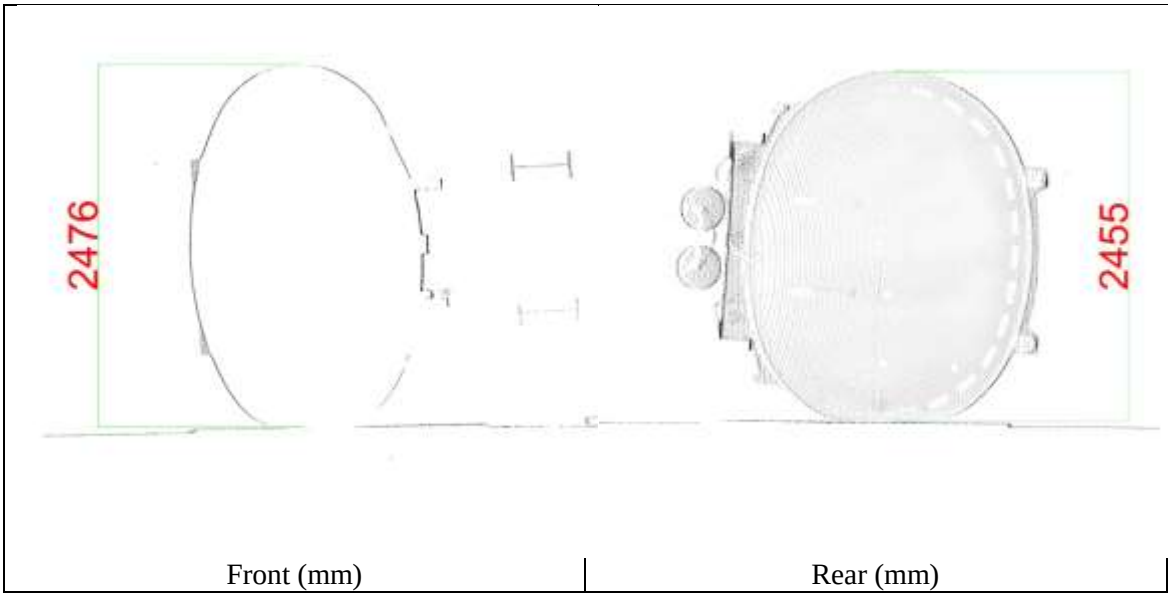

Figure 26 Deformation of tanker from laser scans after test

9.4.3 Length of the damaged section of the shell

The flat lengths were measured at each band (using the laser scan data as for previous tests). Figure 27 gives these values.

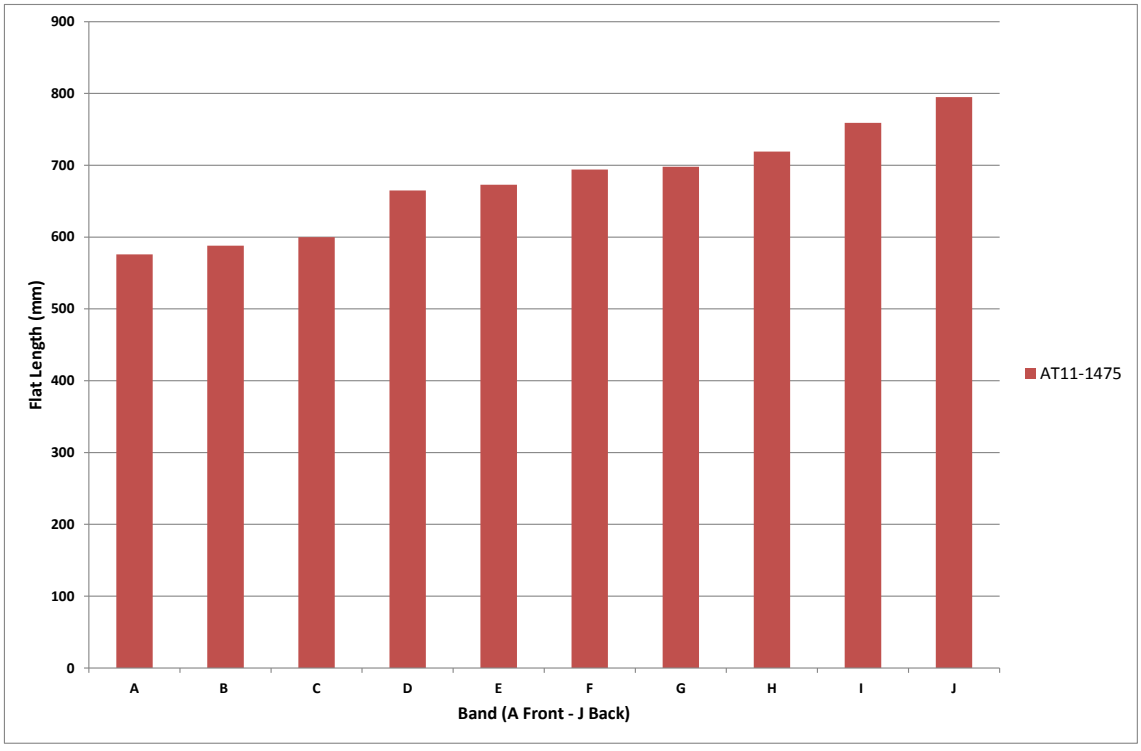

Figure 27 Flat lengths measured at the bands

9.4.4 Visual inspection of exterior damage

Following the topple test, an examination was made of the exterior of the tanker on the side that had come into contact with the ground. This was undertaken in order to identify areas where significant damage had occurred and which may have been the locations where cracks or similar defects could have been generated by the impact of the tanker. Six locations in total were identified for examination which, although not including all of the areas of damage on the tanker, did represent the worst of them. The areas were identified from the degree of surface deformation and cracking of the paintwork. Four areas were associated with extruded band weld seams and two areas were also chosen where significant mechanical abrasion of the shell had occurred. Figure 28 shows the tanker post-testing, with the locations of the six areas identified by ellipses. These were:

- The regions of plastic deformation at the rear end dish and front end of the tanker, identifications Rear 1 and A.
- A smaller region of mechanical deformation towards the front end of the tanker at extruded band C, centred 1,050mm above grey reflective strip, identification C in Figure 28 (labelled D1 in Figure 29b).
- Two areas of mechanical scuffing and scoring of the plate, identification G, and 6. The centre of G is 300mm above the horizontal grey reflective strip, and the centre of 6 is 1,100 mm above the same strip.
- A representative area of weld at extruded band I, 700 mm above the reflective strip.

Figures 29a to 29g show images of the areas prior to paint removal.

HSL used the dye penetrant non-destructive testing technique to determine whether cracking had occurred. The paint layer was removed from the skin/shell in each of the six locations to reveal the underlying metal surface. A proprietary paint remover was used, and the preparation method was carried out in accordance with BS EN ISO 3452-1:2013, "Non-destructive testing – Penetrant testing, Part 1: General principles".

Figures 29h and 29i show the surface quality at locations at the rear dish and on compartment 6, following stripping.

Following paint stripping, and again in compliance with BS EN ISO 3452, the dye penetrant technique was carried out on the six prepared areas. Figures 29j to 29p show the resultant surfaces. It was evident that four out of the six areas showed no indications of cracking. Under initial inspection, the locations at either end of the tanker, where significant crumpling had occurred, appeared to have small indications at the toe of the weld bead where bleed-through of dye appeared to reveal an underlying defect. However, closer examination of these areas indicated that the source of the dye appeared to have been sharp depressions/seams in the weld toe rather than cracking.

Overall, the non-destructive testing of the areas of most significant damage to the tanker, following the topple test, failed to reveal any clear indications of cracking either along weld seams or on the general tanker shell surface. It must be noted that the testing was carried out on-site and although care was taken to ensure that the technique was carried out as effectively as the conditions would permit, this was not as rigorous an inspection as could be achieved under laboratory conditions. It is possible that under these more favourable conditions small defects may have been detected. The author (Liz Geary) is confident however, that gross cracking was not present.

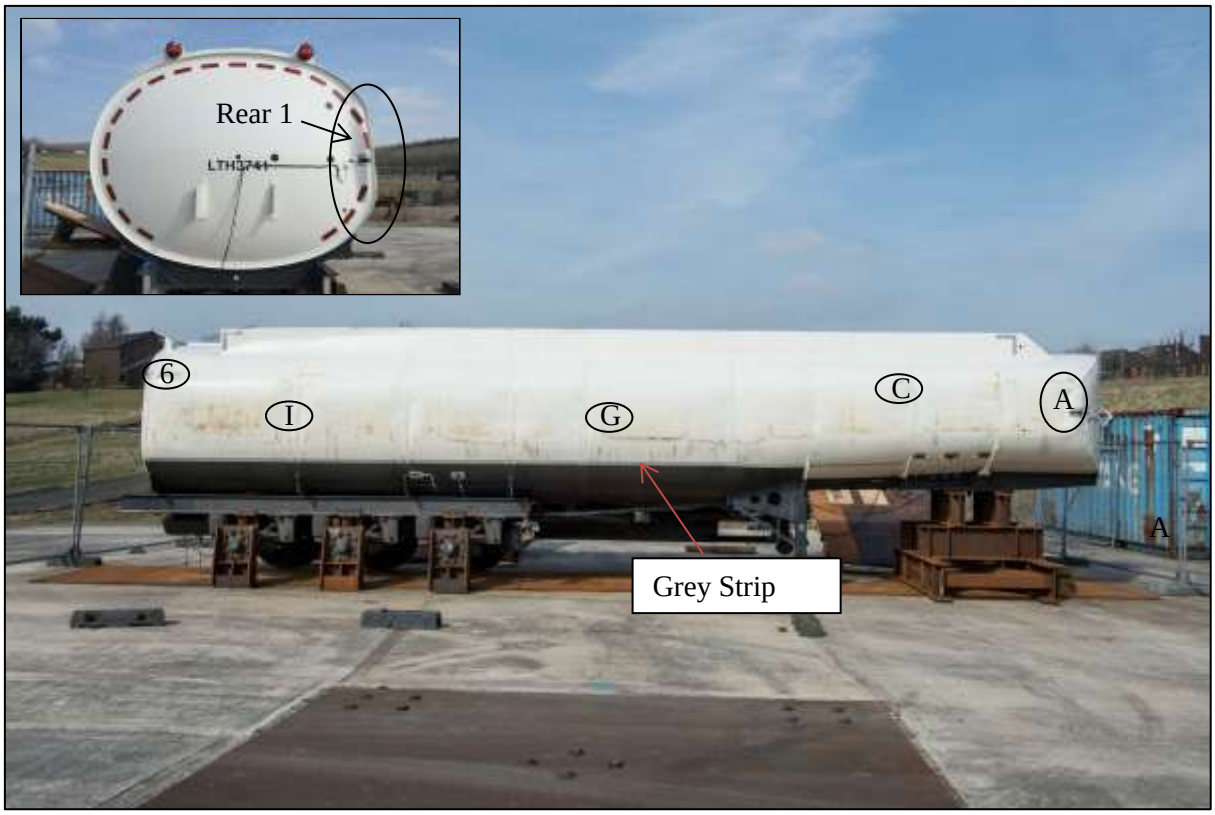

1503050_422

Figure 28. Image of tanker following topple test. Ellipses indicate locations selected for ND testing. Inset shows rear of tanker**.**

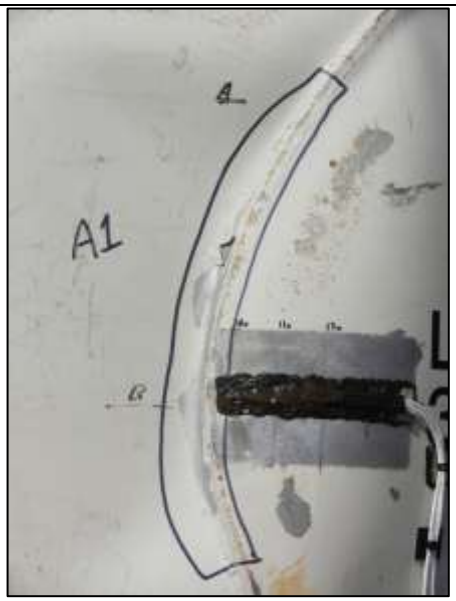

DSCN3438

Figure 29a Deformation zone at front of tanker at the junction of compartment A with front bulkhead.

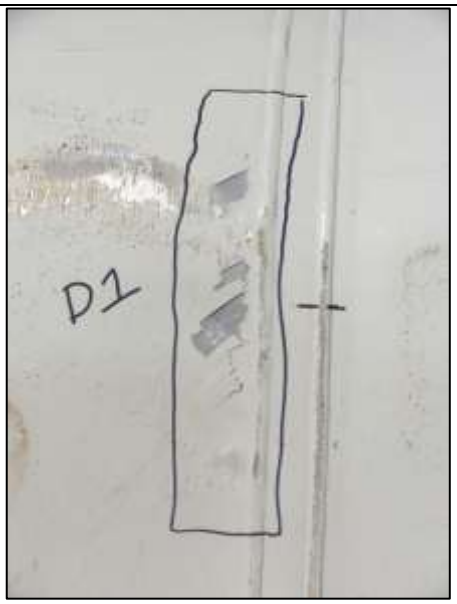

DSCN3437

Figure 29b Deformation in shell at extruded band C (not D as indicated).

DSCN3436

Figure 29c Mechanical damage at extruded band G. (image)

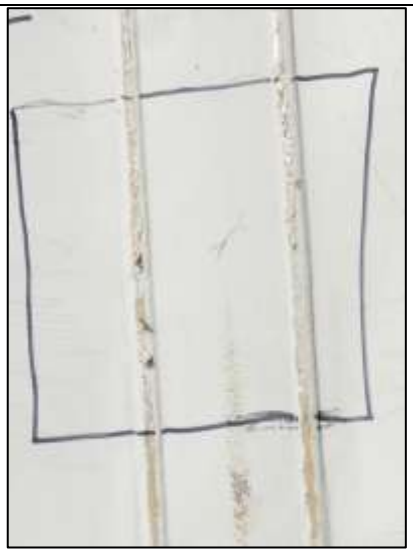

DSCN3434crop

Figure 29d Mechanical abrasion on weld beads at extruded band I.

(DSCN)3433crop

Figure 29e Mechanical abrasion on rear compartment, compartment 6, of shell of tanker.

DSCN 3430

Figure 29f Cracking in paintwork at 2'o clock position along weld seam in rear dish of tanker.

DSCN 3431

Figure 29g Cracking in paintwork at weld seam in rear dish of tanker at 4'o clock position.

DSCN3444

Figure 29h Weld seam at rear dish of tanker following paint stripping.

DSCN3442

Figure 29i Region of mechanical abrasion on surface of compartment 6 following paint stripping.

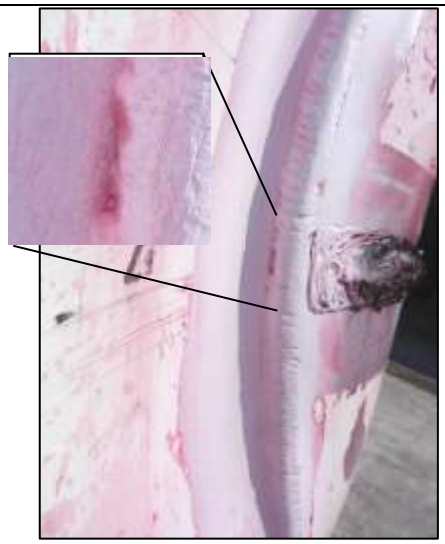

DSCN3456) (inset image DSCN3456 crop)

Figure 29j Area of deformation at front of tanker. Suggestion of an indication on weld seam toe, with close up in inset.

DSCN3478

Figure 29k Area of deformation to the rear side and weld seam at extruded band C.

DSCN3460

Figure 29l Region of mechanical abrasion at G.

DSCN3459

Figure 29m Front facing weld seam at location G.

DSCN3466

Figure 29n Region of mechanical abrasion on surface of compartment 6 .

DSCN3468

Figure 29o Weld seam in crumple zone at rear of tanker, Rear 1.

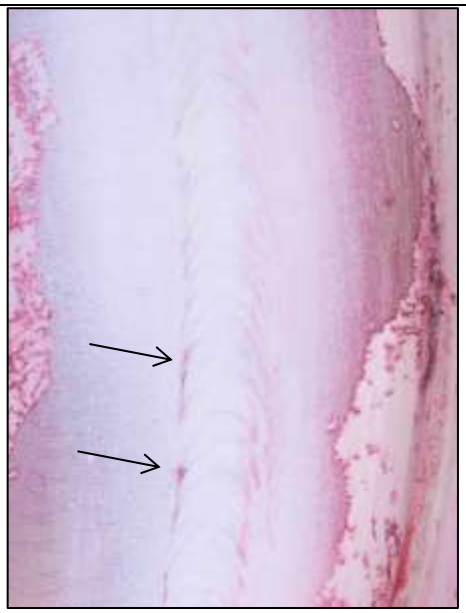

DSCN3471

Figure 29p Weld seam in crumple zone at rear of tanker. Close inspection of indications (arrows) did not reveal cracking.

9.5 STRAIN GAUGE AND PRESSURE TRANSDUCER DATA - PRESENTATION

All strain gauge and pressure transducer measurements have been averaged using a 19-point moving average through the data samples. This is similar to the approach used for previous tests. Also, the zero-time point was the moment that the *first* gauge or transducer started to respond to the impact. The rear accelerometer responded about 8 ms before the front accelerometer, the strain gauges in compartments responded about 4 ms to 8 ms after the rear accelerometer, and the pressure transducers responded about 4 ms to 8 ms after the rear accelerometer. This was due to the rear of the tanker impacting the pad slightly before the front of the tanker.

9.6 STRAIN GAUGE MEASUREMENTS

Strain is measured in micro strain ($\mu\varepsilon$ which is extension/original length multiplied by 10^6).

The data traces for the test are given in Appendix 4. Key features of the data are as follows.

Figure A4.1 shows the measurements for all the strain gauges in both compartments:
The time-base is referenced to zero at the initial impact. The impact event is relatively short (about 0.1 seconds). The non-zero values of strain after this are caused by:

- changes in load on the tanker wall due to water displacement in the tanker (sloshing);
- plastic deformation in the tanker wall; and
- the rocking movement of the tanker as it settled after impact.

Figure A4.2 shows the same measurement on a much shorter time-base to focus on the initial impact event. Strain 10-15 outer (lower rhs) are the gauges on the end dishes. The gauges on the front dish (10, 11, 12) were all damaged during the impact so that their outputs became unreliable. The outputs from these gauges start to show a response around 8 ms after the gauges on the rear, which correspond to the rear of the tanker impacting before the front. The two gauges on the rear dish nearest the weld edge (13, 14) were also damaged during the impact so that their outputs became unreliable. Gauge 15, furthest from the weld edge on the rear dish, continued to operate during the impact and variations in strain associated with the movement of the water inside the compartment and the rocking of the tanker are seen in the gauge 15 trace for Strain 10-15 outer (lower rhs) in Figure A4.1.

The strain gauges pairs mounted at compartment 1b and 4b have been used to obtain the *average membrane strain* and the *average bending strain.* These values have been obtained from equations (1) and (2) in Section 8.1.1.

Figure A4.3 shows SG pair 3 (location H), pair 4 (location M) and pair 6 (location W2) from compartment 1.

Figure A4.4 shows SG pair 1 (location X) from compartment 1.

Figure A4.5 shows SG pair 7 (location H) and pair 9 (location W2) for compartment 4.

The strain gauge data were broadly consistent with expectations based on the impact events, tanker structural design and experience from previous tests. In general, strains near the welds were higher than those at the compartment centre, with some yielding and plastic deformation observed in the strain behaviour near the welds. During impact, high speed video captured free travelling flexural waves propagating away from the impact line around the circumference of the tanker. Such waves should result in more pronounced ripples in the circumferential strain than the longitudinal strain at the centre of the compartment, and there was some evidence of this in the data.

Since there was no modelling of the tanker impact, detailed consideration of the strain gauge data was not within the scope of the work.

9.7 PRESSURE MEASUREMENTS

All pressure measurements were *gauge* measurements; so measurements close to zero were measuring the ambient air pressure. As mentioned in Section 8.1.2, as the tanker begins to topple the hydrostatic pressure at each gauge reduces until the moment of impact - by this time *all* transducers were measuring less than 0.05 bar (0.725 psi). So, assuming the transducers were measuring atmospheric pressure at the point of impact is reasonable.

The data traces for the test are given in Appendix 4. Key features of the data are as follows.

Figure A4.6 shows the measurements from the pressure transducers for compartments 1b and 4b throughout the test. With the tanker in the upright position, HSL have ordered the transducer numbers in the graph legends from the transducer at the 6 o'clock position at the top, to the transducer at the 12 o'clock position at the bottom. The pressure changes directly resulting from the impact occurred in a very short time period immediately after the impact.

Figure A4.7 shows the same measurements over a much shorter time period after the impact. The highest pressures were measured for the transducers closest to the impact point (around the 9 o'clock position) as expected. The transducers at the 6 o'clock and 12 o'clock positions gave little deviation from ambient pressure. The fact that the curves were showing some frequency modulation (sinusoidal short waves being carried on a longer, low frequency wave) suggests that many of the transducers were measuring acoustic waves as well as changes in water pressure.

The maximum pressure was measured on the transducers in the 9 o'clock position (transducer 445886 for compartment 1b, and 445882 for compartment 4b). These transducers measured transient peaks around 10 bar at the moment of impact. About 0.04 seconds after impact, all transducers were measuring pressures below 2 bar, and about 0.06 seconds after impact (compartment 1) and 0.07 seconds after impact (compartment 4) all transducers were reading close to ambient pressure.

The pressure measurements were broadly consistent with expectations based on the impact events, tanker structural design and experience from previous tests. Since there was no modelling of the tanker impact, detailed consideration of the pressure measurements was not within the scope of the work.

10 METALLOGRAPHIC AND ANALYTICAL ASSESSMENT OF AT11-1475

After Section 10.1 which describes the HSL sampling of the tanker, the remainder of this section contains direct quotes (with small modifications or additional text which do not change the findings) from TWI report 24000/13/15 "Department for Transport Technical Assessment of Petroleum Tankers: Metallographic and Analytical Assessment of AT11-1475" dated 04 September 2015 [6], which is given in full in Appendix 5.

10.1 SAMPLES TAKEN

Following the incident and after consultation with TWI and DfT, four sample sections of the tanker were cut from the barrel to be sent to TWI for detailed radiography and analysis. Figure 30 shows the position and approximate dimensions of the samples removed from Bands A and J. The red lines in the top two photographs show where the cuts were made at the end bulkheads, and the lower two figures show the depths of the cuts along the body of the tanker.

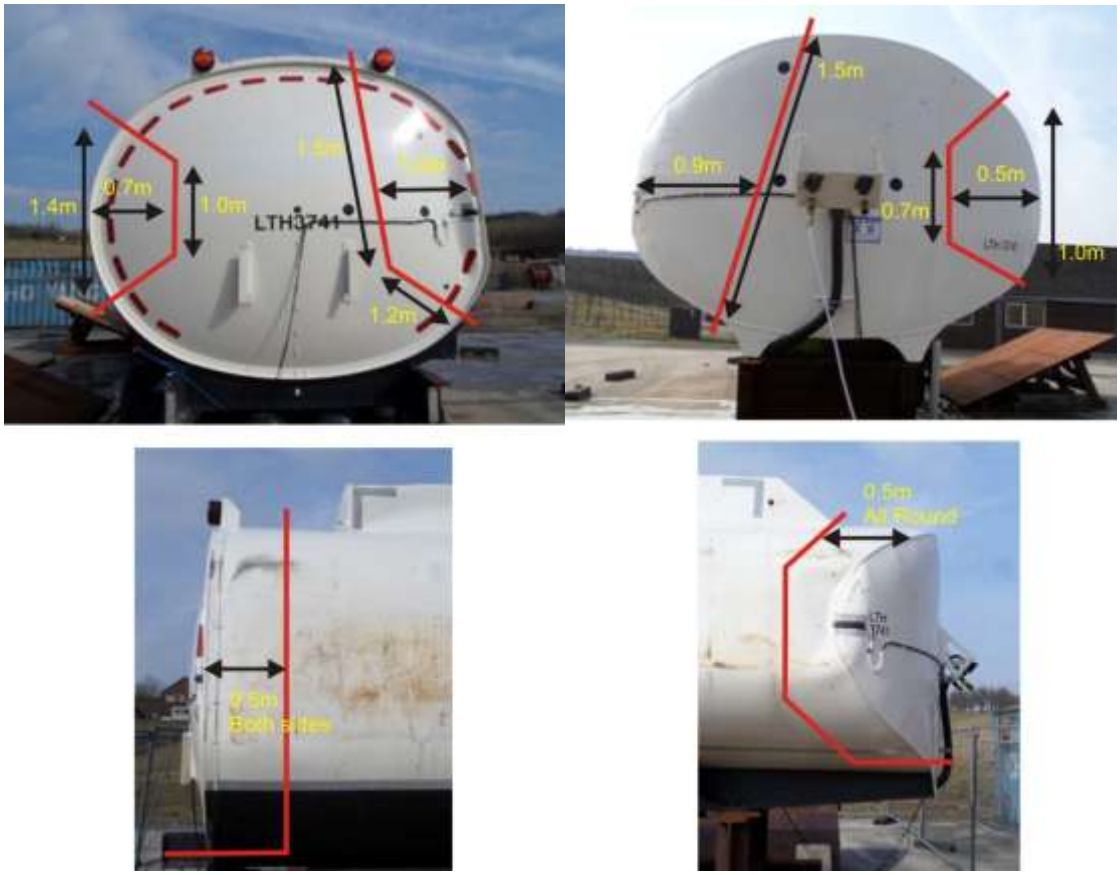

Figure 30 Samples taken from AT11-1475 (dimensions are approximate)

HSL visually inspected the samples before they were sent to TWI, and found some small cracks in the ends of the stitched fillet welds on the rear Band J. These do not appear to have been present on the internal inspection before test (Section 6.3). However, as the fillet welds were not a structural design feature, no loss of bulkhead integrity had been observed after test, and there was no associated damage visible on the extrusion joint, such minor internal damage on roll-over was not considered to be significant.

10.2 OBJECTIVES

The objectives of the work were to undertake:

- A detailed macroscopic and microscopic examination of sections from the front and rear circumferential joints of tanker AT11-1475.
- Tensile testing on samples machined from the parent metal, weld metal and extrusion band metal.
- Finite Element Analysis (FEA) in conjunction with a forming limit diagram to determine the likelihood of failures in the parent metal during a topple test.

10.3 POST-MORTEM AND METALLOGRAPHIC EXAMINATION

10.3.1 Overview

As described in Section 6.1, petroleum road fuel tanker AT11-1475 is an aluminium-bodied, banded-design. Each adjacent barrel, or cylindrical section, of aluminium alloy 5182 tanker shell is joined by a circumferential joint similar to the informative joint design D.14(b) and D.14(c) from BS EN 13094 [4] shown in Figure 31. In this joint configuration, the partition dish, bulkhead, baffle or end dish is also made of AA 5182. For the rear band (Band J/10), where there is no adjacent section of tanker shell, only one primary circumferential weld is made. All other circumferential joints except for the front joint are similar to that shown in Figure 31. However, due to the unique design of the front 'swept' dish of AT11-1475, the front-most circumferential joint (Band A/10) is a double-sided corner joint between the dish and the tanker shell, similar to D.9(b) from BS EN 13094 [4] also shown in Figure 31.

Following receipt from HSL, the sections were photographed, radiographed, and then additional sampling was undertaken to analyse cross sections of the circumferential joints.

10.3.2 Radiographic examination

Radiographic inspection was undertaken to identify the location and position of potential welding defects in each of the sections. For the rear end sections (Band J/10), the primary circumferential welds (i.e. those joining the tanker shell to the extrusion band) were radiographed. For the front end sections (Band A/10), the circumferential joint between the swept front dish and the first tanker compartment was radiographed.

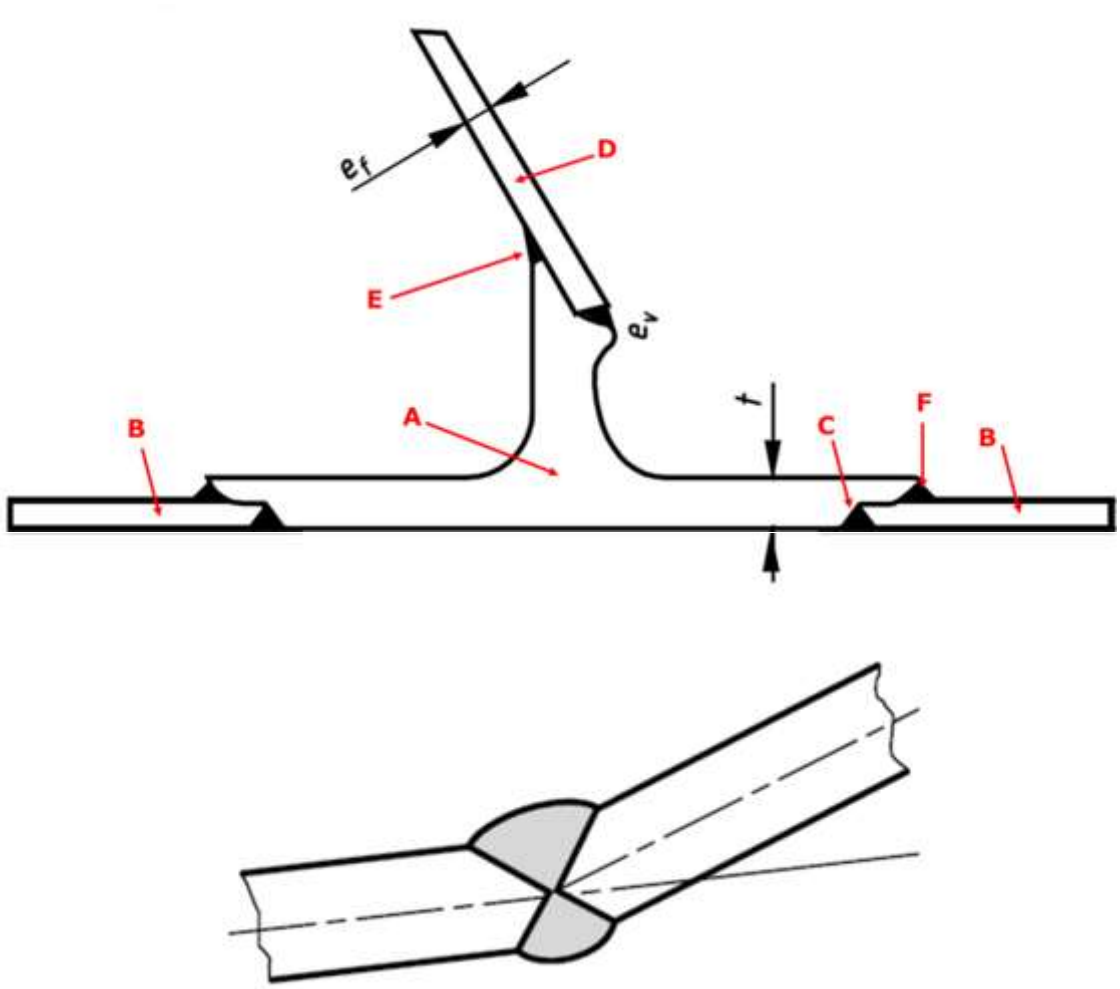

Figure 31 Diagrams of joint designs that are qualitatively similar to the rear and intermediate circumferential, extrusion band joints (top frame) and front end joint (bottom frame) in tanker AT11-1475.
(Figure 1 from TWI report 24000/13/15.)
Images reproduced from Figure D.14(c) for the top frame and D.9(b) for the bottom frame in BS EN 13094 (2015) with red arrows added for this report.
A) Extrusion band (or extrusion profile);
B) Tanker shell;
C) Primary circumferential weld joining tanker shell to the extrusion band;
D) Division plate such as a bulkhead, baffle, surge plate or end dish;
E) 'Top' weld joining the division plate to the extrusion band;
F) Internal fillet weld joining the inner surface of the tanker shell to the extrusion band.

10.3.3 Metallographic examination of samples

Based on the shape of the deformed sections and the results of the radiographic examination, amongst other considerations, the four large sections supplied by HSL were sampled at between three and seven different locations each along their circumferential length.

Seven samples were machined in the longitudinal direction (transverse to the circumferential welds) from the impacted, rear offside section of AT11-1475 (Band J/10). From the seven samples, five were removed from the crushed region of the section that impacted the ground

during the topple test. The remaining two samples were taken from a region remote from the impact zone: one sample (RO-01) was removed where there was no additional internal fillet weld present, and the other (RO-02) was removed from a location near RO-01 where an additional internal fillet weld was present. For the rear band of AT11-1475, the internal fillet welds were 'stitched' around the circumference, with 50 mm weld lengths and 50 mm gaps between the welds.

Samples RO-01 and RO-03 exhibited porosity and lack of penetration into the root of the weld, resulting in an approximately 2.0 mm deep, surface-breaking, lack of fusion defect. Sample RO-02, however, showed good penetration into the root and there was no lack of fusion defect present. In Sample RO-04, the internal fillet weld joining the toe of the extrusion band to the inner surface of the tanker shell had failed, with a crack propagating along the fusion line with the inner surface of the tanker shell. Samples RO-05, RO-06 and RO-07 all exhibited surface-breaking, lack of root fusion defects due to the weld not fully penetrating into the root. The typical depth of these defects ranged from 1.0 mm to 2.0 mm. In samples from all of the primary circumferential welds (RO-01 to RO-07 inclusive), the penetration into the root of the weld was variable. Due to the absence of a through-wall rupture, no additional sampling was undertaken between samples RO-03 and RO-07, and therefore it was not possible to specify the precise circumferential (surface) length of these lack of fusion, surface-breaking defects; however, since the lack of fusion was evident on samples RO-03 through RO-07, in view of the radiography, it is possible to conservatively estimate that the lack of fusion persists continuously between these sampling points and hence has a total surface length of approximately 700 mm. The relevant micrographs from samples RO-01 to RO-07 can be found in Figures 9, 10, 11 and 12 of the TWI report 24000/13/15 in Appendix 5.

Four samples were machined from the undamaged, rear nearside section of AT11-1475 (Band J/10). The four samples were spaced approximately 125 mm apart. As with the rear offside, the penetration into the root of the weld was variable, with sample RN-03 exhibiting good penetration and fusion between the tanker shell and extrusion band, whilst samples RN-01, RN-02 and RN-04 showed signs of lack of fusion at the root of the weld, resulting in surface-breaking defects that were up to 1.5 mm deep. Figure 32 (which is Figure 14 from the TWI report 24000/13/15) contains the micrographs from samples RN-01 to RN-04 inclusive.

The main circumferential welds in the samples from both the rear offside and rear nearside were shown to exhibit weld caps (or overfill) typically in excess of 3.0 mm as measured from the outer surface of the tanker shell. Previous research on tanker performance under topple test conditions [5] has demonstrated the benefits that a large weld cap can have in resisting the bending moments experienced by the joint under topple test conditions. Nevertheless, an excessive weld cap can also be indicative of poor root penetration, which is evident in many of the samples taken from the rear welds. All weld samples from the rear offside and rear near side showed very good alignment, with axial misalignment measurements typically being less than 0.5 mm. The previous TWI research [5] also demonstrated the significant effect of misalignment on the acceptability of defects; specifically, the maximum tolerable defect size under topple test conditions reduced rapidly as the level of axial misalignment increased. Thus, although a surface-breaking, lack of root fusion defect is present in many of the rear weld samples, it is likely that the combination of good joint alignment and relatively large weld cap size contributed to the lack of failure during the topple test.

Six samples were machined in the longitudinal direction from the impacted, front offside section of AT11-1475 (Band A/10). As described in Sections 6.1 and 10.3.1, all circumferential joints in AT11-1475 are geometrically similar to that shown in Figure 31 except for the front-most joint, which is a double-sided corner joint due to the swept design of the front dish. Of the six samples, five were taken from the crush zone (i.e. the large plastic bulge that comprised the

flattened region that impacted the ground) and one additional sample (FO-01) was taken remote from the crush zone. Whilst the front circumferential joint underwent extensive plastic deformation during the topple test as evidenced by the severe bending, none of these exhibited any evidence of cracking. Finally, three samples were machined from the undamaged, front nearside of the tank (Band A/10). The samples from the front circumferential joint did not exhibit any significant lack of fusion defects.

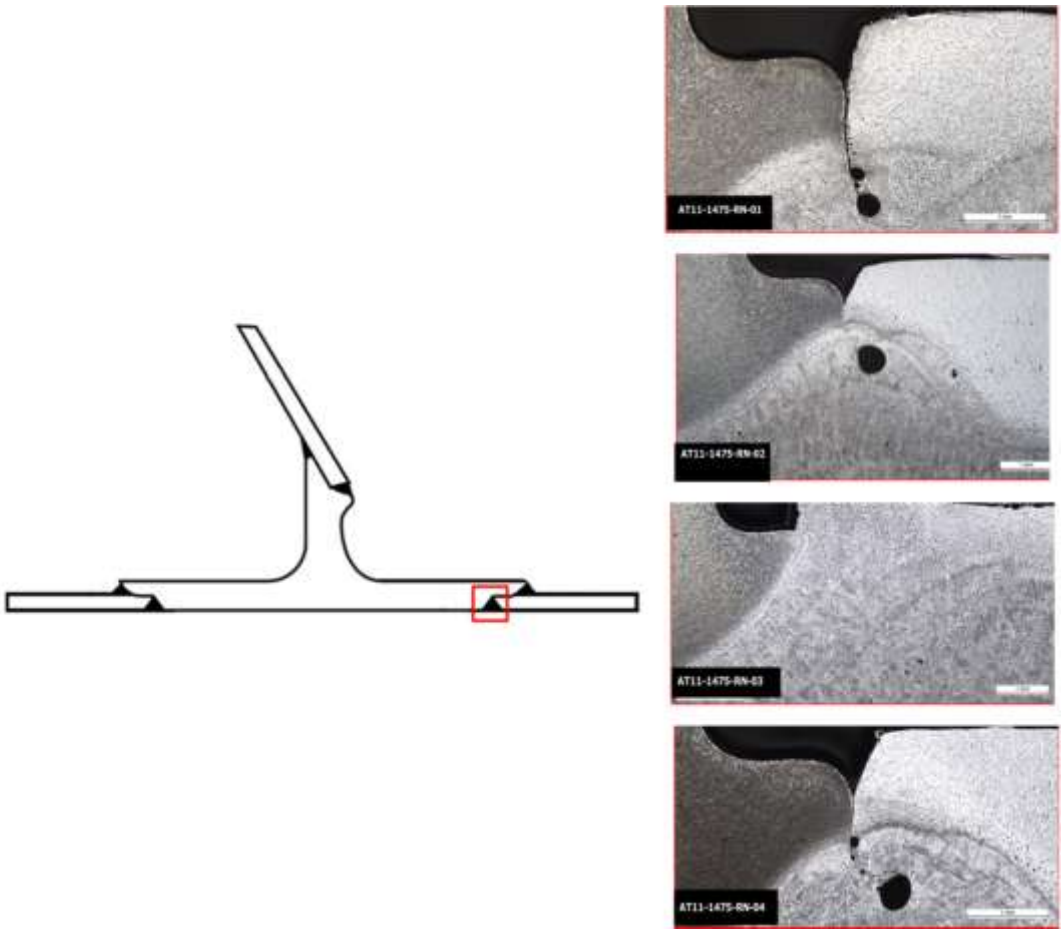

Figure 32 Images of samples RN-01 to RN-04 inclusive.
(Figure 14 from TWI report 24000/13/15.)
RN-01 (top right), RN-02 (second from top right), RN-03 (third from top right), and RN-04 (bottom right), with the reference location shown on the BS EN 13094 indicative joint design D.14(c) on the left. The scale bars on the frames indicate 1.0 mm length. Sample RN-01 shows more significant lack of fusion at the root than RN-02. Sample RN-04 exhibits lack of root fusion.

10.3.4 Tensile testing

Tensile testing was undertaken on material samples machined from the undamaged rear, nearside section of AT11-1475 (Band J/10).

Two tensile specimens were prepared from the tanker shell material in the joints (labelled M01-01 and M01-02). These specimens were taken in the circumferential orientation and machined as flat bar specimens. Weld metal specimens could not be machined from the primary circumferential welds joining the tanker shell to the extrusion band because of the need to avoid the potential presence of lack of fusion defects that could affect the tensile testing results. Instead, two flat bar, all-weld metal specimens were machined from the weld joining the rear dish to the top of the extrusion band. These specimens were labelled M02-01 and M02-02.

Finally, two round bar specimens were machined from circumferentially-oriented material from the centre of the up-stand of the extrusion band. These specimens were labelled M03-01 and M03-02.

The flat bar tensile specimens were of nominal width 6.0 mm and parallel length 32.0 mm, marked with a 25.0 mm gauge length for determination of plastic elongation. The specimens were instrumented with a dual averaging HRD auto extensometer, of gauge length 25.0 mm, for the determination of total elongation (at fracture) and tested at ambient temperature. The choice of ambient temperature instead of the minimum ADR design temperature (-20 ^{o}C) was made to more closely match the conditions of the topple test. The applied strain was recorded through the entire test. Up to the yield point, the applied strain rate was 0.015 strain/min, and beyond the yield point, the applied strain rate was 0.400 strain/min.

The round bar tensile specimens were of nominal diameter 8.0 mm and parallel length 48.0 mm, marked with a 5X diameter gauge length for determination of plastic elongation. The specimens were instrumented with a dual averaging extensometer and tested at ambient temperature.

The stress-strain curves showed that the weld metal slightly overmatched the tanker shell metal, and that the tanker shell metal had tensile properties that were generally in agreement with the anticipated properties of the aluminium alloy Al-5182. The extrusion band metal significantly overmatched both the parent and weld metal curves, exhibiting a higher yield point, ultimate tensile strength and smaller elongation.

10.4 FORMING LIMIT DIAGRAM ASSESSMENT

In order to provide additional numerical and analytical understanding of the performance of the tanker under the topple test conditions, finite element analyses have been conducted on the front and rear circumferential joints. The FEA performed in this report is a simplified, static model of the topple test. The dynamic and inertial effects experienced during the actual topple test are ignored and only the deformation of the tank due to the 'crushing' effect of the ground and the pressure exerted by the water contained in the compartments on the internal surfaces of the tank are considered. The results of the FEA have been assessed using a forming limit diagram methodology to determine whether ruptures in the parent metal or weld metal would occur due to the deformation exceeding the formability limit of the tanker shell material, Al 5182.

10.4.1 Finite element modelling

10.4.1.1 Software

All models were generated using version 6.14-1 of the pre-processing finite element analysis software Abaqus/CAE and the analyses were solved using version 6.14-1 of Abaqus/Standard.

10.4.1.2 Geometry

Two different models were created: one for the rear dish (Band J/10) and one for the front dish (Band A/10). All models were created using the CAD capabilities of Abaqus/CAE and were developed from engineering drawings provided by Lakeland. The dimensions in the engineering drawings were compared with those measured from the sections of AT11-1475 received from HSL and any differences were incorporated into the model as appropriate. Due to symmetry considerations with respect to the geometry and applied loads, only one-quarter of the rear and front sections were modelled.

The rear dish model comprised of the extrusion profile, rear dish and tanker shell. The front dish model was modelled as a single, solid body. Details of the model are given in the full report in Appendix 5.

10.4.1.3 Material properties

Two different material regions were included in the rear dish model: one for the tanker shell, weld metal and rear dish, and one for the extrusion band. For both regions, the lower-bound engineering stress-strain curves obtained from tensile testing were transformed to true stress-true plastic strain curves. For both materials, the Young's modulus was taken to be 70 GPa and the Poisson's ratio was taken to be 0.3, which agree with the test measurements and with the typical elastic constants for this material [7]. A rate independent plasticity model using the Von Mises yield criterion and isotropic strain hardening rule was specified using the incremental plasticity data obtained from sampling the tensile curves. In the front dish model, no extrusion band was present, and the entire model was comprised of the lower bound parent metal material.

10.4.1.4 Loads and boundary conditions

A flat, analytic rigid body was created to model the ground and was coupled to a centrally-positioned reference node. All degrees of freedom of this reference node were restrained (set equal to zero) except for the translational degree of freedom in the crushing direction. A contact definition was created between the ground and the tanker model with hard, normal contact. A 250 mm displacement was applied in the crushing direction (i.e. into the tanker section) to simulate the static impact of the ground and tank. The magnitude of this displacement is somewhat arbitrary, as it was chosen to be sufficiently large so as to ensure the simulation would achieve the same flattened length measured from the specimens after the topple test (see Section 10.4.2). The boundary conditions applied to the tanker geometry were those representing the symmetry planes and axial restraint, simulating the longer adjacent section of tanker that was not incorporated into the model. All simulations were analysed with the finite strain formulation, incorporating the nonlinear effects of large displacements and rotations.

10.4.2 Results

After the topple test, the flattened length of the rear band J/10 (i.e. the length of the crush zone) was approximately 760 mm, and the flattened length of the front circumferential joint (Band A/10) was approximately 580 mm. Therefore, for each simulation, the ground was translated into the tanker model until the flattened length of the deformed model matched that measured on the sections removed from AT11-1475.

The deformation of the rear dish model showed exceptional agreement with the samples taken from the rear, offside section of AT11-1475. In particular, the shape, curvature and dimensions of the crush zone agreed with the samples taken from the centre (sample RO-05) as well as the ends of the crush zone (sample RO-03). For this reason, the model was considered to be a reasonably accurate representation of the topple test. As with the rear band model, the front dish model showed very good agreement with measurements taken from samples of the front, offside section of AT11-1475.

To assess the likelihood of cracking occurring in the parent or weld metal, a forming limit diagram (FLD) approach was employed. Essentially, a forming limit diagram provides a graphical description of material failure tests such as biaxial tension tests and punched dome tests. The diagram comprises a 'safe' region and an 'unsafe' region separated by the forming limit curve. The forming limit curve is defined as a locus of points with x-coordinate minor strain and y-coordinate major strain. FLDs are typically employed in the sheet metal forming industry to determine the propensity for cracks to appear during cold-forming, bending and stamping. Due to the thin nature of sheets, the through-wall strains are negligible, and therefore the strain state at any given point can be wholly described by the minor and major principal strains. For the present analyses, the large span of the end dishes relative to the wall thickness enables the forming limit diagram approach to be used. A literature review of FLDs for Al 5182-O, the aluminium alloy of the end dishes and tanker shell, was undertaken to provide an approximate forming limit curve suitable for the present analysis. Whilst FLDs have some

dependency on strain-rate, thickness, temperature, heat treatment and pre-strain, a representative curve, obtained from the literature review was employed for the present study. The results obtained from this forming limit curve (described below) have provided reasonable comparisons to the topple test results, and therefore these additional dependencies had only secondary influences.

For the rear band model, pairs of minor strain and major strain were plotted on the FLD against the forming limit curve as shown in Figure 33 (Figure 29 from the TWI report 24000/13/15). In this figure, the red curve (strains from the FE model) lies below the forming limit curve (black curve). This indicates that the forming limit diagram approach does not predict failure to occur. This result agrees with the observations from the topple test and subsequent metallographic examinations, where no cracking or failure of the rear dish was seen.

For the front dish model, as with the rear band model, the maximum and minimum principal strains were plotted on the forming limit diagram in Figure 34 (Figure 30 from the TWI report 24000/13/15). Again, the strains from the model all lie below the forming limit curve and hence the FLD approach does not predict failure to occur, which agrees with the lack of failure observed in the front dish after the topple test and subsequent metallographic examinations.

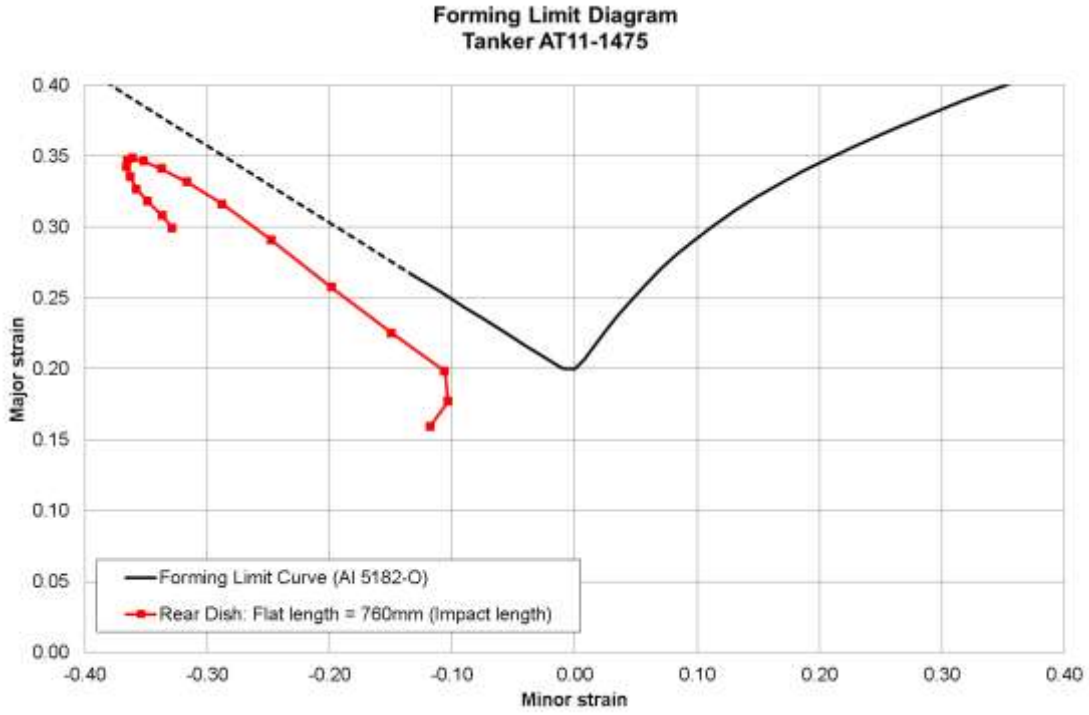

Figure 33 Forming limit diagram for the rear dish simulation.
Each red point represents the minor and major strains output at a node in the circumferential path passing through the most severely strained region of the model. (Figure 29 from TWI report 24000/13/15.)

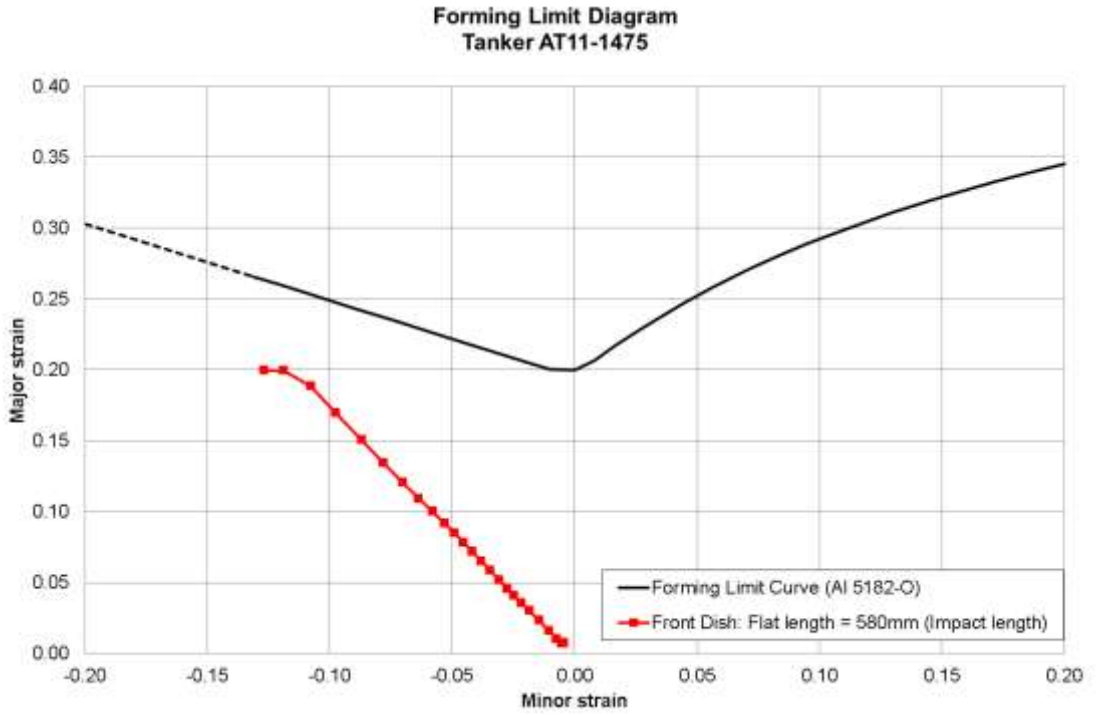

Figure 34 Forming limit diagram for the front dish simulation.
Each red point represents the minor and major strains output at a node in the circumferential path passing through the most severely strained region of the model. (Figure 30 from TWI report 24000/13/15.)

10.5 CONCLUSIONS

Metallographic examinations and detailed numerical analyses have been undertaken to provide supplementary information about the performance of the petroleum road fuel tanker AT11-1475 after topple testing. These investigations found that:

- No through wall ruptures were observed in any of the samples taken from the front or rear welds of AT11-1475.
- The samples from the front circumferential joint did not exhibit any significant lack of fusion defects.
- The samples of the rear circumferential joint exhibited variable root penetration in the main circumferential welds. This resulted in some internal surface-breaking, lack of root fusion defects being observed with typical defect depths ranging from 1.0 mm to 2.0 mm.
- For the rear weld samples, the joints were found to exhibit good alignment, typically within 0.5 mm, and the height of the weld caps of the main circumferential welds was found to be typically in excess of 3.0 mm. The combination of low misalignment and large weld caps likely contributed to the good performance of the joints under the topple test. However, the excessive weld cap size was seen to correlate with lack of root penetration (and lack of root fusion defects) in many samples.
- Finite element modelling of a static, idealised representation of the end dish under topple test conditions, in conjunction with a forming limit diagram methodology, correctly predicted that the front swept dish and rear end dish of AT11-1475 would not rupture during the topple test. The model also accurately predicted the tanker front

swept dish and rear end dish deformations and, therefore, represents a valuable approach for future assessments of tanker performance under these conditions.

10.6 ADDITIONAL NOTE

RTN Lakeland have considered the findings from the examinations of the circumferential welds and are working with TWI to review welding practices, welding procedure qualification records (WPQRs) and associated welding procedure specifications (WPSs). HSL have been informed that the plan is to develop a new suite of preliminary WPSs to accommodate all aspects of the tanker welding process. Welding procedure and welder/welding operator qualification tests will then be undertaken as appropriate and a suite of WPSs developed based on the new WPQRs to take into account the latest best practice and practicalities of manufacture.

11 CONCLUSIONS

The 2011/12 ADR-compliant road fuel tanker AT11-1475, supplied from service by Lakeland tankers maintained its internal and external integrity when subject to the HSL tanker topple test. Radiographic and metallographic examinations revealed some issues relating to the quality of the circumferential welds at the extrusion bands.

Test Methods, including tanker preparation

A single ADR-compliant Lakeland tanker was topple tested using the HSL topple test. This was a 10-banded, 6-compartment road fuel tanker numbered AT11-1475, with the tank manufactured in 2011, and the tanker assembled in 2012.

Tanker AT11-1475 was supplied by Lakeland Tankers after having been taken out of service at the end of a rental contract. Before delivery to HSL, the tanker was radiographed and assessed to obtain information on the condition of the circumferential welds. The same suitably qualified radiographic contractor was used as for the previous work in this research programme. The radiographs indicated defects, to a greater or lesser extent, in all the circumferential welds. The overall percentage of the length of welds radiographed that indicated lack of fusion defects was 23.4%. However, since the design of the circumferential joint has features which are known to complicate radiographic interpretation, these results may require further examination to be certain of the findings, and as such may be viewed as a worst-case. TWI findings from examinations of samples taken from the front and rear circumferential welds, which included radiographic and metallographic assessments, are more definitive and reported at the end of this summary. Prior to delivery to HSL, the tanker was fully ADR inspected by the same qualified inspection body as used for the previous work in this research programme. The minor remedial work arising from the inspection was conducted by Lakeland Tankers before the tanker was prepared for the topple test.

Using the method developed and demonstrated to be reliable in previous work for DfT (TRL report PPR724, 2014), the Lakeland tanker was tilted under controlled conditions until it became unstable and fell onto its offside due to the effect of gravity. The tanker was filled with water because fuels were not practical for environmental and safety reasons. Impact on the offside of the tanker avoided damaging filling ports on the tankers nearside. Information on the tanker was used to calculate the approximate angle at which it would become unstable. The ramps were secured to a concrete test pad, with a plate steel landing pad providing a robust and repeatable impact area. After preparation the empty tanker was lifted onto the ramps with its offside at, and parallel to, the bottom of the ramps.

Once ready for test, the tanker was filled with the required volume of water (equivalent to the maximum mass of fuel that could be carried in service) distributed across all compartments. It was then toppled sideways, pivoting around the outer edge of its offside wheels to fall onto the landing pad. The tanker was tilted into the topple position using two parallel winching systems, with wide slings to spread the load and prevent high stress levels on the tanker barrel and comb when winch forces were applied to the slings. Each winching system included a chain hoist and load cell and was anchored to the concrete pad. Tilting the tanker into the topple position was controlled by ensuring the load on each winch line was similar. When the point of instability was reached, the winching lines slackened and the tanker toppled onto its side due to the effect of gravity.

Rectangular steel supports (‘steel wheels’) replaced the tanker’s offside wheels to remove the risk of the tyres coming off the wheel rims during the test, and to avoid variability from

uncontrolled shear movement in these tyres during the topple. The tanker was not tested with a tractor unit to avoid uncontrolled variations between tests caused by tractor unit rotation and to avoid possible failure of the kingpin due to unconventional loading. Instead, a steel frame (the '5th wheel' assembly) was fitted at the tanker's kingpin plate to give the support normally provided by the tractor and to keep the tanker at the desired coupling height for the test. The tanker's suspension was blocked rigid to remove sources of uncontrolled variation, such as changes in the ride height, and to keep the tank position fixed relative to the suspension during the topple. Any tanker items not integral to the tank and suspension, or which might adversely affect the impact, or which might contain fuel, hydraulic oil or other environmentally harmful materials, were sealed or removed.

The full data gathering instrumentation for the tanker comprised strain gauges, pressure transducers and accelerometers to provide data for comparison and characterisation of general impact behaviour. In total, 40 such instruments were used. Accelerometer blocks were located at the centre point on the outside of both the front and rear bulkheads. Arrays of strain gauges and pressure transducers were affixed to compartments 1b (rear half of front compartment), 4b (third compartment from the rear) and to the front and rear bulkheads as follows:

- seven pressure transducers in each of the two compartments, located at the midpoint of the compartment close to the inner tanker wall, radiating circumferentially top to bottom on the offside (impact side), the centre being at the estimated point of impact;
- twelve strain gauges for compartment 1b, mounted as gauge pairs in matching positions on the inside and outside of the offside tanker shell. Two gauge pairs measuring longitudinal strain near the rear bulkhead weld, two gauge pairs measuring longitudinal strain near the front bulkhead and two gauge pairs measuring longitudinal and hoop strain at the midpoint.
- six strain gauges for compartment 4b, mounted as gauge pairs in matching positions on the inside and outside of the offside tanker shell. Two gauge pairs measuring longitudinal strain near the rear bulkhead weld, and one gauge pair measuring hoop strain at the midpoint.
- three strain gauges on each end bulkhead, mounted on the outside, towards the offside tanker shell, measuring radial strain.

Two independent data loggers were used: one for compartment 1b and the other for 4b and the end bulkheads. During the test these loggers were synchronised with the high speed video and acquired data at 50,000 samples per second, or one sample every 0.02 millisecond. The test was recorded using fifteen video cameras ranging from standard speed (25 frames per second) to high speed (1,000 frames per second). Frames from the high speed video were analysed to obtain accurate measurements of acceleration and impact velocity at the front and rear of the tanker.

After preparation, and before the topple test, the tanker was pressure tested to confirm that the integrity of the tanker had not been adversely affected by the preparations for the topple test. Also, before the topple test, the internal welds at the extrusion bands were visually inspected and the locations and characteristics of fillet welds between the extrusion band and the shell were mapped. The external circumferential weld caps were surveyed and were found to be broadly comparable with expectations based on the experience from previous tests. The tanker was laser scanned on arrival at HSL, after being lifted onto the ramps, immediately after testing (lying on its side), and after being lifted back onto its wheels. This was to confirm that tanker preparation and recovery had caused no damage to the tanker, and to record any changes to the tanker shape after impact.

Once surveyed and prepared, including fitting all instrumentation, the manway lids were refitted and pneumatic pressure tests conducted to confirm that the tanker was fully sealed and loadworthy. Immediately before the test, the tanker was filled with water (using a calibrated water meter) to give a mass that was equivalent to the maximum rated laden mass of the tanker. The tanker was, thus, filled with 31,244 litres of water, with each compartment filled to about 70% of its maximum capacity. These volumes were below the maximum rated laden volumes for fuel because of the higher density of water.

Immediately after impact, impact features found by visual examination were recorded. The tanker was then emptied and lifted back upright onto its wheels. After recovery, further visual examinations and pressure tests were conducted to establish the internal and external integrity of the tank and its compartments.

Topple test results

The overall event duration was a few seconds with most deformation occurring in the first 100 ms. The impact was close to uniform along the length of the tanker, with the rear hitting the ground approximately 8 ms before the front of the tanker. The impact velocities of 4.8 m/s (1.94 rad/s) at the front and 4.1 m/s (1.97 rad/s) at the rear of the tanker lay within the range of 1.75 to 2.62 rad/s which has been reported for rollovers in real accidents.

The pressure and strain data in both compartments were broadly consistent with expectations based on the impact events, tanker structural design and experience from previous tests.

Peak pressures occurred at the 90 degrees from bottom dead centre position which is where the initial impact occurred. In general, strains near the welds were higher than those at the compartment centre, with some yielding and plastic deformation observed in the strain behaviour near the welds. During impact, high speed video captured free travelling flexural waves propagating away from the impact line around the circumference of the tanker. Such waves should result in more pronounced ripples in the circumferential strain than the longitudinal strain at the centre of the compartment, and there was some evidence of this in the data.

After the test, the tanker exhibited a deformation shape with the impact area flattened along the length of the tanker. The impact caused a permanent reduction in tanker diameter of approximately 90 mm at the rear and 61 mm at the front of the tanker.

Immediately after the test, no external leaks could be seen, although there were slow drips from some pressure relief valves on the tanker's manlids. During emptying there was no evidence of internal leaks at any of the bulkheads. **Importantly, after the tanker was righted, ADR pressure tests confirmed that external and internal integrity had been maintained for all compartments and pressure relief valves, and detailed visual examination of the impact damage did not reveal any cracks that would compromise the integrity of the tanker.**

HSL supplied TWI with samples from the front and rear of the tanker, including both the damaged offside and the undamaged nearside, for radiographic and metallographic examinations and in support of detailed numerical analyses.

Metallographic examinations and detailed numerical analyses

Metallographic examinations and detailed numerical analyses have been undertaken to provide supplementary information about the performance of the petroleum road fuel tanker AT11-1475 after topple testing. These investigations found that:

- No through wall ruptures were observed in any of the samples taken from the front or rear welds of AT11-1475.
- The samples from the front circumferential joint did not exhibit any significant lack of fusion defects.
- The samples of the rear circumferential joint exhibited variable root penetration in the main circumferential welds. This resulted in some internal surface-breaking, lack of root fusion defects being observed with typical defect depths ranging from 1.0 mm to 2.0 mm.
- For the rear weld samples, the joints were found to exhibit good alignment, typically within 0.5 mm, and the height of the weld caps of the main circumferential welds was found to be typically in excess of 3.0 mm. The combination of low misalignment and large weld caps likely contributed to the good performance of the joints under the topple test. However, the excessive weld cap size was seen to correlate with lack of root penetration (and lack of root fusion defects) in many samples.
- Finite element modelling of a static, idealised representation of the end dish under topple test conditions, in conjunction with a forming limit diagram methodology, correctly predicted that the front swept dish and rear end dish of AT11-1475 would not rupture during the topple test. The model also accurately predicted the tanker front swept dish and rear end dish deformations and, therefore, represents a valuable approach for future assessments of tanker performance under these conditions.

In light of the metallographic examinations, RTN Lakeland have considered the findings from the examinations of the circumferential welds and are working with TWI to review welding practices, welding procedure qualification records and associated welding procedure specifications. HSL have been informed that the plan is to develop a new suite of welding procedure specifications which accommodate all aspects of the tanker welding process and take into account the latest best practice and practicalities of manufacture.

12 REFERENCES

[1] Project Report PPR724 "Technical Assessment of Petroleum Road Fuel Tankers - Summary Report (all Work Packages)", TRL 2014

[2] European Agreement on the Carriage of Dangerous Goods by Road (ADR) (2013) http://www.unece.org/trans/danger/publi/adr/adr2013/13contentse.html (summary information can be found on the HSE website at http://www.hse.gov.uk/cdg/manual/adrcarriage.htm)

[3] EN ISO 10042: 2005, Welding. Arc-welded joints in aluminium and its alloys. Quality levels for imperfections, BSI Standards Publication.

[4] BS EN 13094: 2015, Tanks for the transport of dangerous goods – Metallic tanks with a working pressure not exceeding 0.5bar – Design and Construction, BSI Standards Publication.

[5] 'Department for Transport Technical Assessment of Petroleum Tankers: Work Package 2 – Detailed Engineering Critical Assessment', TWI Report 24000/9/15, 25 August 2015.

[6] 'Department for Transport Technical Assessment of Petroleum Tankers: Metallographic and Analytical Assessment of AT11-1475', TWI report 24000/13/15, 04 September 2015

[7] MatWeb (2015): 'MatWeb.com: Material Property Data', http://www.matweb.com/search/datasheettext.aspx?matid=9217 accessed 24/07/2015 at 13.54.00.

13 APPENDIX 1 – TANKER RADIOGRAPHY

Band A

Item Reference			COMMENTS	Result
AT11 1475	A10	A-B	LOF Approx 30mm @ A & 68mm @ B. Porosity Noted	Rej
AT11 1475		B-C	LOF/Linear Porosity 80mm. Gas Pores Noted.	Rej
			Note; Due to vareying configuration only this shot was taken. Shot DWSI through the	
			tank body (see skatch)	

Band B

Item Reference			COMMENTS	Result
AT11 1475	B10A	35-470	Groove line noted. Porosity @ 50 to 53cm noted. Root profile noted.	Acc
AT11 1475	B10A	70-105	Groove line noted.	Acc
AT11 1475	B10A	105-134	Groove line ntd. Porosity @ 111 to 113cm noted.	Acc
AT11 1475	B10B	0-30	Groove line noted. Root profile, Linear porosity @ 7 to 10. LOF 12 to 16, 20 to 22cm	Rej
AT11 1475	B10B	30-65	Groove line noted. LOF 40 to 43, 44 to 46 & 62 to 65cm.Porosity @55 to 57 ntd.	Rej
AT11 1475	B10B	65-96	Grove line noted. LOF 65 to 88cm. Root profile @ 89 to 95cm intermittent Ntd.	Rej
AT11 1475	B10C	0-35	Groove line noted. LOF 15 to 22cm. Root profile noted.	Rej
AT11 1475	B10C	35-70	Groove line noted. Root profile noted. Pressure mark @ 40cm noted.	Acc
AT11 1475	B10C	70-102	Groove line noted. LOF 75 to 77. Root profile 90 to 95cm noted.	Rej
AT11 1475	B10C	102-113	Groove line noted.	Acc

Band C

Item Reference			COMMENTS	Result
AT11-1475	C10A	0-35	Groove line noted. Gas pore @ 5cm noted. Pressure mark @ 5 noted.	Acc
AT11-1475	C10A	35-70	Groove line noted. Pores @ 49, 54, 60 & 65cm noted.	Acc
AT11-1475	C10A	70-105	Groove line noted. Linear porosity @ 77 to 85cm. Pressure mark @ 77cm noted.	Rej
AT11-1475	C10A	105-134	Groove line noted. Linear porosity @ 124 to 130cm. Gas pores @ 112, 115, 121cm. Root profile noted.	Rej
AT11-1475	C10A	-4-0-30	Groove line noted. Gas pore @ 21cm noted. Fillet weld profile noted.	Acc
AT11-1475	C10A	30-62	Groove line noted. Root profile ntd. Gas pores 5.5mm @ 44cm, 2x4.4mm @ 42 & 46cm.	Rej
AT11-1475	C10A	64-98	Groove line noted. Fillet weld profile noted. Pressure mark @ 96cm noted.	Acc
AT11-1475	C10A	0-35	Groove line noted. Linear porosity @ 25 to 29cm. Gas pore @ 8cm. Fillet weld profile ntd.	Rej
AT11-1475	C10A	35-70	Groove line noted. Linear porosity @ 52 to 60cm noted.	Rej
AT11-1475	C10A	70-105	Groove line noted. LOF @ 77 to 82cm.	Rej
AT11-1475	C10A	105-118	Groove line noted.	Acc

Band D

Item Reference			COMMENTS	Result
AT11-1475	D10A	0-35	Groove line. Gas pore @ 5, 8, 12, 16, 20 & 27cm. Fillet weld profile noted.	Acc
AT11-1475	D10A	35-70	Groove line. Gas pore @ 41, 45, 50, 52, 55, 60 & 67cm. Fillet weld profile noted.	Acc
AT11-1475	D10A	70-105	Groove line. Linear porosity @ 93 to 100cm. Gas pore @ 76, 84, 102 &105cm ntd. Fillet weld profile noted. Pressure mark @ 75cm noted.	Rej
AT11-1475	D10A	107-142	Groove line. Linear porosity @ 114 to 117cm. Elongated cavity @ 136cm. Fillet weld profile noted.	Rej
AT11-1475	D10B	0-34	Groove line. Fillet weld profile noted.	Acc
AT11-1475	D10B	34-70	Groove line. Gas pores @ 40 & 43cm noted. Fillet weld profile noted.	Acc
AT11-1475	D10B	70-96	Groove line. Fillet weld profile noted. Pressure mark @ 90 noted.	Acc
AT11-1475	D10C	0-35	Groove line. Pores @ 1 & 35cm noted. Fillet weld profile noted.	Acc
AT11-1475	D10C	35-70	Groove line. Pores @ 35, 37 & 55cm noted. Root profile noted. Fillet weld profile ntd.	Acc
AT11-1475	D10C	70-105	Groove line. LOF 77 to 82, 95 to 100cm noted. Linear porosity @ 100 to 105cm noted. Fillet weld profile noted.	Rej
AT11-1475	D10C	105-140	Groove line. Linear porosity @ 105 to 113cm. LOF @ 115 to 124 & 140cm. Elongated cavity's @ 126 & 127cm. Pore @ 130cm. Fillet weld profile noted.	Rej

Band E

Item Reference			COMMENTS	Result
AT11-1475	E10A	0-35	Groove Line. Pore @ 5cm noted. Pressure mark @ 6cm noted. Fillet weld profile Ntd.	Acc
AT11-1475	E10A	35-70	Groove Line. Elongated gas pore @ 40 noted. Fillet weld profile noted.	Acc
AT11-1475	E10A	70-105	Groove Line. LOF 84 to 86cm. Linear porosity @ 95 to 105cm. Gas pores @ 74, 75, 77, 80, 82, 87 & 92cm noted.	Rej
AT11-1475	E10A	105-145	Groove Line. LOF 124 to 142 & 145cm. Gas pores @ 116 & 117cm ntd. Pressure mark @ 114 noted.	Rej
AT11-1475	E10A	145-165	Groove Line. LOF 150 to 153cm. Cavity @ 145cm. Root profile noted.	Rej
AT11-1475	E10B	0-30	Groove Line. LOF @ 4 to 10, 22 to 25cm. Pick up @ 28cm ntd. Fillet weld profile ntd.	Rej
AT11-1475	E10B	30-64	Groove Line. Root profile noted.	Acc
AT11-1475	E10B	64-92	Groove Line. Pores @ 90cm noted.	Acc
AT11-1475	E10C	0-35	Groove Line. Pores @ 20, 32 & 35cm noted. Fillet weld profile noted.	Acc
AT11-1475	E10C	35-70	Groove Line. Pores @ 35, 37, 40, 42, 55, 62 & 67 to 68cm noted. Fillet weld profile noted.	Acc
AT11-1475	E10C	70-105	Groove Line. Pores @ 70 & 95cm noted. Linear porosity @ 83 to 87, 90 to 92cm.	Rej
AT11-1475	E10C	105-145	Groove Line. LOF 124 to 131cm. Pores @ 134 & 136cm. Fillet weld profile ntd.	Rej
AT11-1475	E10C	145-154	Groove Line. Pores @ 144 & 145cm noted	Acc

Band F

Item Reference			COMMENTS	Result
AT11-1475	F10A	0-35	Groove line. Intermittent porosity @ 10 to 15cm. Fillet weld profile.	Acc
AT11-1475	F10A	35-70	Groove line. Porosity @ 40 to 45cm noted. Fillet weld profile.	Acc
AT11-1475	F10A	70-105	Groove line. Porosity @ 82, 87, 92 & 100cm noted. Fillet weld profile. Pressure mark @ 75cm noted.	Acc
AT11-1475	F10A	105-140	Groove line. Gar pore @ 110 to 115 & 117cm noted. Pore 2.8mm dia @ 118cm. Fillet weld profile noted.	Rej
AT11-1475	F10A	140-165	Groove line. Root profile noted.	Acc
AT11-1475	F10B	-2-0-32	Groove line. LOF -2 to 0 to 5, 20 to 21, 24 & 26cm. Pores @ 6cm ntd. Root profile ntd.	Rej
AT11-1475	F10B	32-62	Groove line. Linear porosity @ 10, 36 to 38, 44cm. LOF 48 to 49, 60 to 62cm. Root profile and fillet weld profile noted.	Rej
AT11-1475	F10B	64-92	Groove line. Porosity @ 84 to 88cm. Root profile noted.	Acc
AT11-1475	F10C	0-35	Groove line. LOF 3 to 5, 6, 15, 17 to 24, 25 to 35cm. Root profile noted.	Rej
AT11-1475	F10C	35-70	Groove line. LOF 37 to 43, 45 to 47, 50 to 60cm. Porosity @ 62cm. Fillet weld profile.	Rej
AT11-1475	F10C	70-105	Groove line. LOF 72 to 75, 96 to 97cm. Pore @ 105cm noted. Fillet weld profile ntd.	Rej
AT11-1475	F10C	105-140	Groove line. LOF 110 to 115, 139 to 140cm. Root profile noted. Fillet weld profile ntd.	Rej
AT11-1475	F10C	140-155	Groove line. LOF 140 to 145, 147 to 151cm. Root profile noted, Fillet weld profile ntd.	Rej

Band G

Item Reference			COMMENTS	Result
AT11-1475	G10A	0-35	Groove Line. LOF 0 to 7, 10 to 18, 20 to 35cm. Fillet weld profile noted.	Rej
AT11-1475	G10A	35-70	Groove Line. LOF 35 to 40, 47 to 48, 50 to 65cm.	Rej
AT11-1475	G10A	70-105	Groove Line. LOF 82 to 97cm. Porosity @ 75cm noted.	Rej
AT11-1475	G10A	105-140	Groove Line. LOF 114 to 124cm. Linear porosity @ 129 to 135cm. Root profile noted.	Rej
AT11-1475	G10A	140-165	Groove Line. LOF 142 to 145cm. Root profile @140 to 150, 169 to 145cm.	Rej
AT11-1475	G10B	0-32	Groove Line. LOF 3 to 13, 14cm (5mm) & 22 to 32cm.	Rej
AT11-1475	G10B	32-64	Groove Line. LOF 32 to 34, 42 to 49 @ 50 to 56cm.	Rej
AT11-1475	G10B	64-94	Groove Line. LOF 66 to 79, 83 to 94cm. Root profile @ 63 to 67cm.	Rej
AT11-1475	G10C	0-35	Groove Line. Pores @ 18 to 20, 25 to 27cm	Acc
AT11-1475	G10C	35-70	Groove Line. LOF @ 44, 47, 48 to 50, 52 to 60, 63 to 65cm.	Rej
AT11-1475	G10C	70-105	Groove Line. LOF @ 73 to 75, 95 to 103cm. Porosity @ 80 to 93cm.	Rej
AT11-1475	G10C	105-140	Groove Line. LOF@ 112 to 115, 116 to 130, 135 to 140cm.	Rej
AT11-1475	G10C	140-155	Groove Line. LOF @ 140 to 147cm. Linear porosity @ 150 to 155cm.	Rej

Band H

Item Reference			COMMENTS	Result
AT11-1475	H10A	0-35	Groove line. Pore @ 14cm.	Acc
AT11-1475	H10A	35-70	Groove line. Linear porosity 35 to 41, 60 to 70cm.	Rej
AT11-1475	H10A	70-105	Groove line. Linear porosity 70 to 105cm intermittent full length.	Rej
AT11-1475	H10A	105-140	Groove line. Linear porosity intermittent. Pore @ 132cm (3.5mm Dia.).	Rej
AT11-1475	H10A	140-165	Groove line. Linear porosity @ 147 to 156cm.	Rej
AT11-1475	H10B	-2-0-32	Groove line. Linear porosity full length intermittent. Fillet weld profile noted.	Rej
AT11-1475	H10B	32-64	Groove line. Linear porosity @ 50 to 52cm. Poros @ 33, Pore's at 38, 42, 45, 47, 57, 58 & 60cm.	Rej
AT11-1475	H10B	64-94	Groove line. Porosity @ 72 & 77cm.	Acc
AT11-1475	H10C	-2-0-32	Groove line. Linear porosity @ 13 to 15cm. Porosity 4, 5, 10, 12 & 34cm noted.	Rej
AT11-1475	H10C	35-68	Groove line. Porosity @ 37, 44, 50, 53, 57 & 60 to 63cm. Piping @ 60cm.	Rej
AT11-1475	H10C	68-103	Groove line. Porosity @ 80, 85 to 87 & 97cm.	Acc
AT11-1475	H10C	105-140	Groove line. LOF 120 to 130cm. Linear porosity @132 to 140. Debris in groove @ 119 to 120. Weld root profile in groove. Fillet weld profile noted.	Rej
AT11-1475	H10C	140-155	Groove line. Linear porosity @ 144 to 145 & 149 to 155cm.	Rej

Band I

Item Reference			COMMENTS	Result
AT11-1475	I10A	2-35	Groove. Porosity @ 12cm noted.	Acc
AT11-1475	I10A	35-70	Groove.	Acc
AT11-1475	I10A	70-107	Groove line @ 105 to 107cm. Linear porosity @ 94 to 105cm. Poros @ 85 & 95cm. Fillet weld profile profile noted.	Rej
AT11-1475	I10A	107-140	Groove line @ 107 to 115 & 137cm. Pores @ 125, 127 & 131cm.	Acc
AT11-1475	I10A	140-165	Groove line @ 141 to 164cm. Fillet weld profile noted.	Acc
AT11-1475	I10B	0-34	Groove line. Fillet weld profile noted.	Acc
AT11-1475	I10B	34-64	Groove line 34 to 38 & 58 to 60cm. Fillet weld profile noted.	Acc
AT11-1475	I10B	64-94	Groove line. LOF @74cm. Linear porosity @ 74 to 80, 82 to 84cm. Profile noted.	Rej
AT11-1475	I10C	0-35	Groove line 0 to 5, 10 to 25 & 32 to 35cm. Fillet weld profile noted.	Acc
AT11-1475	I10C	35-70	Groove line. Linear porosity full length intermittent.	Rej
AT11-1475	I10C	70-105	Groove line. Intermittent porosity full length.	Acc
AT11-1475	I10C	105-140	Groove. LOF 107 to 120cm. Linear porosity @ 126 to 140cm.	Rej
AT11-1475	I10C	140-155	Groove. LOF 140 to 14, 146 to 147 & 149 to 154cm.	Rej

Band J

Item Reference			COMMENTS	Result
AT11-147	J10A	0-35	Groove noted. LOF 0 to 8 & 17 to 34cm. Gas pores @ 7, 8 & 14cm noted.	Rej
AT11-147	J10A	35-70	Groove noted. LOF 43 to 70cm. Fillet weld profile noted.	Rej
AT11-147	J10A	75-104	Groove noted. LOF 70 to 104cm.	Rej
AT11-147	J10A	105-140	Groove noted. LOF 105 to 140cm. Fillet weld profile noted.	Rej
AT11-147	J10A	140-158	Groove noted. LOF full length. Fillet weld profile noted.	Rej
AT11-147	J10A	188-222	Groove noted. LOF 188 to 201 & 203 to 222cm. Fillet weld profile ntd. Pressure mark	Rej
AT11-147	J10A	222-255	Groove noted. LOF 222 to 226 & 230 to 255cm. Fillet weld profile noted.	Rej
AT11-147	J10A	255-283	Groove noted LOF full length*. Porosity @ 256cm (3.1mm). Cables noted @ 260cm.	Rej
AT11-147	J10A	283-320	Groove noted. LOF 283 to 285, 287 to 307 & 310 to 320cm. Fillet weld profile noted.	Rej
AT11-147	J10A	351-388	Groove noted. LOF intermittent full length. Fillet weld profile noted.	Rej
AT11-147	J10A	388-425	Groove noted. LOF intermittent full length. Fillet weld profile noted.	Rej
AT11-147	J10A	425-460	Groove noted. LOF intermittent full length. Fillet weld profile noted.	Rej
AT11-147	J10A	460-495	Groove noted. LOF intermittent full length. Fillet weld profile noted.	Rej

Test locations

X-Ray										
Equipment		Rigaku RF-200SPS			kV	100		mA	3	
Focal Spot		2 x 2mm								
Image Plate:		Flex HR			Plate Size:	10cm x 40cm		FFD		mm
Window:		Level:			Exposure Time:					mA Mins.
Screens:	Pb.	Front	0.375	Rear 0.375	IQI Type:	10 AL EN	Sensitivity:	Wire	5	%

TEST LOCATIONS

Item Reference	COMMENTS	Result

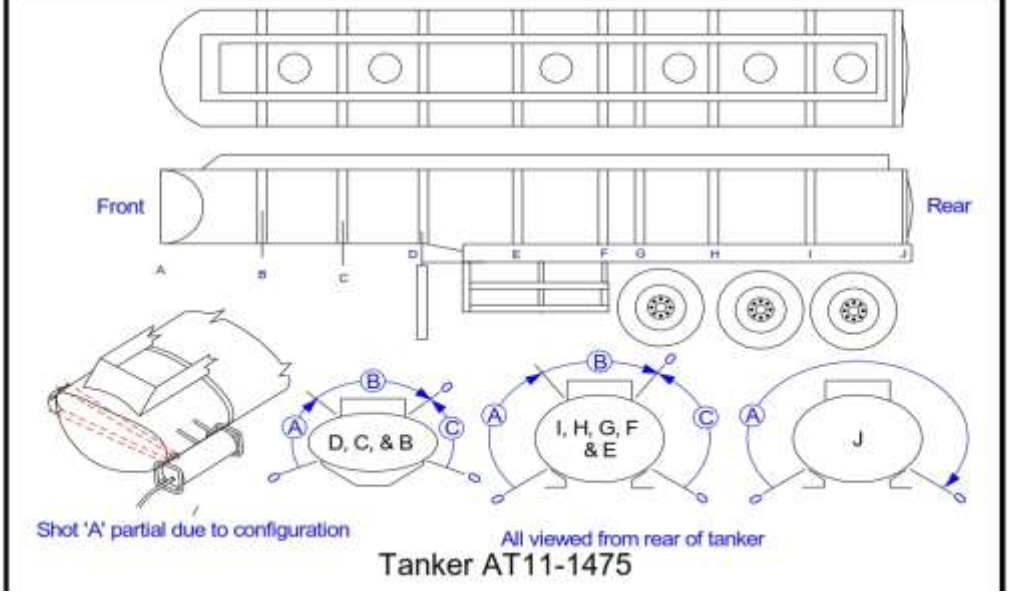

14 APPENDIX 2 - INTERNAL SURVEY – WELD MAPS

Detailed fillet weld location maps for AT11-1475

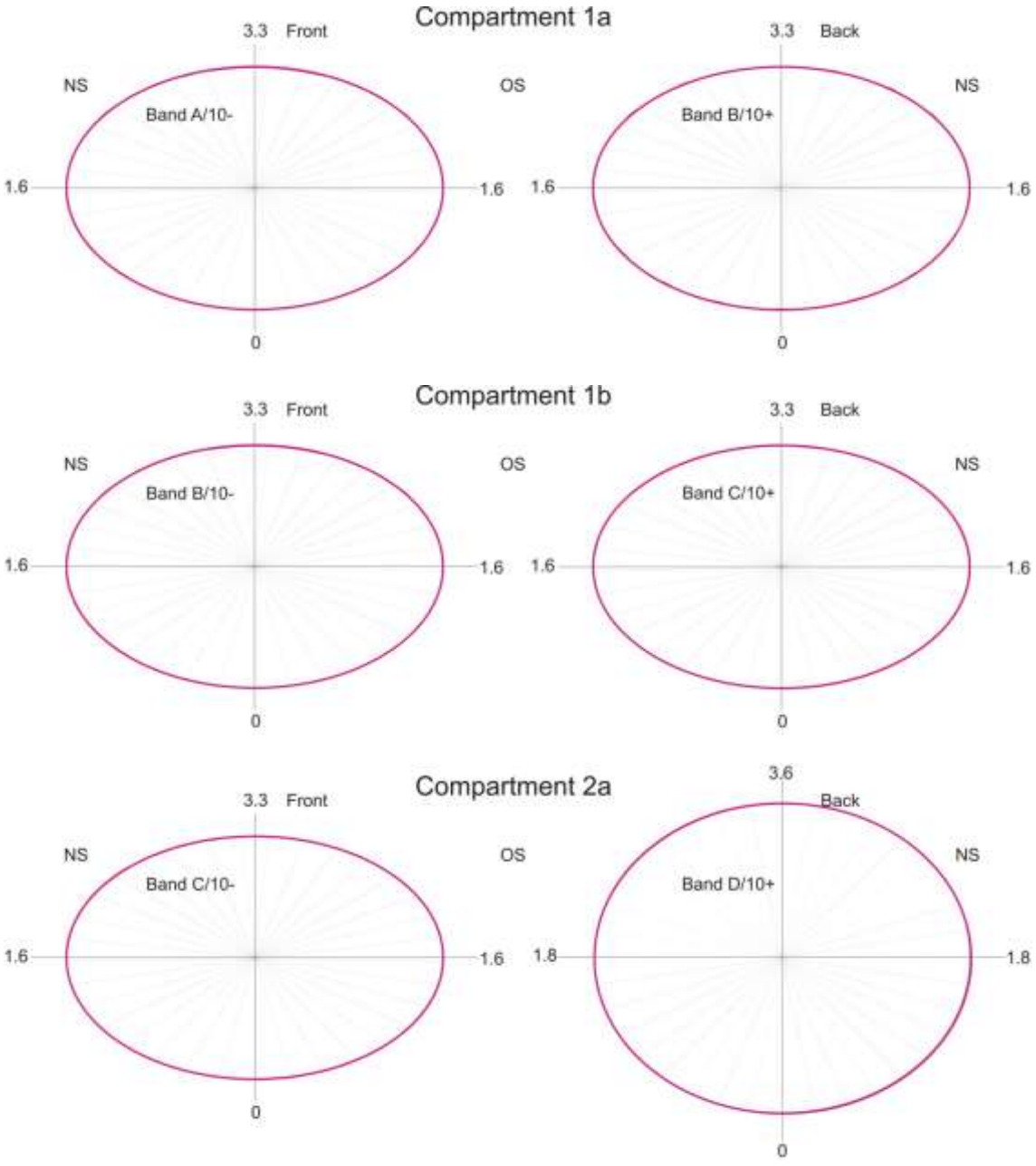

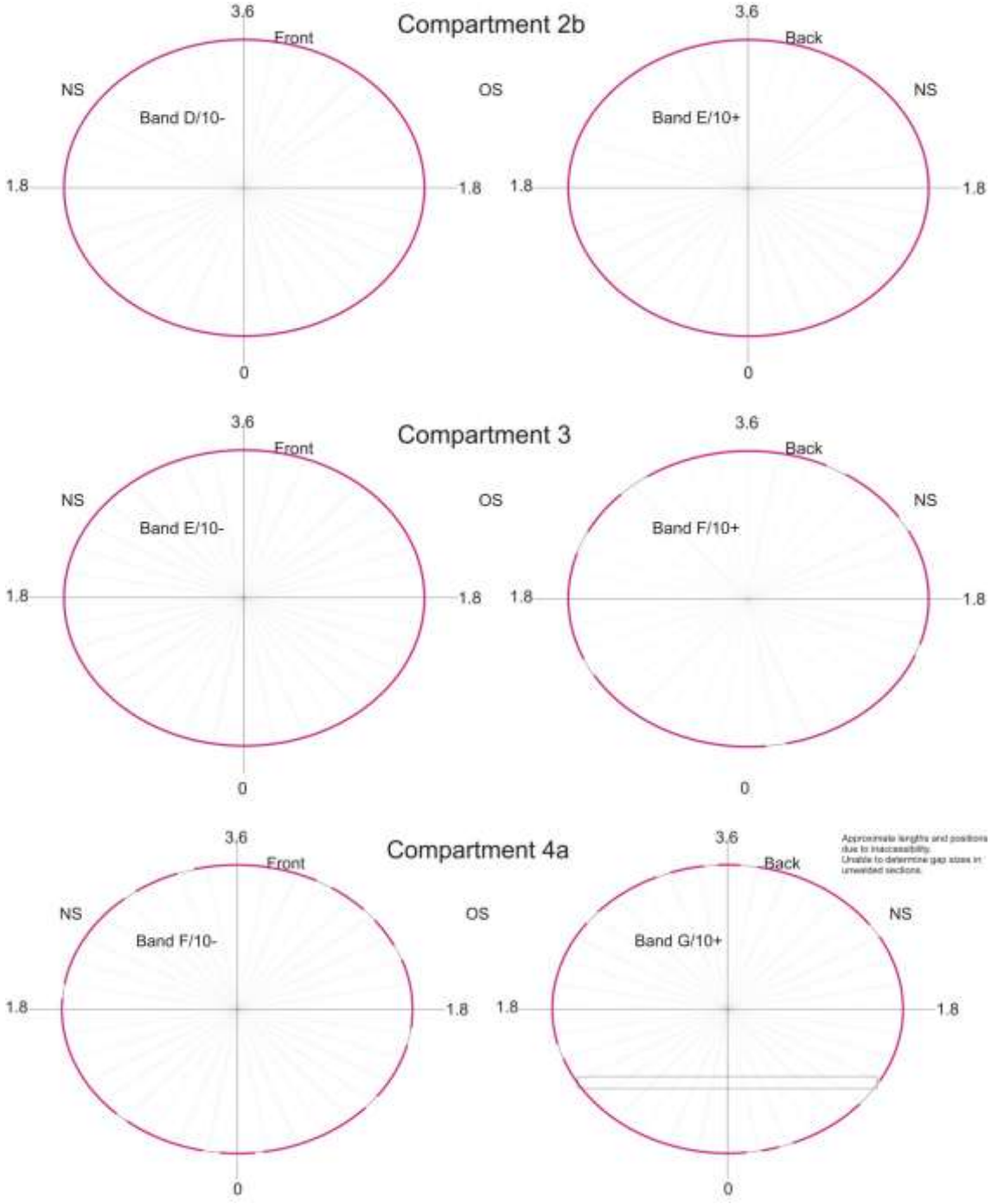
Compartment 2b
3.6
Front
NS
OS
Band D/10-
1.8
1.8
0
3.6
Back
NS
Band E/10+
1.8
1.8
0
Compartment 3
3.6
Front
NS
OS
Band E/10-
1.8
1.8
0
3.6
Back
NS
Band F/10+
1.8
1.8
0
Compartment 4a
3.6
Front
NS
OS
Band F/10-
1.8
1.8
0
3.6
Back
NS
Band G/10+
1.8
1.8
0

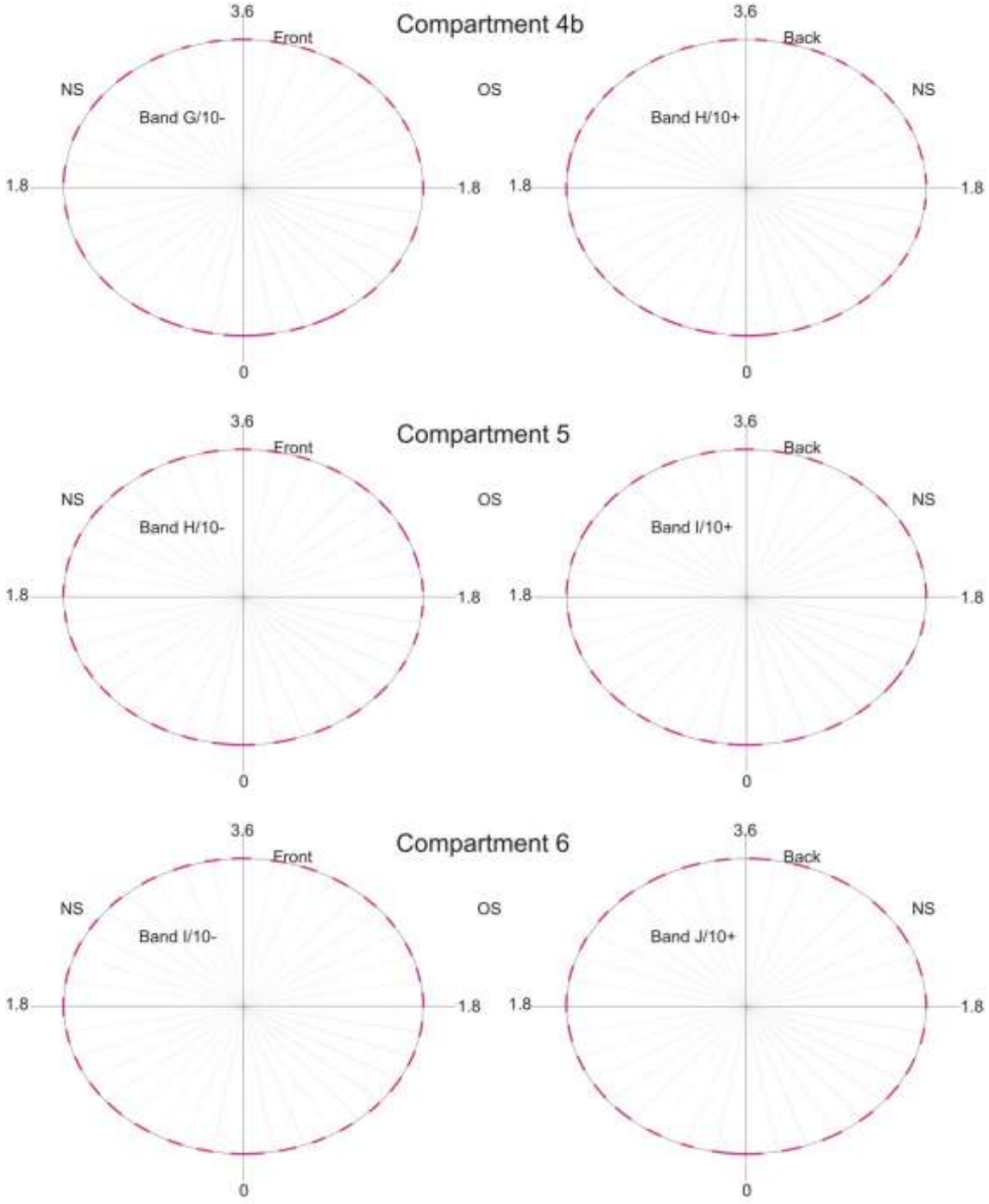
Compartment 4b
3.6
Front
NS
Band G/10-
OS
1.8
1.8
0
3.6
Back
NS
Band H/10+
1.8
1.8
0
Compartment 5
3.6
Front
NS
Band H/10-
OS
1.8
1.8
0
3.6
Back
NS
Band I/10+
1.8
1.8
0
Compartment 6
3.6
Front
NS
Band I/10-
OS
1.8
1.8
0
3.6
Back
NS
Band J/10+
1.8
1.8
0

15 APPENDIX 3 - WELD CAP SURVEY

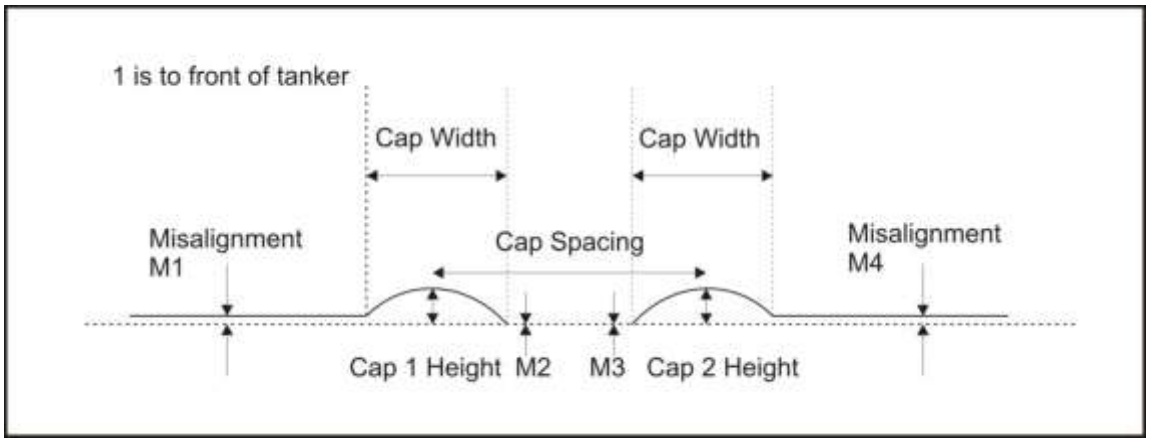

Figure A3.1 Schematic showing the weld cap survey variables

Measurements were carried out on both the offside and nearside of the tanker.
For the front and rear bands (A and J), there was only one weld cap.
For all cap and misalignment measurements - 1 is the nearest to the front of the tanker

Misalignment measurements were obtained as follows (shown in Figure A3.2):

1. Draw a line from the outer two positions of the scan data in each position (i.e. two points nominally on the main tanker surface)
2. Offset this line so it touches only the inner-most point on the scan profile
3. Take the misalignment measurements from the weld profile to this line

M1 is always to the front of the tanker

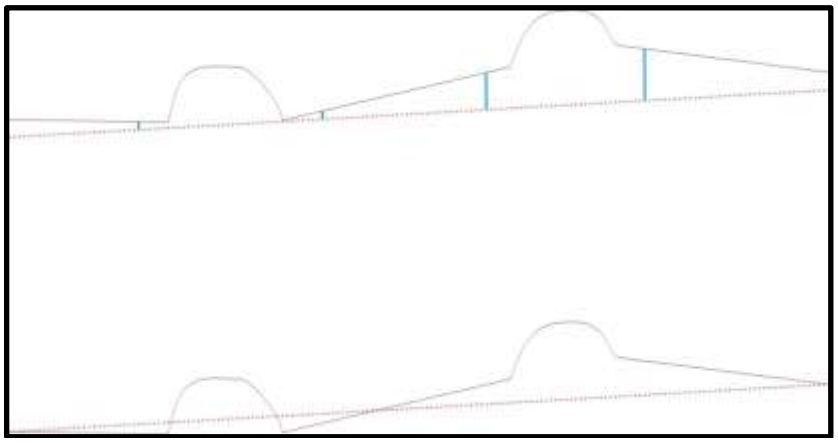

Actions 2 and 3- offset line and measure
Measurements M1 on left to M4 on right as in key above
M1 is always to the front of the tanker

Action 1 - draw line

Figure A3.2 Measuring misalignment

Measurement samples (slices) were taken in three positions on the tanker surface at:

- 30° above the mid-height horizontal plane at;
- the mid-height horizontal plane; and
- 30° below the mid-height horizontal plane.

Figure A3.3 shows these positions.

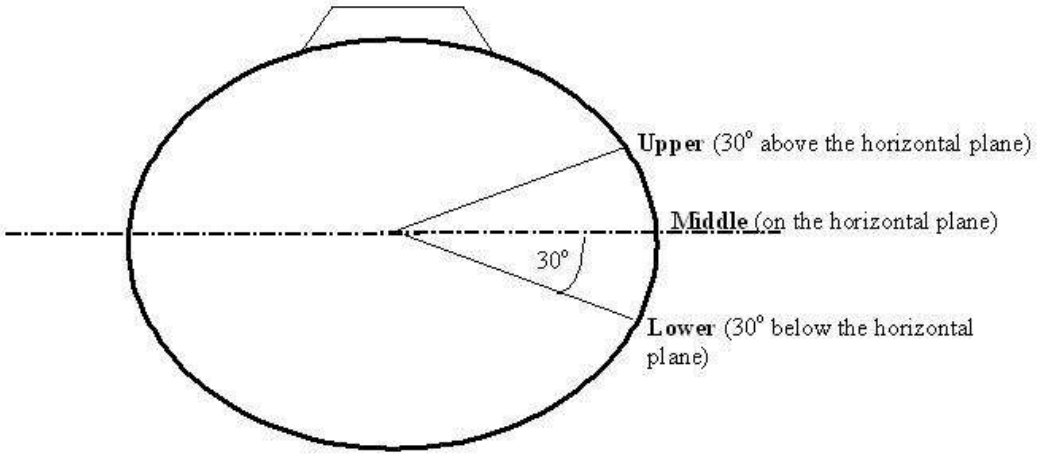

Figure A3.3 Measurement slices for the weld cap survey

Table A3.1 provides the weld cap survey dimensions.

Table A3.1 Weld cap survey data

LAKELAND WELD CAP DATA FROM LASER SCAN - all dimensions mm

Caps and misalignment - 1 is nearest front of tanker

Vehicle Offside slice	Band	Cap Height		Cap Width		Cap Spacing	Misalignment			
		1	2	1	2		1	2	3	4
Upper	B	2.4	2.3	17.4	16	51.1	0.36	0.47	0.56	0.68
30 degrees	C	1.6	2.2	19.2	16.1	50.9	0.67	0.33	0.31	0.64
above horizontal	D	2.6	2.4	14.9	16.2	50.6	0.36	0.54	0.65	0.99
	E	2	2.5	15.7	16.2	49.7	1.72	0.94	0.22	0.39
	F	2.4	2.5	16.9	14.8	50.7	0.52	0.01	0.05	0.28
	G	2.8	2.4	17.1	16.1	90.7	0.48	0.65	0.35	0.42
	H	2.8	2.3	16	16.6	90.5	0.14	0.06	0.19	0.41
	I	2.2	2.8	16.5	14.6	91.8	0.85	0.52	0.06	0.72
Middle	B	2.7	2.5	17	17.1	51.4	0.32	0.2	0.38	0.99
horizontal	C	1.8	2.3	17.2	16	51.1	0.98	0.12	0.21	0.77
(3 o'clock)	D	2.1	2.3	14.9	16.4	50.8	0.17	0.36	0.7	1.15
	E	2.7	2.3	17.2	17.2	50.7	0.78	0.57	0.34	0.49
	F	2.6	2.6	16.8	16.7	51.5	0.69	0.06	0.04	0.35
	G	2.5	2.5	15.5	16.9	91.4	0.4	0.5	0.28	0.55
	H	2	2	17.8	15.8	89.6	0.71	0.07	0.61	1.17
	I	2.2	2.8	17.2	17.5	91.7	0.53	0.13	0.13	0.54
Lower	B	2.7	2.5	17.5	16.7	50.7	0.67	0.11	0.5	0.96
25 degrees	C	1.9	2.4	16.4	16.2	50.6	0.9	0.01	0.51	0.73
below horizontal	D	2	2.1	16.5	15.7	48.9	0.33	1.22	1.95	2.89
	E	2.9	2.3	15.7	15.6	48	0.6	0.94	1.03	1.07
	F	2.3	2.8	16.8	15.8	49.6	0.76	0.11	0.17	0.44
	G	2.3	2.4	17.4	16	91	1.11	0.37	0.31	0.58
	H	2.1	2.4	18.5	17.3	90.2	1.03	0.1	0.83	1.53
	I	2.3	2.5	17	15.6	90.8	0.76	0.48	0.06	1.03

LAKELAND WELD CAP DATA FROM LASER SCAN - all dimensions mm

Caps and misalignment - 1 is nearest front of tanker

Vehicle Nearside slice	Band	Cap Height		Cap Width		Cap Spacing	Misalignment			
		1	2	1	2		1	2	3	4
Upper	B	2.2	2.4	15.9	15.2	50.1	0.26	0.32	0.44	0.55
30 degrees	C	2.4	1.8	15.6	17.2	51.3	0.78	0.53	0.31	0.67
above horizontal	D	2.2	2.3	15.5	16.6	49.7	0.83	0.24	0.29	0.76
	E	2.4	2.7	16.4	17	49	0.21	0.05	0.61	1.26
	F	2.5	2.5	15.7	16.4	50.7	0.22	0.01	0.11	0.6
	G	2.2	2.5	14.9	17.5	90.5	0.22	0.17	0.13	0.6
	H	2.3	2	15.4	17.6	89.6	1.49	0.64	0.05	0.73
	I	2.1	2.3	15.5	16.9	91.9	1.52	0.14	0.47	1.09
Middle	B	2.4	2.4	17.5	16	50.9	0.25	0.01	0.33	0.71
horizontal	C	2.5	2.7	16	15.9	51.2	0.04	0.01	0.08	0.38
(3 o'clock)	D	2.3	2.9	16.6	16.7	49	0.79	0.3	0.2	0.48
	E	2.7	2.7	16.5	16.6	48.3	0.61	0.22	0.32	0.32
	F	2.6	2.5	15.9	15.8	50.3	0.26	0.04	0.02	0.37
	G	2.5	2.6	16.9	17.6	90.7	0.59	0.34	0.39	0.49
	H	2.5	2.4	16.4	17.7	90	1.61	1.06	0.45	0.87
	I	2.5	2.2	16.1	16.8	90.6	0.54	0.21	0.02	0.09
Lower	B	2.4	2.5	16.7	16.7	50.3	0.69	0.17	0.76	0.49
25 degrees	C	2.8	2.7	15.2	16.2	51	0.78	0.53	0.31	0.67
below horizontal	D	2.4	2.5	16.5	16.3	49.9	2.17	1.46	0.46	0.21
	E	2.7	2.7	16.1	16.5	48.1	1.16	0.44	0.41	0.43
	F	2.6	2.4	17.9	16.1	51.4	0.13	0.04	0.28	0.61
	G	2.6	2.7	15.6	17.9	90.7	0.5	0.11	0.05	0.51
	H	2.5	2.1	17.1	16.6	90.3	1.67	0.77	0.1	0.48
	I	2.7	2.3	16.7	17.7	91.7	0.48	0.18	0.21	0.5

Upper slice on band 4 scan only covered one weld

16 APPENDIX 4 – INSTRUMENTATION TEST DATA

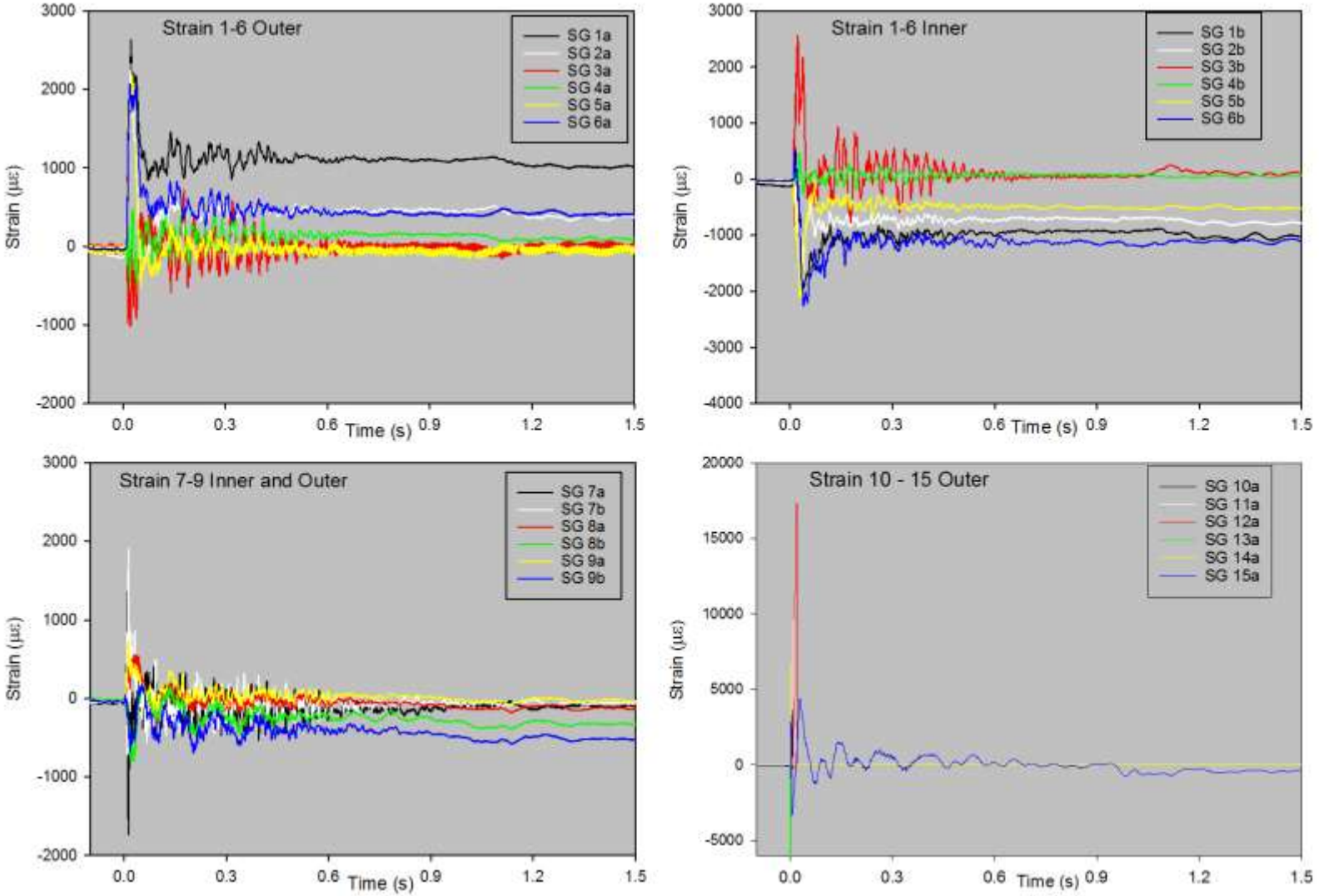

Figure A4.1 AT11-1475 Strain measurements – all gauges (full time history)

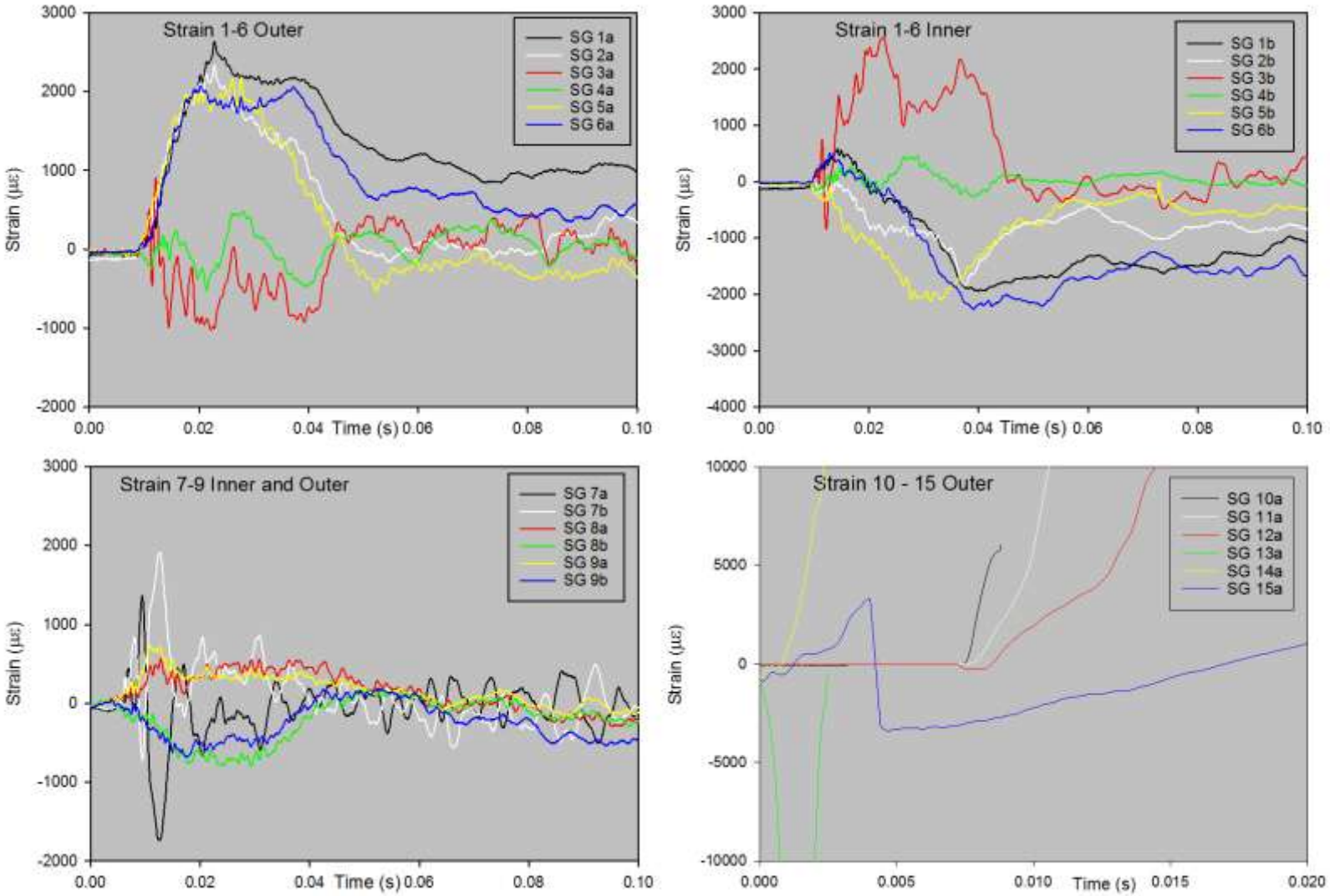

Figure A4.2 AT11-1475 Strain measurements – all gauges (event only)

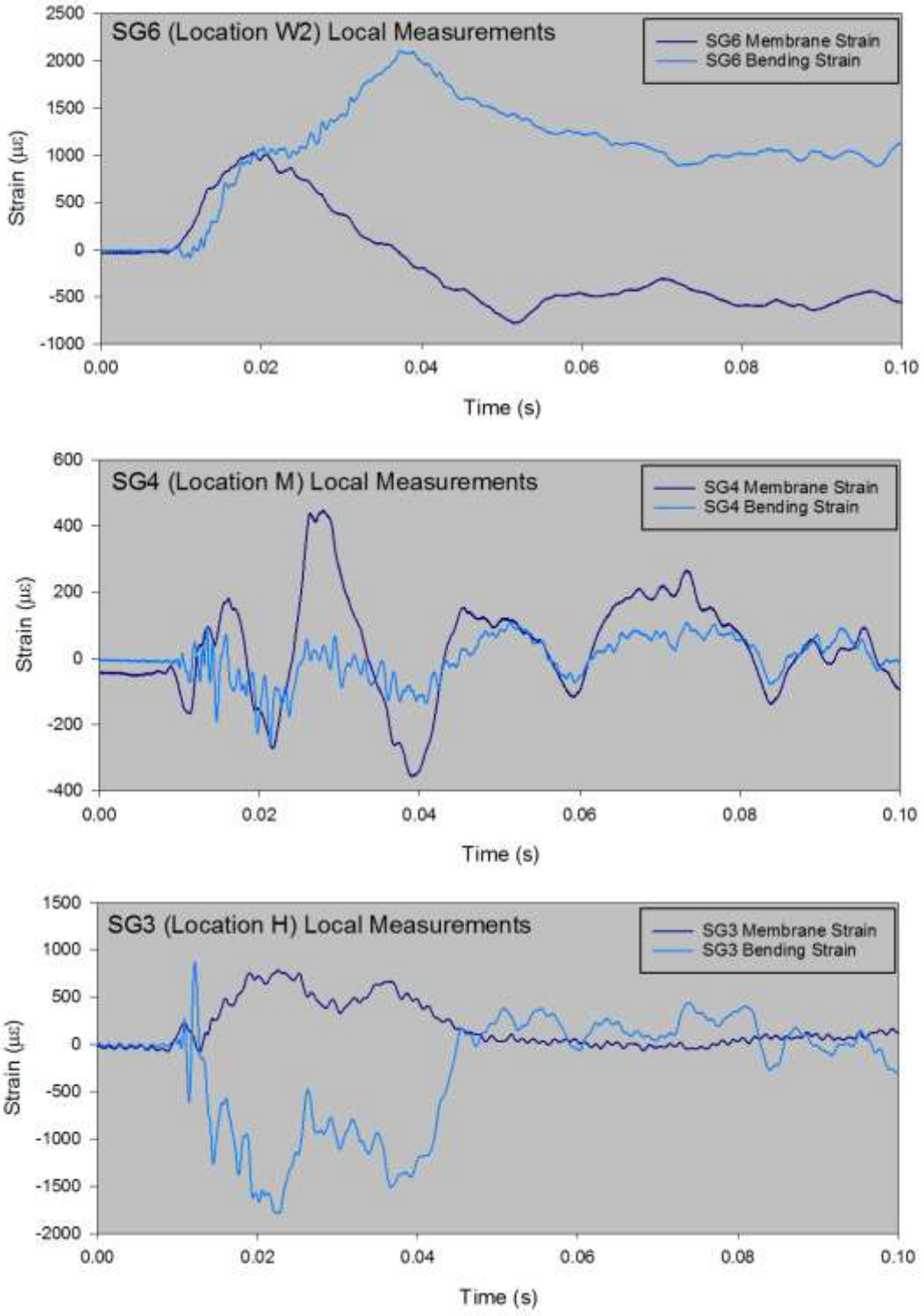

Figure A4.3 AT11-1475 Membrane and bending strain compartment 1

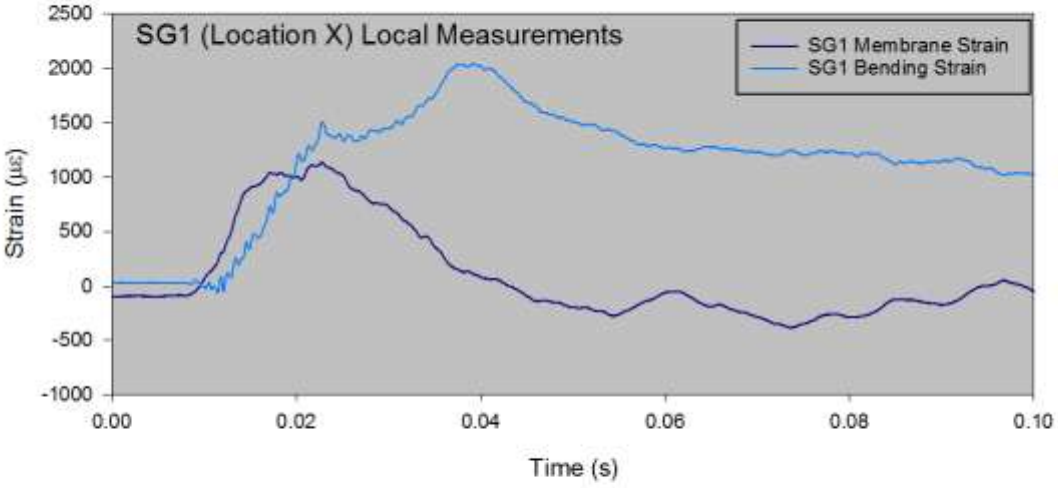

Figure A4.4 AT11-1475 Membrane and bending strain compartment 1 (continued)

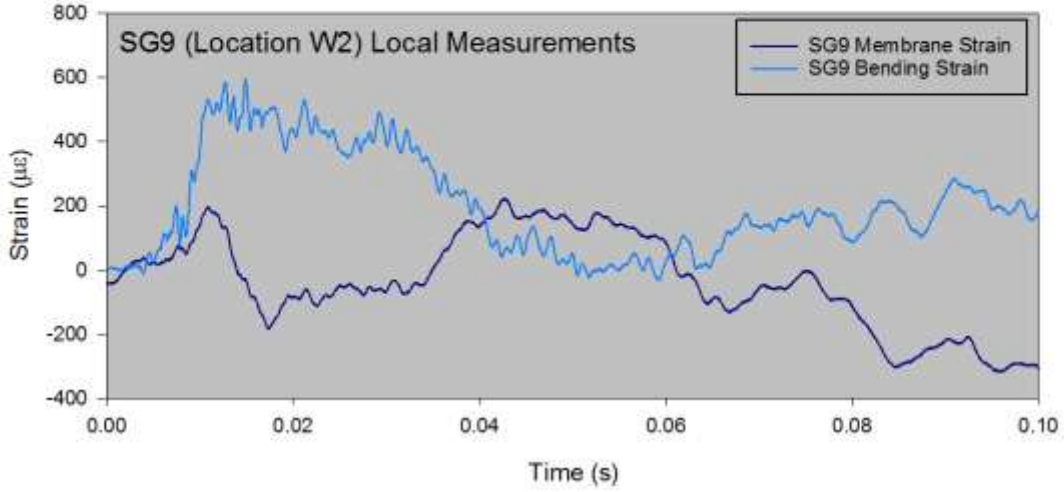

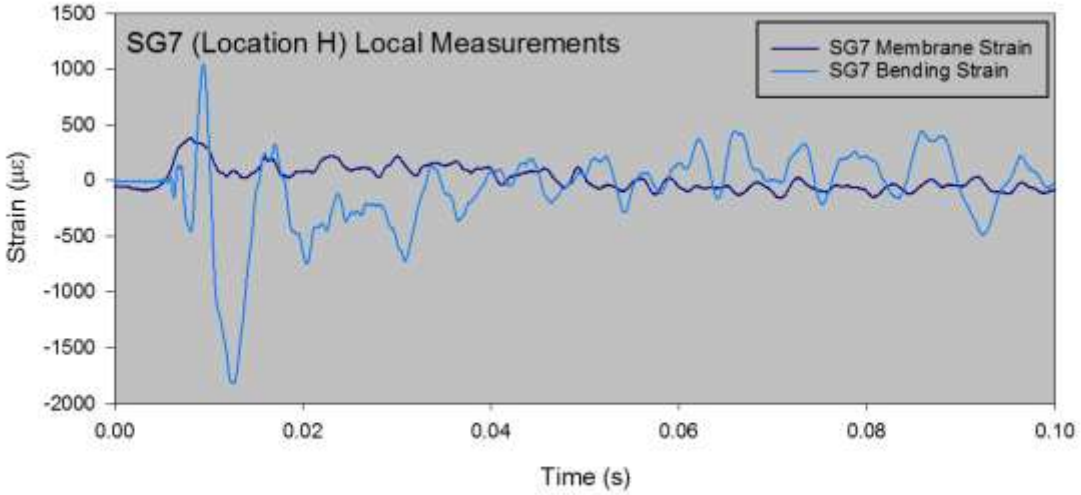

Figure A4.5 AT11-1475 Membrane and bending strain compartment 4

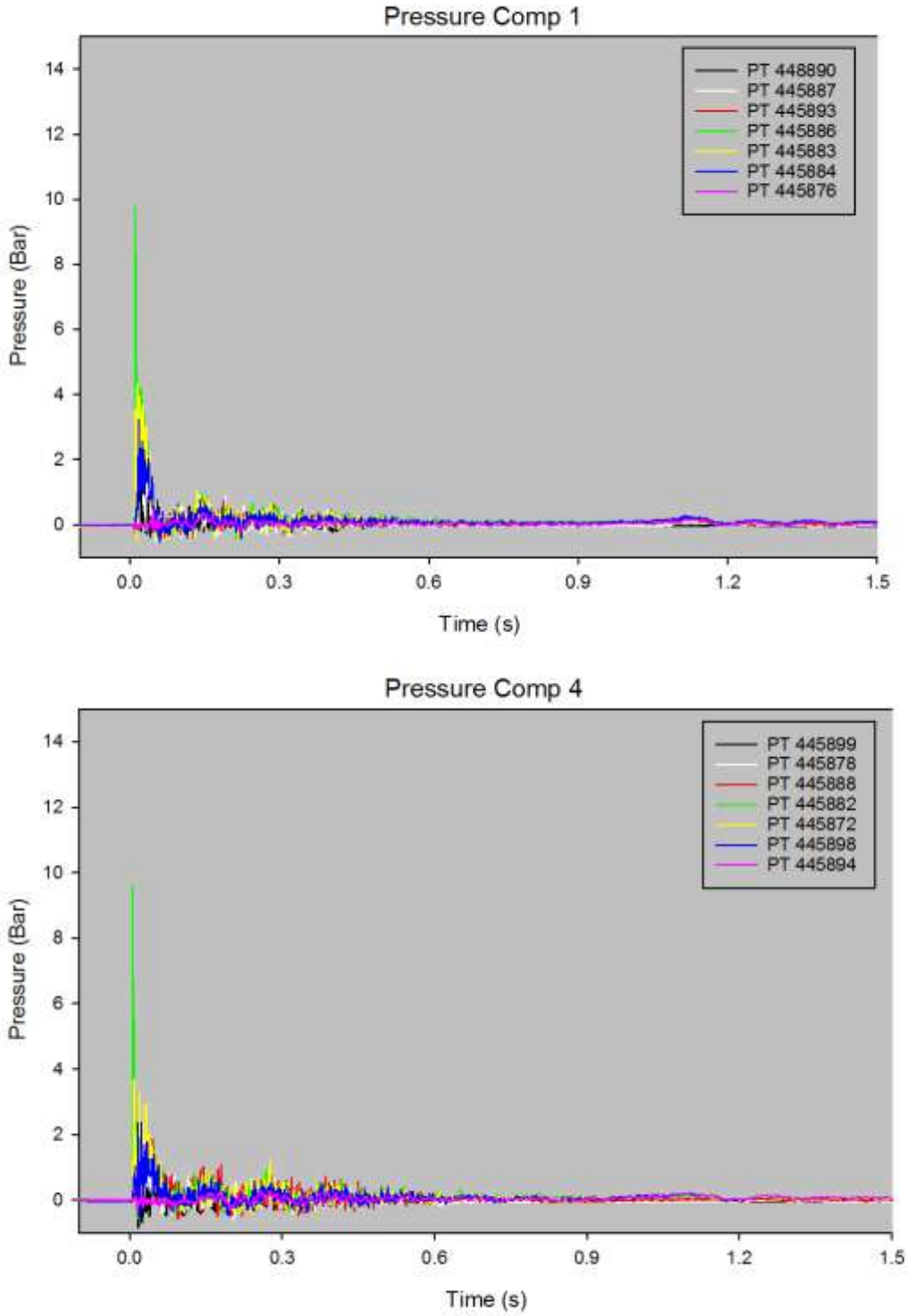

Figure A4.6 Pressure measurements – all transducers (full time history)

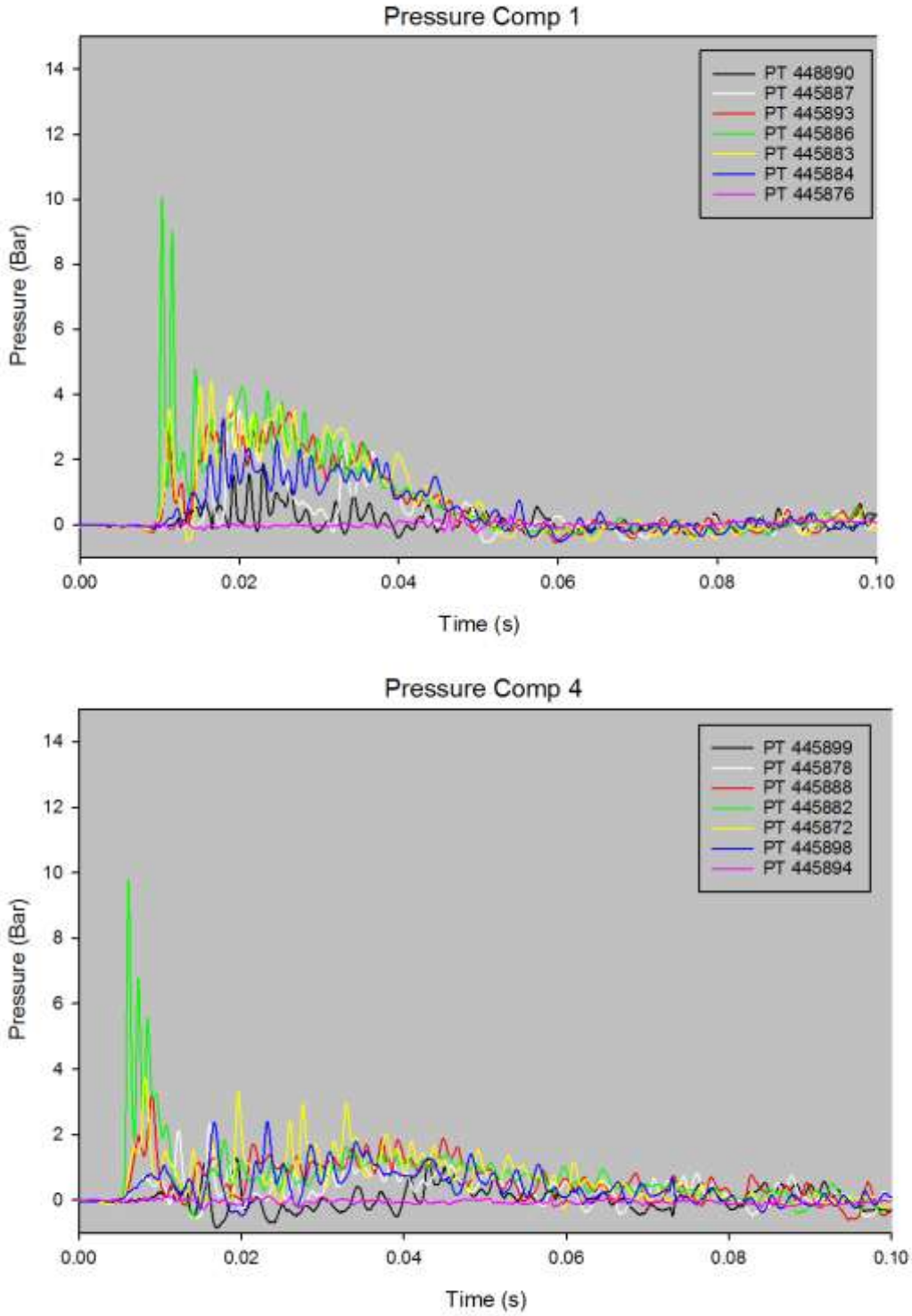

Figure A4.7 Pressure measurements – all transducers (impact event only)

17 APPENDIX 5 – TWI REPORT 24000/13/15

Report No: 24000/13/15

Date: 04 September 2015

For: Department for Transport

TWI Ltd

TWI is one of the world's foremost independent research and technology organisations, with expertise in solving problems in all aspects of manufacturing, fabrication and whole-life integrity management technologies.

Established at Abington, Cambridge, UK in 1946 and with facilities across the globe, the company has a first-class reputation for service through its teams of internationally respected consultants, scientists, engineers and support staff. The company employs over 900 staff, serving over 700 Member companies across 4500 sites in 80 countries.

TWI is a non-profit distributing company, limited by guarantee and owned by its Members. It can therefore offer confidential, independent advice and is internationally renowned for employing multidisciplinary teams to implement established or advanced joining technology or to address issues associated with initial design, materials selection, production and quality assurance, through to service performance and repair.

Supported by a successful international training and examinations network, TWI also takes technical and practical knowhow to regions looking for growth through skills development.

TWI houses the National Structural Integrity Research Centre for postgraduate education, and a professional institution, The Welding Institute, which has a separate membership of over 6000 individuals.

The company operates a management system certificated by LRQA to BS EN ISO 9001:2008. It also has certificated management systems for health and safety (BS OHSAS 18001) and environment (BS EN ISO 14001).

(See inside back cover TWI Management System.)

TWI Ltd, Granta Park, Great Abington, Cambridge CB21 6AL, United Kingdom. Tel: +44 (0)1223 899000

TWI Report: Department for Transport Technical Assessment of Petroleum Tankers: Metallographic and Analytical Assessment of AT11-1475

Report No: 24000/13/15

Date: 04 September 2015

Prepared for: Department for Transport
c/o Zone 2/31
Great Minster House
33 Horseferry Road
London
SW1P 4DR

Contact: Steve Gillingham

Author: Tyler London

TWI Endorsement

This report has been reviewed in accordance with TWI Policy

Project Leader (Signature) Tyler London

Print name: Tyler London

Technical Reviewer (Signature) pp CM Worrall

Print name: Simon Smith

Approved by Ian Norris
Product Manager
(Signature)

Print name: Ian Norris

Approved by
Group Commercial Manager
(Signature)

Print name: Andrew Carey

Administrator (Signature) ERaven

Print name: Emma Raven

er

Published Version History

Date	Version	Reason
29/05/2015	0.1	Draft Issue
10/07/2015	0.2	Draft issue incorporating consortium comments
27/07/2015	0.3	Additional editorial changes
04/09/2015	1.0	Incorporation of consortium comments

er

Contents

1 Introduction

As part of the Department for Transport (DfT) research programme on petroleum road fuel tankers, the Health and Safety Laboratory (HSL) has performed a full-scale topple test of the petroleum road fuel tanker AT11-1475. Under Work Package 2 Extensions of the DfT research programme, TWI has been requested to provide numerical analysis and metallographic examinations of sections removed from AT11-1475 after the topple test in order to provide supporting information for the Health and Safety Laboratory (HSL) technical report.

This report details the examination of sections removed from the front and rear ends of the tanker as well as finite element analyses (FEA) that were undertaken to provide insight into the performance of AT11-1475 under the topple test conditions.

2 Objectives

The objectives of the present work are to undertake:

- A detailed macroscopic and microscopic examination of sections from the front and rear circumferential joints of tanker AT11-1475.
- Tensile testing on samples machined from the parent metal, weld metal and extrusion band metal.
- FEA in conjunction with a forming limit diagram to determine the likelihood of failures in the parent metal during a topple test.

3 Post-mortem and Metallographic Examination

3.1 Overview

Petroleum road fuel tanker AT11-1475 is an aluminium-bodied, banded-design. Each adjacent barrel or cylindrical section of aluminium alloy 5182 (henceforth referred to as the 'tanker shell') is joined by a circumferential joint similar to the informative joint design D.14(b) and D.14(c) from BS EN 13094 (2015) shown in Figure 1. In this joint configuration, the partition dish, bulkhead, baffle or end dish is also made of AA 5182. For the rear band (referred to in the main report as band J/10 rear), where there is no adjacent section of tanker shell, only one primary circumferential weld is made. All other circumferential joints except for the front joint are similar to that shown in Figure 1. However, due to the unique design of the front 'swept' dish of AT11-1475 (see, for example, Figure 3), the front-most circumferential joint (referred to in the main report as band A/10 front) is a double-sided corner joint between the dish and the tanker shell, similar to D.9(b) from BS EN 13094 (2015) also shown in Figure 1.

Following the topple test, sections of the undamaged nearside and the impacted offside were removed from AT11-1475 from both the front and rear of the tanker and sent to TWI by HSL. Images of the approximate locations of the sections are shown in Figure 2 for the rear of the tank and in Figure 3 for the front of the tank. Following receipt, the sections were photographed, radiographed, and then additional sampling was undertaken to analyse cross-sections of the circumferential joints.

3.2 Radiographic examination

Radiographic inspection was undertaken to identify the location and position of potential welding defects in each of the sections.

For the rear end sections, the primary circumferential welds (ie those joining the tanker shell to the extrusion band) were radiographed. For the rear offside

(impacted side) section, the datum markers are shown in Figure 4 and the radiographic interpretation is summarised in Table 1. For the rear nearside section, the datum markers are shown in Figure 5 and the radiographic interpretation is summarised in Table 2.

For the front end sections, the circumferential joint between the swept front dish and the first tanker compartment was radiographed. For the front offside (impacted side) section, the datum markers are shown in Figure 6 and the radiographic interpretation is summarised in Table 3. For the front nearside section, the datum markers are shown in Figure 7 and the radiographic interpretation is summarised in Table 4.

3.3 Metallographic examination of samples

Based on the shape of the deformed sections and the results of the radiographic examination, amongst other considerations, the four large sections were sampled at between three and seven different locations each along their circumferential length. Table 5 summarises the sample IDs, the section from which they were machined, and an approximate description of the location of each sample.

Seven samples were machined in the longitudinal direction (transverse to the circumferential welds) from the impacted, rear offside section of AT11-1475. The locations of the samples are shown in Figure 8. From the seven samples, five were removed from the crushed region of the section that impacted the ground during the topple test. The remaining two samples were taken from a region remote from the impact zone: one sample (RO-01) was removed where there was no additional internal fillet weld present (see 'F' in Figure 1), and the other (RO-02) was removed from a location near RO-01 where an additional internal fillet weld was present. For the rear band of AT11-1475, the internal fillet welds were 'stitched' around the circumference, with 50mm weld lengths and 50mm gaps between the welds. In Figure 9, images of samples RO-01, RO-02 and RO-03 are shown. Sample RO-01 and RO-03 exhibit porosity and lack of penetration into the root of the weld, resulting in an approximately 2.0mm deep, surface-breaking, lack of fusion defect. Sample RO-02, however, shows good penetration into the root and there is no lack of fusion defect present. Images of the remaining samples (RO-04 to RO-07) are shown in Figures 10 and 11. In Sample RO-04 (Figure 10), the internal fillet weld joining the toe of the extrusion band to the inner surface of the tanker shell has failed with a crack propagating along the fusion line with the inner surface of the tanker shell. Images of the RO-05, RO-06 and RO-07 from the rear offside are shown in Figure 11. All of these samples exhibit surface-breaking, lack of root fusion defects due to the weld not fully penetrating into the root. The typical depth of these defects ranges from 1.0mm to 2.0mm. For comparison, macro-images of all of the primary circumferential welds (see 'C' in Figure 1) are shown together in Figure 12. In these images, the penetration into the root of the weld is variable. Due to the absence of a through-wall rupture, no additional sampling was undertaken between samples RO-03 and RO-07, and therefore it is not possible to specify the precise circumferential (surface) length of these lack of fusion, surface-breaking defects; however, since the lack of fusion is evident on samples RO-03 through RO-07, in view of the radiography, it is possible to conservatively estimate that the lack of fusion persists continuously between these sampling points and hence has a total surface length of approximately 700mm.

Four samples were machined from the undamaged, rear nearside section of AT11-1475. The locations of the samples are shown in Figure 13. The four

samples were spaced approximately 125mm apart. Samples RN-01 to RN- are shown in Figure 14. All of the primary circumferential welds from the rear nearside samples are shown in Figure 15. As with the rear offside, the penetration into the root of the weld is variable, with sample RN-03 exhibiting good penetration and fusion between the tanker shell and extrusion band, whilst samples RN-01, RN-02 and RN-04 show signs of lack of fusion at the root of the weld, resulting in surface-breaking defects that are up to 1.5mm deep.

The main circumferential welds in the samples from both the rear offside and rear nearside were shown to exhibit weld caps (or overfill) typically in excess of 3.0mm as measured from the outer surface of the tanker shell. Previous research on tanker performance under topple test conditions (TWI, 2015) has demonstrated the benefits that a large weld cap can have in resisting the bending moments experienced by the joint under topple test conditions. Nevertheless, an excessive weld cap can also be indicative of poor root penetration, which is evident in many of the samples taken from the rear welds. All weld samples from the rear offside and rear near side showed very good alignment, with axial misalignment measurements typically being less than 0.5mm. The previous TWI research (2015) also demonstrated the significant effect of misalignment on the acceptability of defects; specifically, the maximum tolerable defect size under topple test conditions reduced rapidly as the level of axial misalignment increased. Thus, although a surface-breaking, lack of root fusion defect is present in many of the rear weld samples, it is likely that the combination of good joint alignment and relatively large weld cap size contributed to the lack of failure during the topple test.

Six samples were machined in the longitudinal direction from the impacted, front offside section of AT11-1475. As described in Section 3.1, all circumferential joints in AT11-1475 are geometrically similar to that shown in Figure 1 except for the front-most joint, which is a double-sided corner joint due to the swept design of the front dish. Of the six samples, five were taken from the crush zone (ie the large plastic bulge that comprises the flattened region that impacted the ground) and one additional sample (FO-01) was taken remote from the crush zone. The locations of the samples are illustrated in Figure 16. In Figure 17, images of the corner joint are shown for each sample from the front offside. Whilst the front circumferential joint has undergone extensive plastic deformation during the topple test as evidenced by the severe bending shown in Figure 17, none of these exhibit any evidence of cracking.

Finally, three samples were machined from the undamaged, front nearside of the tank as illustrated in Figure 18. Images of the welds from these samples are shown in Figure 19.

3.4 Tensile testing

Tensile testing was undertaken on material samples machined from the undamaged rear, nearside section of AT11-1475.

Two tensile specimens were prepared from the tanker shell material in the joints shown in Figure 20 (labelled M01-01 and M01-02). These specimens were taken in the circumferential orientation and machined as flat bar specimens. Weld metal specimens could not be machined from the primary circumferential welds joining the tanker shell to the extrusion band because of the need to avoid the potential presence of lack of fusion defects that could affect the tensile testing results. Instead, two flat bar, all-weld metal specimens were machined from the weld joining the rear dish to the top of the extrusion band (see the top weld labelled 'E' in Figure 1). These specimens are labelled M02-01

and M02-02 in Figure 20. Finally, two round bar specimens were machined from circumferentially-oriented material from the centre of the up-stand of the extrusion band. These specimens are labelled M03-01 and M03-02 in Figure 20.

The flat bar tensile specimens were of nominal width 6.0mm and parallel length 32.0mm, marked with a 25.0mm gauge length for determination of plastic elongation. The specimens were instrumented with a dual averaging HRD auto extensometer of gauge length 25.0mm for the determination of total elongation (at fracture) and tested at ambient temperature. The choice of ambient temperature instead of the minimum ADR design temperature (-20°C) was made to more closely match the conditions of the topple test. The applied strain was recorded through the entire test. Up to the yield point, the applied strain rate was 0.015 strain/min, and beyond the yield point, the applied strain rate was 0.400 strain/min.

The round bar tensile specimens were of nominal diameter 8.0mm and parallel length 48.0mm, marked with a 5X diameter gauge length for determination of plastic elongation. The specimens were instrumented with a dual averaging extensometer and tested at ambient temperature.

The stress-strain curves showed that the weld metal slightly overmatches the tanker shell metal, and that the tanker shell metal has tensile properties that are generally in agreement with the anticipated properties of the aluminium alloy Al-5182. The extrusion band metal significantly overmatches both the parent and weld metal curves, exhibiting a higher yield point, ultimate tensile strength and smaller elongation.

4 Forming Limit Diagram Assessment

4.1 Overview

In order to provide additional numerical and analytical understanding of the performance of the tanker under the topple test conditions, finite element analyses have been conducted on the front and rear circumferential joints. The FEA performed and described in this report is a simplified, static model of the topple test. The dynamic and inertial effects experienced during the actual topple test are ignored and only the deformation of the tank due to the 'crushing' effect of the ground and the pressure exerted by the water contained in the compartments on the internal surfaces of the tank are considered. The results of the FEA have been assessed using a forming limit diagram methodology to determine whether ruptures in the parent metal or weld metal would occur due to the deformation exceeding the formability limit of the tanker shell material, Al-5182.

4.2 Finite element modelling

4.2.1 Software

All models were generated using version 6.14-1 of the pre-processing finite element analysis software Abaqus/CAE and the analyses were solved using version 6.14-1 of Abaqus/Standard (SIMULIA, 2014).

4.2.2 Geometry

Two different models were created: one for the rear dish and one for the front dish. All models were created using the CAD capabilities of Abaqus/CAE and were developed from engineering drawings provided by Lakeland Ltd (2004a-c, 2005, 2011, 2015). The dimensions in the engineering drawings were compared with those measured from the sections of AT11-1475 received from HSL and

any differences were incorporated into the model as appropriate. Due to symmetry considerations with respect to the geometry and applied loads, only one-quarter of the rear and front sections were modelled.

The rear dish model comprised of the extrusion profile, rear dish and tanker shell. In order to facilitate the accurate resolution of the extensive bending that the rear dish undergoes during the topple test, the rear dish was modelled as a shell part and meshed with quadratic, reduced-integration, shell elements (type S8R in Abaqus) with nine integration points through thickness. The rest of the geometry was modelled as a solid body. Except for the regions that were in contact with the ground, all solid regions were meshed with 20-node, quadratic-displacement, reduced-integration elements (type C3D20R in Abaqus). In order to improve contact convergence, several layers of elements that would be in contact with the ground were meshed with 8-node, linear-displacement, reduced-integration elements (type C3D8R in Abaqus). A tie constraint was used to join the incompatible interfaces between the solid linear elements and solid quadratic elements. A shell-to-solid coupling was defined between the shell part (rear dish) and the solid part (extrusion band) to ensure continuity of displacements and rotations across this interface. Images of the geometry, finite element mesh and boundary conditions for the rear dish are shown in Figure 21 and 22.

The front dish model was modelled as a single, solid body and comprised entirely of solid, quadratic continuum elements. Images of the geometry, finite element mesh, and boundary conditions for the front dish are shown in Figure 23 and 24.

4.2.3 Material properties

Two different material regions were included in the rear dish model: one for the tanker shell, weld metal and rear dish, and one for the extrusion band. For both regions, the lower-bound engineering stress-strain curves obtained from tensile testing were transformed to true stress-true plastic strain curves and sampled at 20-30 equally-spaced points. For both materials, the Young's modulus was taken to be 70GPa and the Poisson's ratio was taken to be 0.3, which agree with the test measurements and with the typical elastic constants for this material (MatWeb, 2015). A rate-independent plasticity model using the Von Mises yield criterion and isotropic strain hardening rule was specified using the incremental plasticity data obtained from sampling the tensile curves. In the front dish model, no extrusion band was present, and the entire model was comprised of the lower-bound parent metal material.

4.2.4 Loads and boundary conditions

A flat, analytic rigid body was created to model the ground and was coupled to a centrally-positioned reference node. All degrees of freedom of this reference node were restrained (set equal to zero) except for U2, the translational degree of freedom in the crushing direction. A contact definition was created between the ground and the tanker model with hard, normal contact and a penalty friction coefficient of 0.1. A 250mm displacement was applied in the crushing direction (ie into the tanker section) to simulate the static impact of the ground and tank. The magnitude of this displacement is somewhat arbitrary, as it was chosen to be sufficiently large so as to ensure the simulation would achieve the same flattened length measured from the specimens after the topple test (see Section 4.2.5). The boundary conditions applied to the tanker geometry were those representing the symmetry planes and axial restraint, simulating the longer adjacent section of tanker that was not incorporated into the model. All

simulations were analysed with the finite strain formulation, incorporating the nonlinear effects of large displacements and rotations.

4.2.5 Results

After the topple test, the flattened length of the rear band (ie the length of the crush zone) was approximately 760mm, and the flattened length of the front circumferential joint was approximately 580mm. Therefore, for each simulation, the ground was translated into the tanker model until the flattened length of the deformed model matched that measured on the sections removed from AT11-1475.

The deformation and Von Mises stress contour for the rear dish model is shown in Figure 25 at the solution increment when the flattened length was 760mm. The deformation of the rear dish model showed exceptional agreement with the samples taken from the rear, offside section of AT11-1475. In particular, the shape, curvature and dimensions of the crush zone agreed with the samples taken from the centre (sample RO-05, see Figure 26) as well as the ends of the crush zone (sample RO-03, see Figure 27). For this reason, the model was considered to be a reasonably accurate representation of the topple test.

The deformation and Von Mises stress contour for the front dish model is shown in Figure 28 at the solution increment when the flattened length was approximately 580mm. As with the rear band model, the front dish model showed very good agreement with measurements taken from samples of the front, offside section of AT11-1475.

To assess the likelihood of cracking occurring in the parent or weld metal, a forming limit diagram (FLD) approach was employed. Technical details about the forming limit diagram methodology are provided in Li (2011), Abedrabbo et al (2006) and Soare (2007). Essentially, a forming limit diagram provides a graphical description of material failure tests such as biaxial tension tests and punched dome tests. The diagram comprises a 'safe' region and an 'unsafe' region separated by the forming limit curve. The forming limit curve is defined as a locus of points with x-coordinate minor strain and y-coordinate major strain. FLDs are typically employed in the sheet metal forming industry to determine the propensity for cracks to appear during cold-forming, bending and stamping. Due to the thin nature of sheets, the through-wall strains are negligible, and therefore the strain state at any given point can be wholly described by the minor and major principal strains. For the present analyses, the large span of the end dishes relative to the wall thickness enables the forming limit diagram approach to be used. A literature review of FLDs for Al 5182-O, the aluminium alloy of the end dishes and tanker shell, was undertaken to provide an approximate forming limit curve suitable for the present analysis. Whilst FLDs have some dependency on strain-rate, thickness, temperature, heat treatment and pre-strain, a representative curve, obtained from the literature review (Wu et al, 2003), was employed for the present study. The results obtained from this forming limit curve described below have provided reasonable comparisons to the topple test results, and therefore these additional dependencies had only secondary influences.

For the rear band model, a circumferential path of nodes was created in the region where the principal strains were largest. This path of nodes was located on the inner surface of the rear dish at the extrados (tensile side) of the bend comprising the crushed zone. For each node in this path, the maximum principal (major) strain and minimum principal (minor) strain were output at the solution increment when the flattened length was 760mm. The pairs of

minor strain and major strain were plotted on the FLD against the forming limit curve from Wu et al (2003) as shown in Figure 29. In this figure, the red curve (strains from the FE model) lies below the forming limit curve (black curve). This indicates that the forming limit diagram approach does not predict failure to occur. This result agrees with the observations from the topple test and subsequent metallographic examinations, where no cracking or failure of the rear dish was seen.

For the front dish model, a circumferential path of nodes was created along the corner joint between the swept design front dish and the tanker shell. As with the rear band model, the maximum and minimum principal strains were extracted at each node on this path and the results were plotted on the forming limit diagram in Figure 30. Again, the strains from the model all lie below the forming limit curve and hence the FLD approach does not predict failure to occur, which agrees with the lack of failure observed in the front dish after the topple test and subsequent metallographic examinations.

5 Conclusions

Metallographic examinations and detailed numerical analyses have been undertaken to provide supplementary information about the performance of the petroleum road fuel tanker AT11-1475 after topple testing. These investigations found that:

1. No through wall ruptures were observed in any of the samples taken from the front or rear welds of AT11-1475.
2. The samples from the front circumferential joint did not exhibit any significant lack of fusion defects.
3. The samples of the rear circumferential joint exhibited variable root penetration in the main circumferential welds. This resulted in some internal surface-breaking, lack of root fusion defects being observed with typical defect depths ranging from 1.0mm to 2.0mm.
4. For the rear weld samples, the joints were found to exhibit good alignment, typically within 0.5mm, and the height of the weld caps of the main circumferential welds was found to be typically in excess of 3.0mm. The combination of low misalignment and large weld caps likely contributed to the good performance of the joints under the topple test. However, the excessive weld cap size was seen to correlate with lack of root penetration (and lack of root fusion defects) in many samples.
5. Finite element modelling of a static, idealised representation of the end dish under topple test conditions in conjunction with a forming limit diagram methodology correctly predicted that the front swept dish and rear end dish of AT11-1475 would not rupture during the topple test. The model also accurately predicted the tanker front swept dish and rear end dish deformations and therefore represents a valuable approach for future assessments of tanker performance under these conditions.

6 References

Abedrabbo N, Pourbogrhat F and Carsley J (2006): 'Forming of AA5182-O and AA5754-O at elevated temperatures using coupled thermo-mechanical finite element models', International Journal of Plasticity, Vol 23, pp 841-875.

BSI (2015): 'BS EN 13094:2015 Tanks for the transport of dangerous goods – Metallic tanks with a working pressure not exceeding 0.5bar – Design and Construction', BSI Standards Publication.

Li J (2011): 'Characterization of post-annealing mechanical behaviour of preformed aluminium alloy 5182-O', University of Michigan PhD Dissertation.

Lakeland (2004a): 'Main Division – Semi-trailer', Document Ref: DRG.NO.C2076.

Lakeland (2004b): 'Division – Semi-trailer', Document Ref: DRG.NO.C2082.

Lakeland (2004c): 'Joint Ring 2', Engineering drawing of extrusion profile design, Document Ref: 77605.

Lakeland (2005): 'Large Division / Baffle Extrusion', Document Ref: DRG.NO.C2939.

Lakeland (2011): 'G.A. – 42800L-6C AL.-ADR-BLVF', Document Ref: DRG.NO.B1404.

Lakeland (2015): 'AT11.1475 Test Tank – Front End 1'. Engineering drawing of AT11-1475 tank front end.

MatWeb (2015): 'MatWeb.com: Material Property Data', http://www.matweb.com/search/datasheettext.aspx?matid=9217, accessed 24/07/2015 at 13.54.00.

SIMULIA (2015): 'Abaqus Analysis User's Guide', SIMULIA.

Soare SC (2007): 'On the use of homogeneous polynomials to develop anisotropic yield functions with applications to sheet forming', University of Florida PhD Dissertation.

TWI (2015): 'Department for Transport Technical Assessment of Petroleum Tankers: Work Package 2 – Detailed Engineering Critical Assessment', TWI Report 24000/9/15, 31 March 2015.

Wu PD, Jain M, Savoie J, MacEwen SR, Tugcu P and Neale KW (2003): 'Evaluation of anisotropic yield functions for aluminium sheets', International Journal of Plasticity, Vol 19.

Table 1 Rear offside (impacted side) primary circumferential weld radiographic interpretation for AT11-1475 (see Figure 4)

Radiograph Number	Weld Number	Datum Points	Comments
P0117	W1	A-B	Groove Noted, minor isolated pores throughout <0.8mm ø.
P0118	W1	B-C	Groove Noted, linear aligned pores throughout <1.0mm ø.
P0119	W1	C-D	Groove Noted, linear aligned pores throughout <1.0mm ø.
P0120	W1	D-E	Groove Noted, linear aligned pores throughout <1.0mm ø.
P0121	W1	E-F	Groove Noted, linear aligned pores throughout <1.0mm ø.
P0122	W1	F-G	Groove Noted, linear aligned pores throughout <1.0mm ø.
P0123	W1	G-H	Groove Noted, linear aligned pores throughout <1.0mm ø.

Table 2 Rear nearside primary circumferential weld radiographic interpretation for AT11-1475 (see Figure 5)

Radiograph Number	Weld Number	Datum Points	Comments
P0112	W3	A-B	Groove Noted, linear aligned pores throughout <1.0mm ø.
P0113	W3	B-C	Groove Noted, linear aligned pores throughout <1.0mm ø.
P0114	W3	C-D	Groove Noted, linear aligned pores throughout <1.0mm ø.
P0115	W3	D-E	Groove Noted, linear aligned pores throughout <1.0mm ø.

Table 3 Front offside weld radiographic interpretation for AT11-1475 (see Figure 6)

Radiograph Number	Weld Number	Datum Points	Comments
P0151	W1	A-B	Linear lack of penetration noted throughout radiograph. Isolated porosity noted no greater than 1mm ø.
P0152	W1	B-C	Linear lack of penetration noted throughout radiograph. Isolated porosity noted no greater than 1mm ø.
P0153	W1	C-D	Linear lack of penetration noted throughout radiograph. Isolated porosity noted no greater than 1mm ø.
P0154	W1	D-E	Linear lack of penetration noted throughout radiograph. Isolated porosity noted no greater than 1mm ø.
P0155	W1	E-F	Isolated porosity noted no greater than 1mm ø throughout.
P0156	W1	F-G	Linear porosity noted, F + 10mm for a length of 25mm. Isolated porosity noted no greater than 1.5mm ø throughout.
P0157	W1	G-H	Porosity noted no greater than 1.5mm ø throughout.
P0158	W1	H-I	Porosity noted no greater than 1.5mm ø throughout.
P0159	W1	I-J	Porosity noted no greater than 1.5mm ø throughout. Lack of penetration 20mm up to J.
P0160	W1	J-K	Porosity noted no greater than 1.0mm ø throughout, transverse void noted positioned J+15mm,4mm long
P0161	W1	K-L	Porosity noted no greater than 1.0mm ø throughout. Two large pores noted 25mm before L.
P0162	W1	L-M	Porosity noted no greater than 1.0mm ø throughout. Two gas pores noted, position L +10mm, and L +18mm. Lack of penetration starting 60mm from L to M.
P0163	W1	M-N	Minor porosity noted throughout. Intermittent Lack of Penetration, position M +20mm.
P0164	W1	N-O	Minor porosity noted throughout. Intermittent Lack of Penetration, position N +25mm to O.
P0165	W1	O-P	Minor porosity noted throughout. Linear Pore noted, 4mm ø.
P0166	W1	P-Q	Minor porosity noted no greater than 0.2mm ø throughout. Lack of penetration throughout.
P0167	W1	Q-R	Minor porosity noted no greater than 0.5mm ø throughout. 1 gas pore noted, position Q +35mm. Intermittent lack of penetration throughout.
P0168	W1	R-S	Minor porosity noted no greater than 0.5mm ø throughout. Intermittent lack of penetration throughout.
P0169	W1	S-T	Minor porosity noted no greater than 0.7mm ø throughout. Intermittent lack of penetration throughout.
P0170	W1	T-U	Minor porosity noted no greater than 0.5mm ø throughout. Intermittent lack of penetration throughout.
P0171	W1	U-V	Intermittent lack of penetration throughout.
P0172	W1	V-W	Intermittent lack of penetration throughout.
P0173	W1	W-X	4 gas pores noted, 4mm ø. Minor porosity noted no greater than 0.5mm ø throughout. Intermittent lack of penetration noted at X position.

Table 4 Front nearside weld radiographic interpretation for AT11-1475 (see Figure 7)

Radiograph Number	Weld Number	Datum Points	Comments
P0096	W1	A-B	Porosity noted throughout radiograph between 0.2 to 1.3mm ø. Linear lack of fusion noted 60mm from A to 30mm behind B.
P0097	W1	B-C	Isolated porosity noted throughout radiograph <1.0mm ø. Linear lack of fusion noted 20mm long, 50mm behind C.
P0098	W1	C-D	Isolated scattered porosity noted throughout radiograph <0.5mm ø. 2 large pores noted at the stop/start no greater than 1.5mm ø.
P0099	W1	D-E	Isolated porosity noted throughout radiograph <0.5mm ø. Intermittent lack of fusion noted.
P0100	W1	E-F	Isolated porosity noted throughout radiograph <0.5mm ø. Intermittent lack of fusion noted.

Table 5 Summary of cross-section samples for the metallographic examination of AT11-1475

Section	Sample ID	Description
Rear offside Figure 8	AT1-1475-RO-01	Remote from impact site where there is no internal fillet weld
	AT1-1475-RO-02	Remote from impact side site where this is an internal fillet weld
	AT1-1475-RO-03	End of the crush zone towards the top of the tank
	AT1-1475-RO-04	Located between RO-03 and RO-05 in crush zone
	AT1-1475-RO-05	Centre of the crush zone/bulge
	AT1-1475-RO-06	Located between RO-05 and RO-07 in crush zone
	AT1-1475-RO-07	End of the crush zone towards the bottom of the tank
Rear nearside Figure 13	AT1-1475-RN-01	Centrally-located, no internal fillet weld
	AT1-1475-RN-02	Centrally-located, internal fillet weld present
	AT1-1475-RN-03	Centrally-located, no internal fillet weld
	AT1-1475-RN-04	Centrally-located, internal fillet weld present
Front offside Figure 16	AT1-1475-FO-01	Remote from the impact site towards top of tank
	AT1-1475-FO-02	End of the crush zone towards the top of the tank
	AT1-1475-FO-03	Located between FO-02 and FO-04
	AT1-1475-FO-04	Centre of the crush zone
	AT1-1475-FO-05	Located between FO-04 and FO-06
	AT1-1475-FO-06	End of the crush zone towards the bottom of the tank
Front nearside Figure 18	AT1-1475-FN-01	Centrally-located
	AT1-1475-FN-02	Centrally-located
	AT1-1475-FN-03	Centrally-located

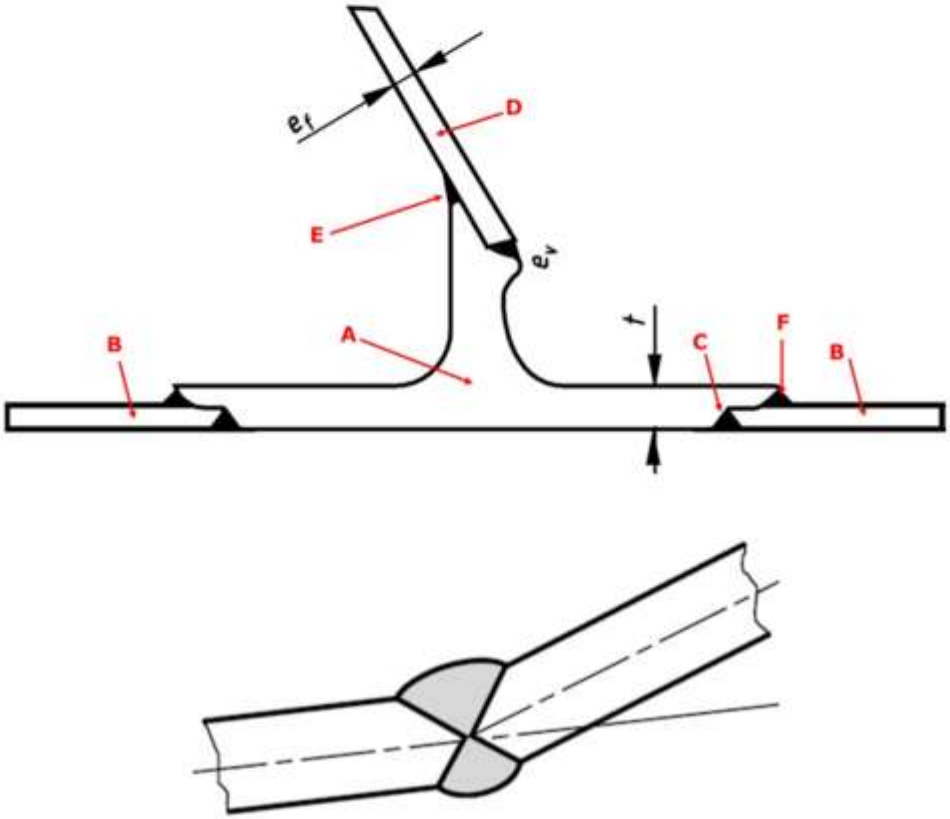

Figure 1 Diagrams of a joint designs that are qualitatively similar to the rear and intermediate circumferential, extrusion band joints (top frame) and front end joint (bottom frame) in tanker AT11-1475. Images reproduced from Figure D.14(c) for the top frame and D.9(b) for the bottom frame in BS EN 13094 (2015) with red arrows added for this report.

A) Extrusion band (or extrusion profile);
B) Tanker shell;
C) Primary circumferential weld joining tanker shell to the extrusion band;
D) Division plate such as a bulkhead, baffle, surge plate or end dish;
E) 'Top' weld joining the division plate to the extrusion band;
F) Internal fillet weld joining the inner surface of the tanker shell to the extrusion band.

Figure 2 Locations of the sections removed from the impacted, rear offside of AT11-1475 (Position B) and the undamaged, rear nearside (Position A). Images provided courtesy of HSL.

Figure 3 Location of the section removed from the impacted, front offside of AT11-1475. Images courtesy of HSL. The position A indicates the approximate dimensions of the section received by TWI.

Figure 4 Image of the section from the rear offside of AT11-1475 showing the datum markers (A-H for the primary circumferential weld) for the radiographic examination (see Table 1).

Figure 5 Image of the section from the rear nearside of AT11-1475 showing the datum markers (A-E) for the radiography (Table 2).

Figure 6 Image of the section from the front offside of AT11-1475 showing the datum marks (A-X) for the radiography (Table 3).

Figure 7 Image of the section from the front nearside of AT11-1475 showing the datum markers (A-F) for the radiography (Table 4).

Figure 8 Diagram of the sampling plan for the rear offside (impacted) section of AT11-1475.

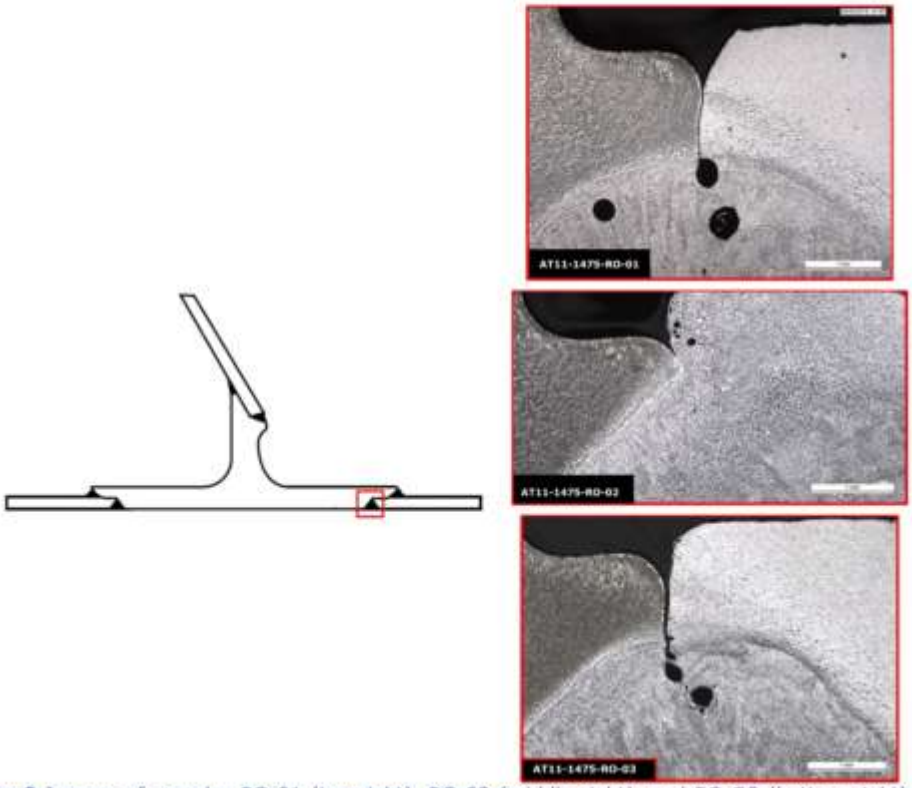

Figure 9 Images of samples RO-01 (top right), RO-02 (middle right), and RO-03 (bottom right) with the reference location shown on the BS EN 13094 indicative joint design D.14(c) on the left. The scale bars on the right indicate 1.0mm. Samples RO-01 and RO-03 exhibit lack of root fusion defects, whilst RO-02 exhibits good penetration and fusion.

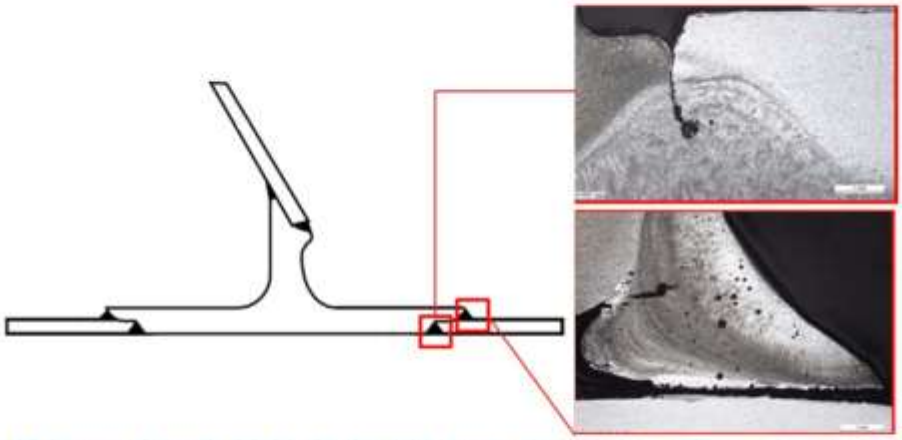

Figure 10 Images of sample RO-04. On the right images, the scale bars indicate 1.0mm length. The top right image shows the lack of root fusion defect, and the right frame shows the fracture between the internal fillet weld and the inner surface of the tanker shell along the fusion line.

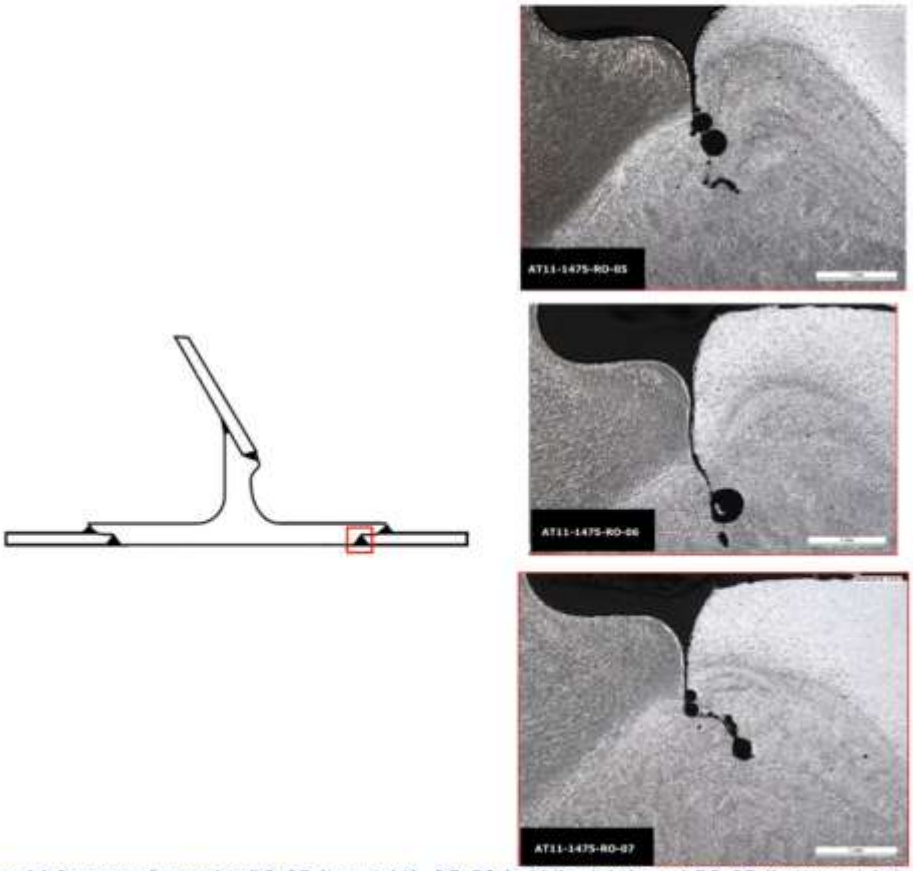

Figure 11 Images of samples RO-05 (top right), RO-06 (middle right), and RO-07 (bottom right), with the reference location shown on the BS EN 13094 indicative joint design D.14(c) on the left. On the left frames, the scale bar indicates 1.0mm length. All three samples exhibit lack of root fusion defects.

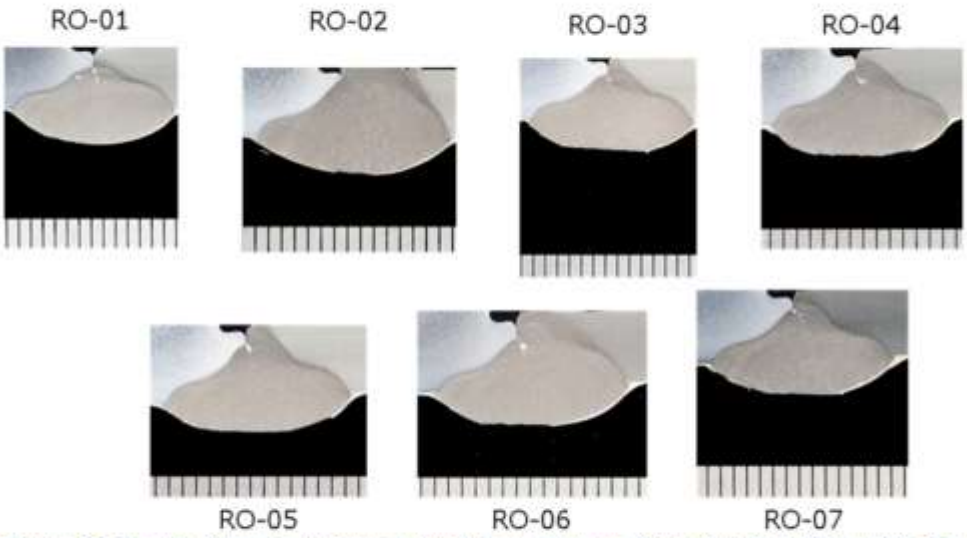

Figure 12 Images of the circumferential welds from the rear offside section of AT11-1475. Tick marks indicate 1.0mm length. The locations are shown in Figure 8.

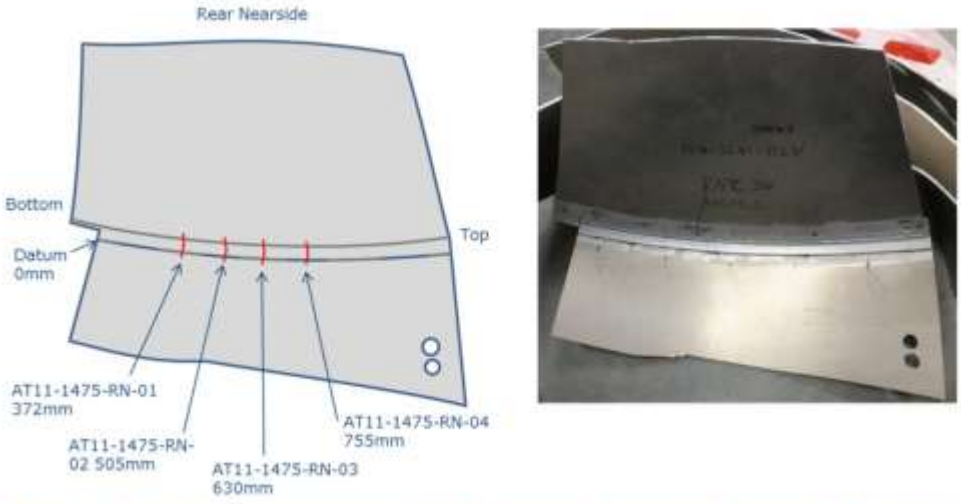

Figure 13 Diagram of the sampling plan for the rear nearside (undamaged) section of AT11-1475.

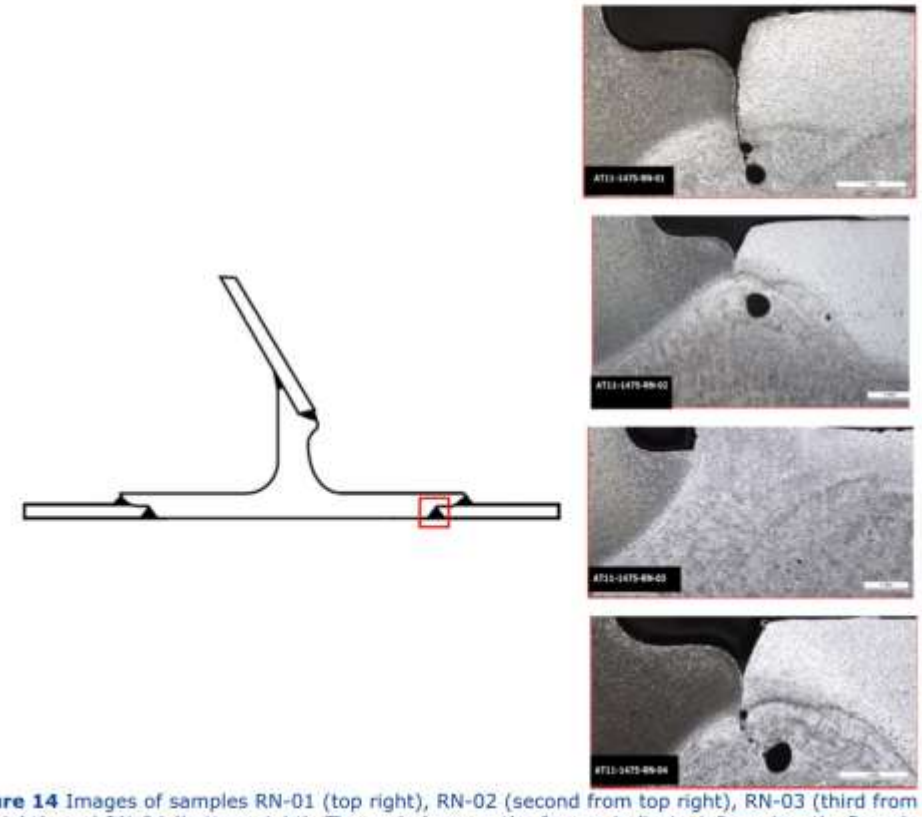

Figure 14 Images of samples RN-01 (top right), RN-02 (second from top right), RN-03 (third from top right), and RN-04 (bottom right). The scale bars on the frames indicate 1.0mm length. Sample RN-01 shows more significant lack of fusion at the root than RN-02. Sample RN-04 exhibits lack of root fusion.

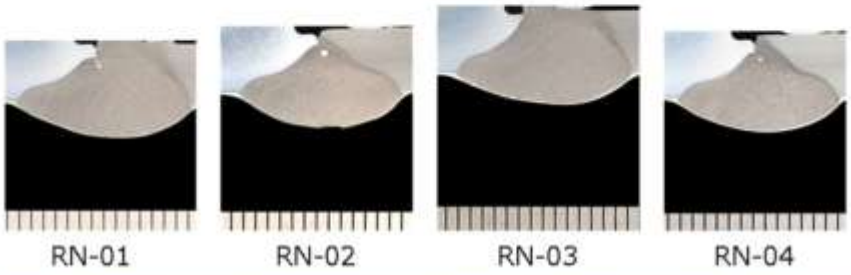

Figure 15 Images of the circumferential welds from the rear nearside section of AT11-1475. Tick marks indicate 1.0mm length scale. The locations are shown in Figure 13.

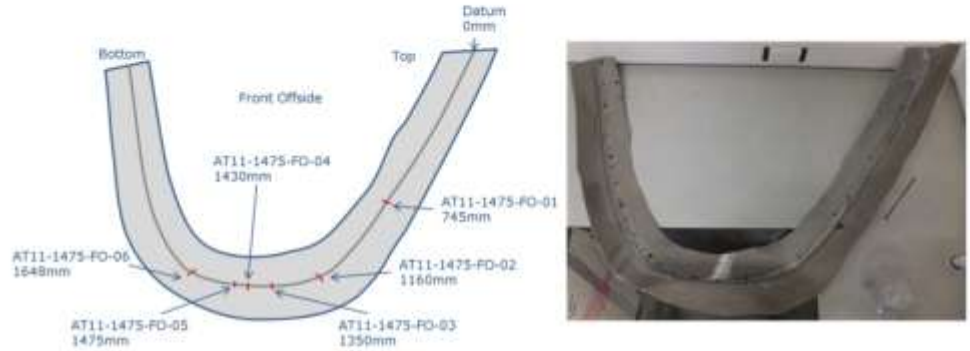

Figure 16 Diagram of the sampling plan for the front offside (impacted) section of AT11-1475.

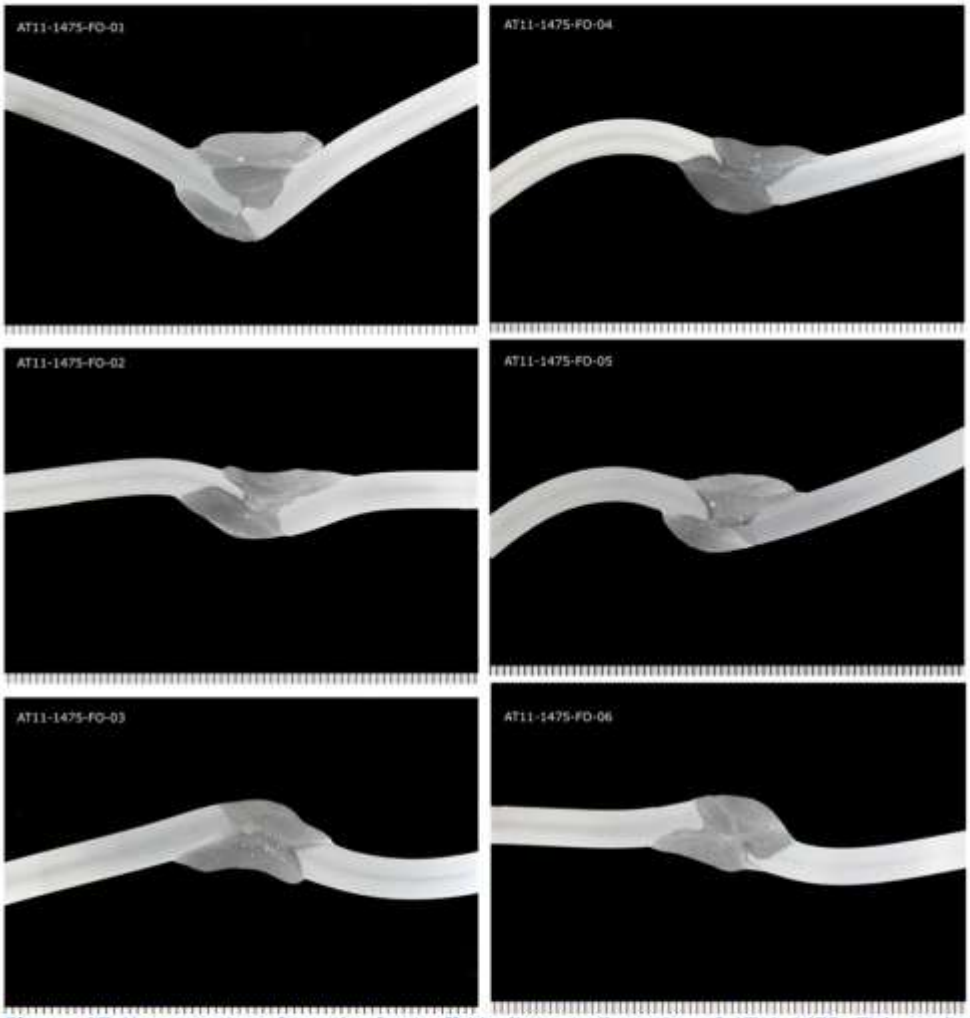

Figure 17 Macro-sections from the front offside (impacted) section of AT11-1475. Tick marks indicate a 1.0mm length scale. The locations are shown in Figure 8.

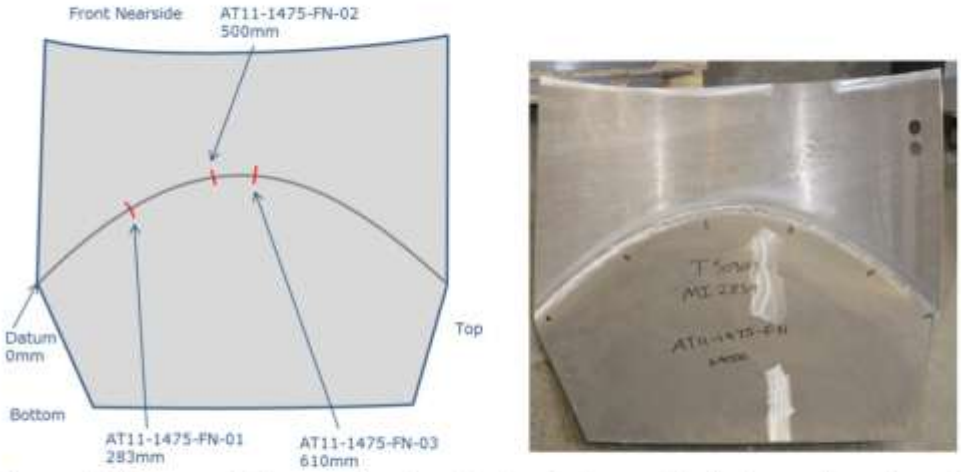

Figure 18 Diagram of the sampling plan for the front nearside (undamaged) section of AT11-1475.

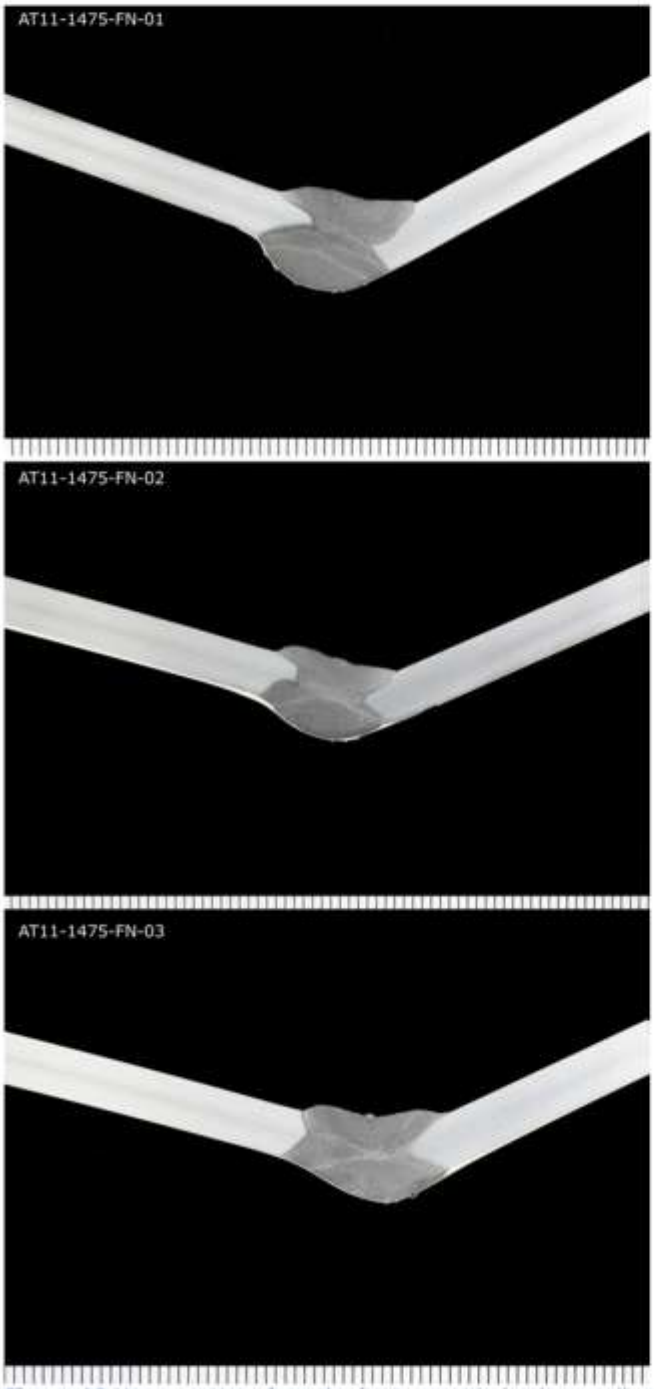

Figure 19 Macro-sections from the front nearside (undamaged) section of AT11-1475. Tick marks indicate 1.0mm length scale. The locations are shown in Figure 10.

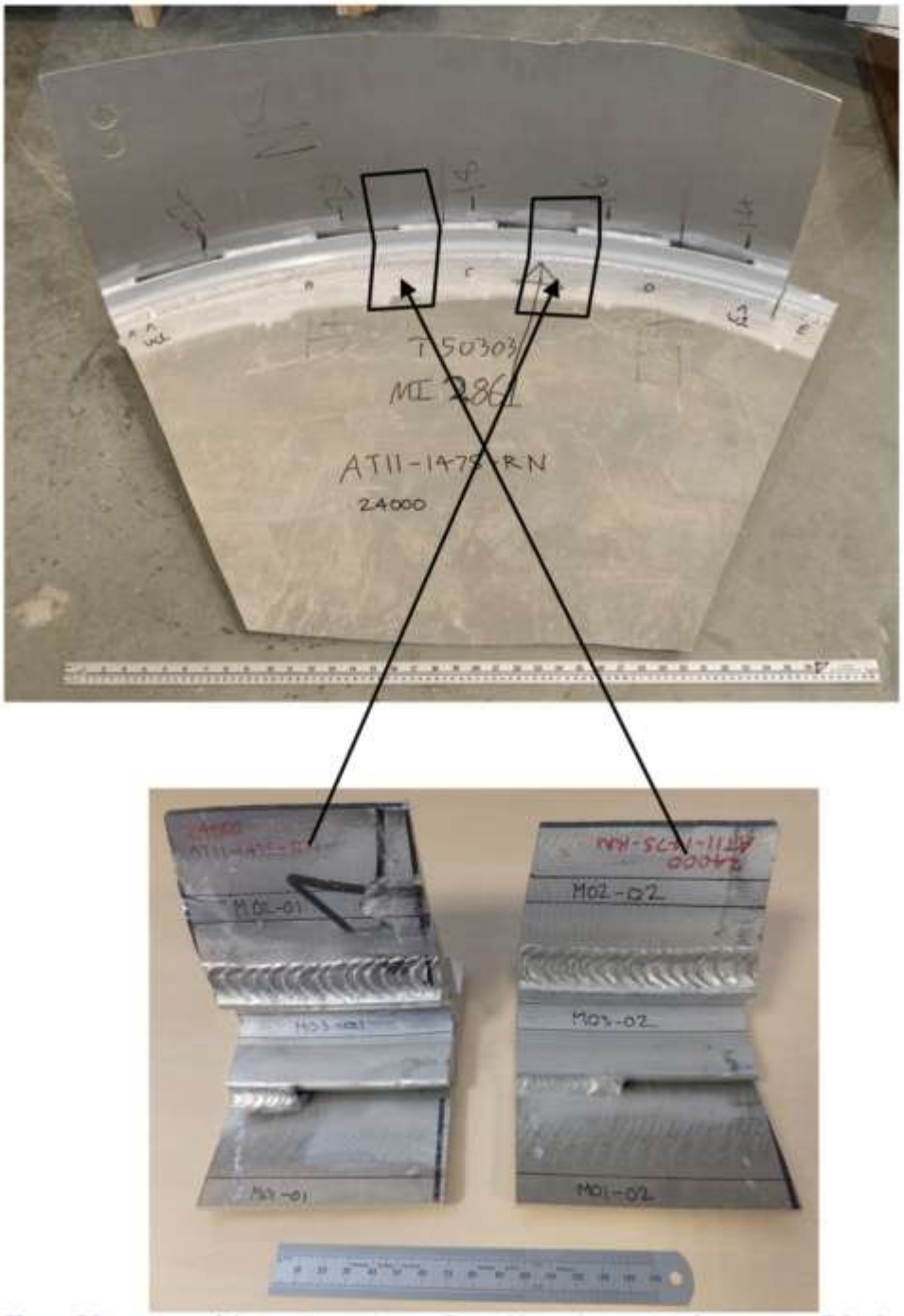

Figure 20 Locations of the tensile specimens. The weld metal was taken from position E (top) as shown in Figure 1.

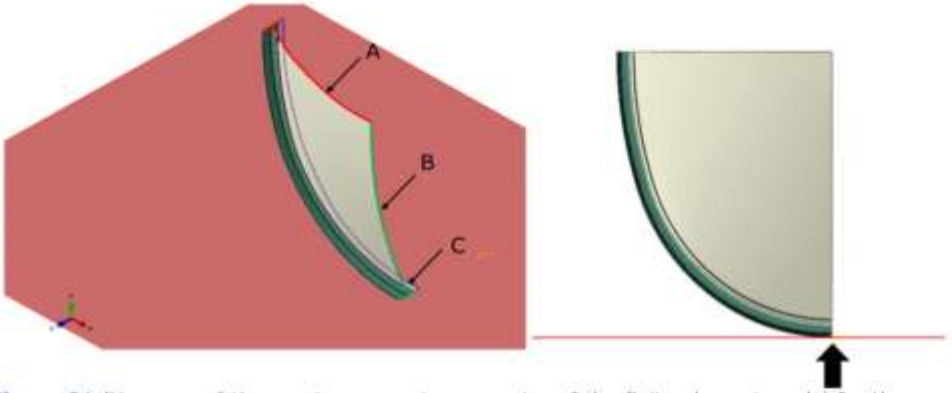

Figure 21 Diagrams of the quarter-symmetry geometry of the finite element model for the rear dish, side impact model. A) Y-direction restraint; B) X-direction restraint, C) Z-direction restraint. The movement of the ground is shown by the black arrow. The beige colour corresponds to parent and weld metal and the green corresponds to the extrusion band metal.

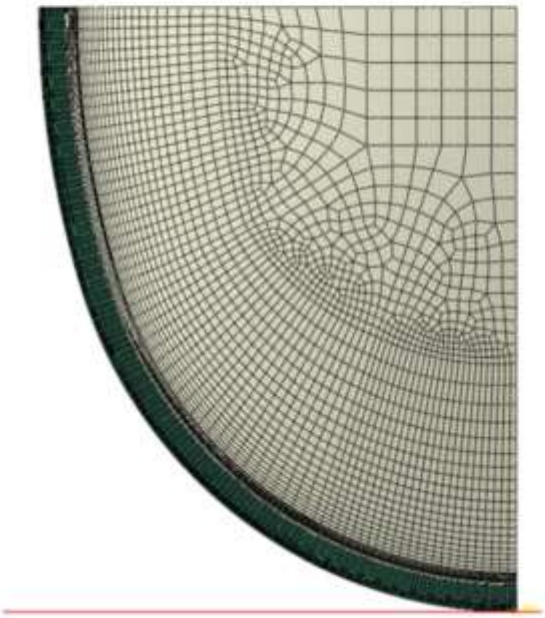

Figure 22 Finite element mesh used for the rear dish, side impact model. The beige colour corresponds to parent and weld metal and the green corresponds to the extrusion band metal. Viewed from the front.

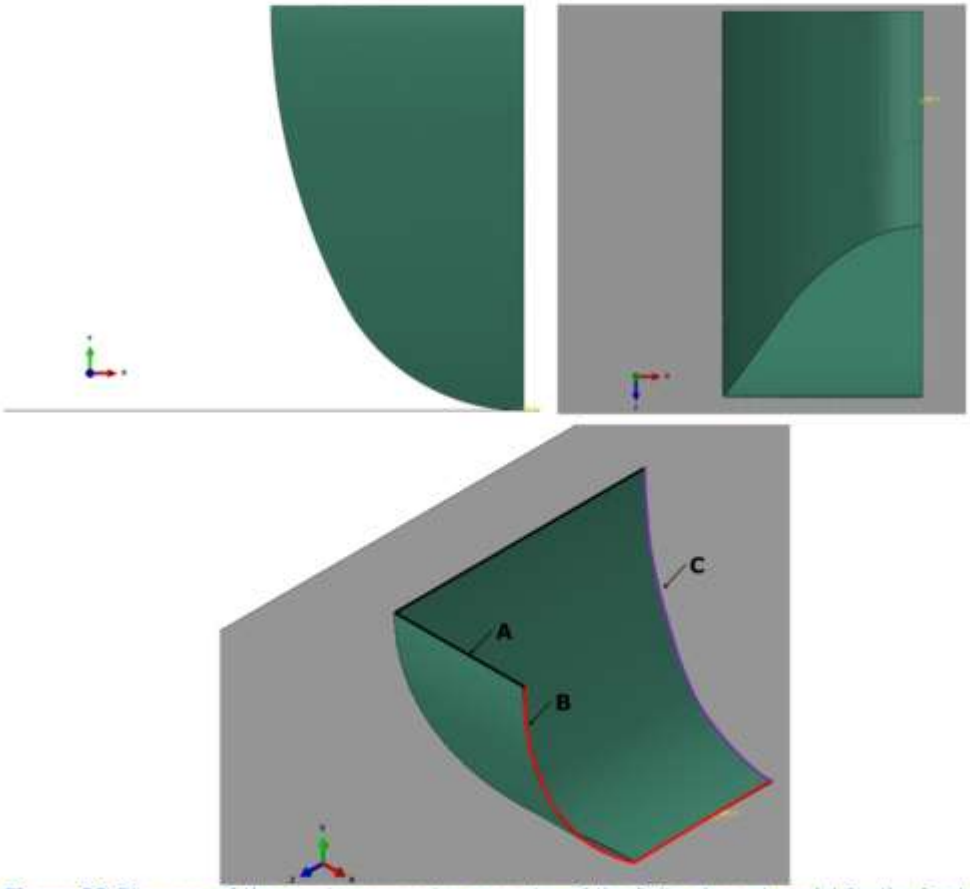

Figure 23 Diagrams of the quarter-symmetry geometry of the finite element model for the front end, side impact model. A) Y-direction restraint; B) X-direction restraint; C) Z-direction restraint. The top right frame shows the profile of the swept end front dish designed as viewed from the 3 o'clock position looking towards the 9 o'clock position of the tank with upright.

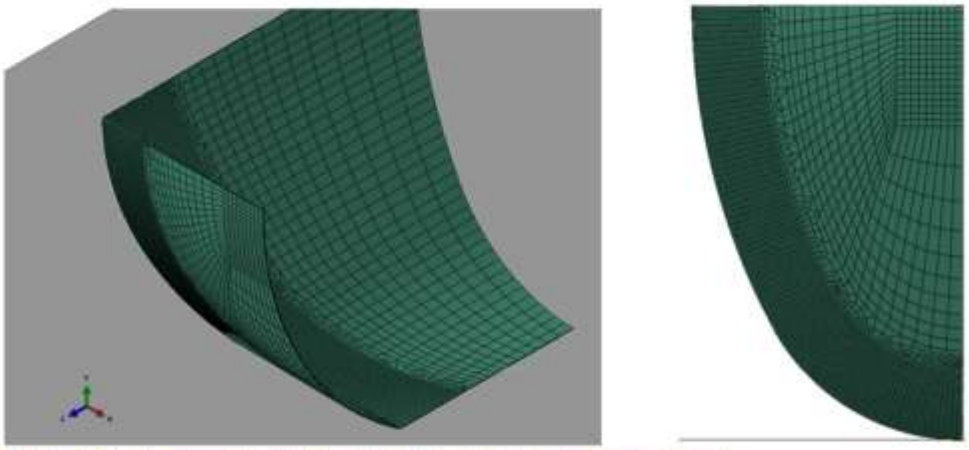

Figure 24 Finite element mesh used for the front dish, side impact model.

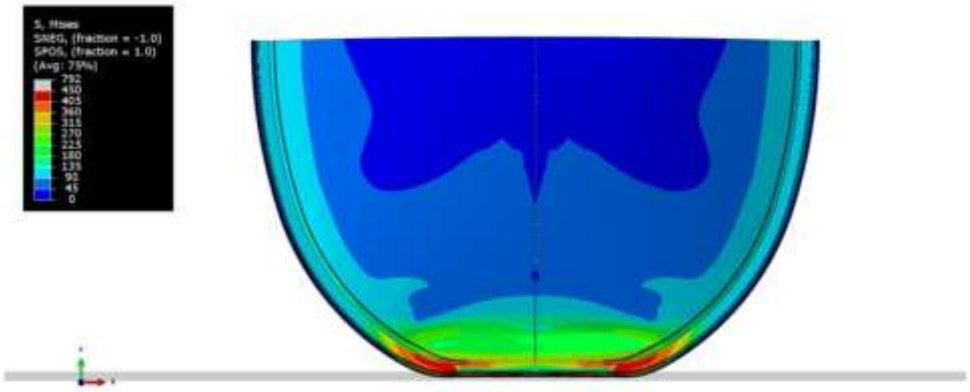

Figure 25 Image of the rear dish (viewed from the back of the tanker) when the flattened length is approximately 760mm. The symmetric half of the quarter model has been added for visualisation purposes.

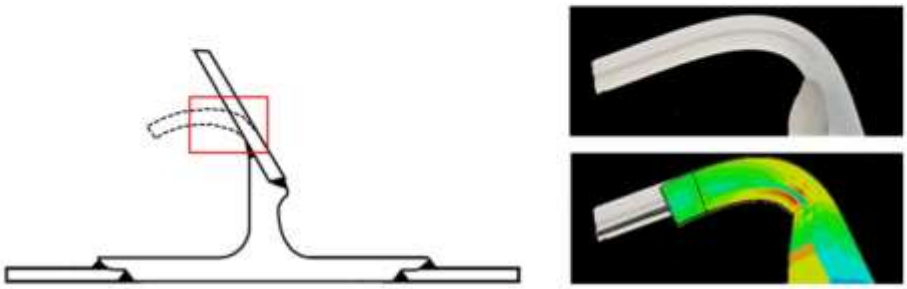

Figure 26 FEA results superimposed on the macro-section AT11-1475-RO-05 taken from the centre of the crush zone (equivalent to the symmetry plane in the FE model). Deformation not magnified, and equivalent plastic strain contour shown for reference.

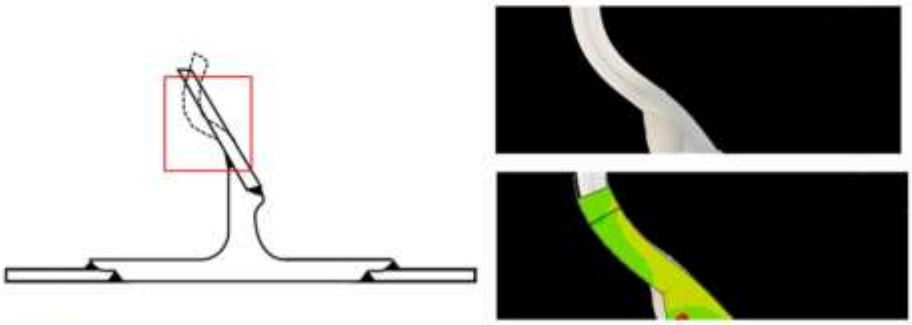

Figure 27 FEA results superimposed on the macro-section AT11-1475-RO-03 taken from the end of the crush zone approximately 400mm from the centre of the crush zone.

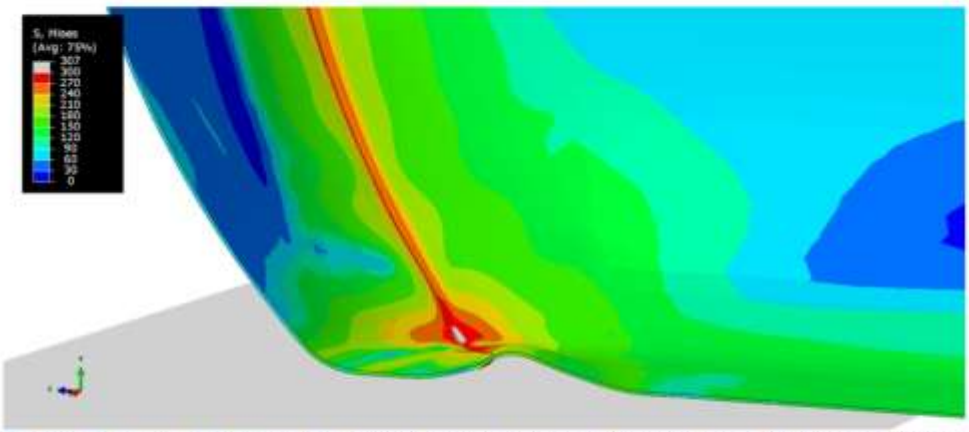

Figure 28 Image of the front dish viewed along the central symmetry plane (ie the plane cutting the tank from 3 o'clock to 9 o'clock when upright) showing the deformation at the centre of the crush zone (see the right frames of Figure 17 for similar bending deformation).

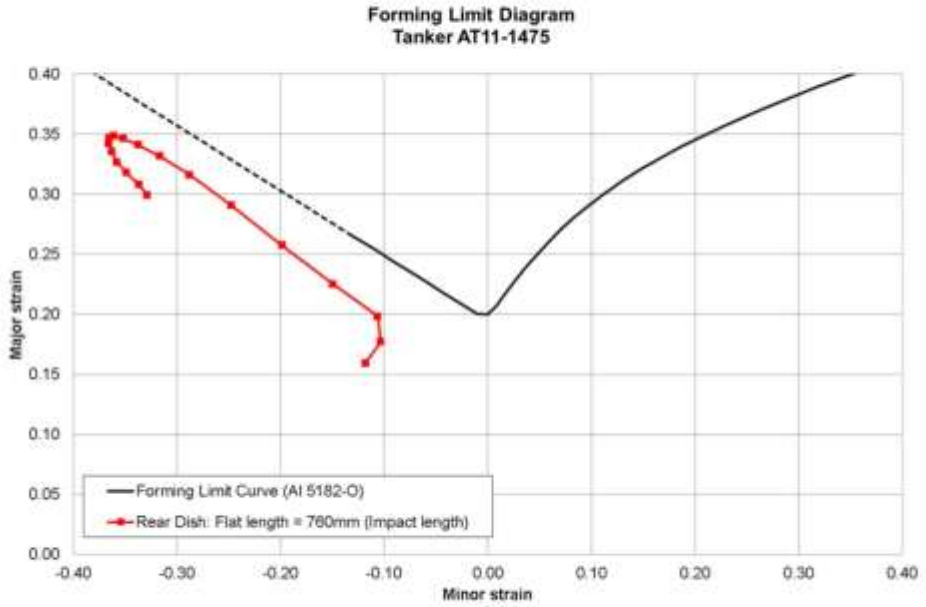

Figure 29 Forming limit diagram for the rear dish simulation. Each red point represents the minor and major strains output at a node in the circumferential path passing through the most severely strained region of the model.

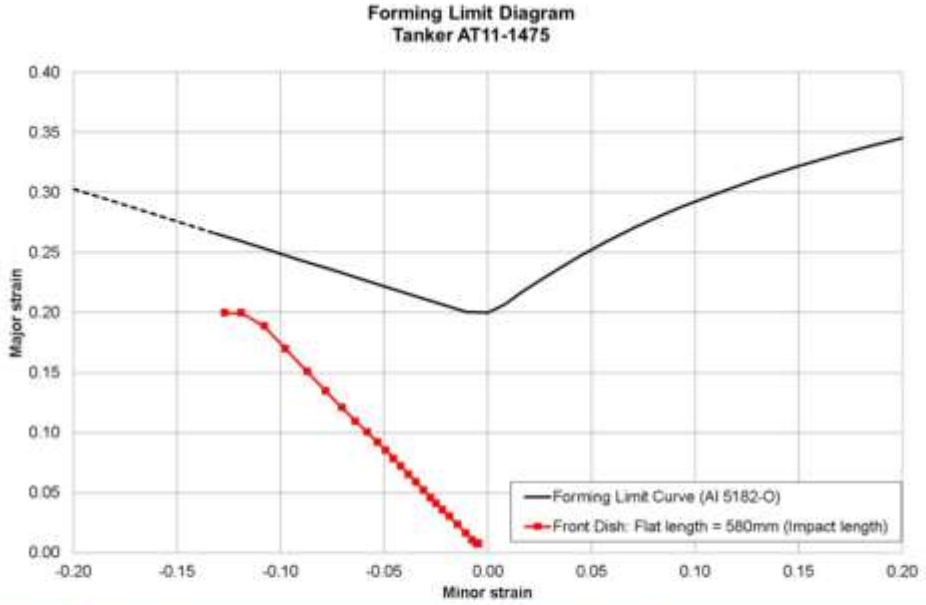

Figure 30 Forming limit diagram for the front dish simulation. Each red point represents the minor and major strains output at a node in the circumferential path passing through the most severely strained region of the model.

TWI Management System

TWI operates a Management System designed to ensure that customer requirements are met and that any work carried out is conducted in a planned and controlled manner. Customer satisfaction is a key measure of the success of TWI, which remains committed to delivering world-class solutions. To this end:

- All technical activities are controlled by a management system that complies with the general requirements of the BS EN ISO 9000:2008 series of standards.
- Project management, examination and training services are audited by LRQA as complying with BS EN ISO 9001:2008 and software development in accordance with TickITplus, Certification Number 0925004.
- TWI is a UKAS accredited testing laboratory No. 0088. Specific details are given on the UKAS Schedule of Accreditation, available at www.ukas.org. Reports may contain information not included in the TWI schedule of accredited tests. Enquiries concerning accreditation of tests should be directed to the Quality and Safety Group.
- Examination activities are assessed by PCN to BINDT requirements and by TWI Certification Ltd to CSWIP requirements.
- TWI is certificated by LRQA to BS EN ISO 14001:2004, certificate number LRQA 4000756.
- TWI's Occupational Health and Safety Management System is certificated to BS OHSAS 18001:2007 by LRQA, certificate number 4004571.

The Management System operated by TWI includes the following features that are particularly relevant to ensuring the success of projects:

- Close and frequent contact with the customer is requested of the Project Leader throughout the project. In particular, changes in personnel involved in the project or equipment availability are discussed together with any project delays or contractual changes.
- Regular management reviews of projects are held throughout the life of a project and upon its completion. These cover finance, technical progress and adherence to schedule.
- Project sponsors are formally contacted on project completion by senior TWI management to determine their satisfaction with the work carried out. Moreover, TWI management welcomes feedback on project progress at all times during the course of the work. Significant lapses in service are subjected to a structured management review so that inadequate procedures are identified and improved.

TWI Ltd
Granta Park, Great Abington
Cambridge CB21 6AL
United Kingdom

Tel: +44 (0)1223 899000
Fax: +44 (0)1223 892588
Web: www.twi-global.com

VAT Number GB 700 1708 69

Registered Number 3859442 England